

**CHROMATOGRAPHY AND PURIFICATION  
OF  
ENDOHEDRAL METALLOFULLERENES**

by

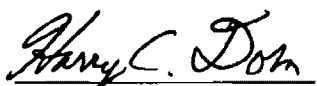
Steven A. Stevenson



Dissertation submitted to the Faculty of the  
Virginia Polytechnic Institute and State University  
in partial fulfillment of the requirements for the degree of  
Doctor of Philosophy

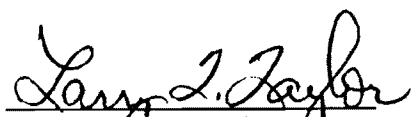
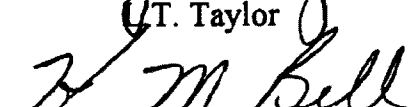
in

Chemistry

APPROVED:

  
H.C. Dorn, Chairman

  
M.R. Anderson  
  
K. Brewer

  
T. Taylor  
  
H. Bell

December 1995

Blacksburg, Virginia

Key words: Metallofullerenes, Chromatography, Isolation, HPLC-EPR

# Chromatography and Purification of Endohedral Metallofullerenes

by  
Steven Alan Stevenson

H.C. Dorn, Chairman  
Chemistry

## (ABSTRACT)

At the conception of this research, a separation methodology for obtaining purified metallofullerene [ $A_m@C_{2n}$ ;  $m = \#$  of metal atoms,  $A$ , and  $C_{2n} = \#$  of carbons in the surrounding cage] samples was not yet developed. Isolation of these metal-encapsulated fullerenes was strongly desired for characterization of their physical and chemical properties. Predicted applications for these novel species include their use as possible superconductors, catalysts, and non-linear optical devices. However, initial purification efforts have been hindered by several difficulties. These factors include a low abundance (<1%) in the raw extract, uncertain stability in aerobic environments, co-elution of  $A_m@C_{2n}$  with empty-cage fullerenes, and the need for selective chromatographic detection.

In this research, these difficulties have been overcome with the development of a continuous-flow, on-line HPLC-EPR apparatus. Advantages include a selective, non-invasive detector with chromatographic separations being performed in a controlled anaerobic environment. This on-line approach permits the selective detection of only those metallofullerenes with an odd-number of encapsulated atoms. The ability to continually monitor separations of these paramagnetic species ultimately permits the optimization of chromatographic parameters. The methodology developed from this on-line HPLC-EPR approach has ultimately resulted in purified empty-cage ( $C_{60}$ ,  $C_{70}$ ... $C_{96}$ ) and metallofullerene samples ( $Sc_2@C_{74}$ ,  $Sc_2@C_{76}$ ,  $Sc_2@C_{78}$ ,  $Sc_2@C_{80}$ ,  $Sc_2@C_{82}$ ,  $Sc_2@C_{84}$  - two isomers,  $Sc_2@C_{86}$ ,  $Sc_2@C_{88}$ ,  $Sc_2@C_{90}$ ,  $Sc_3@C_{82}$ ,  $Sc_4@C_{82}$ ,  $La_2@C_{72}$ ,  $Er@C_{82}$ ,  $Er_2@C_{82}$  - two isomers, and  $Er_2@C_{92}$ ).

## DEDICATION

This dissertation is dedicated to my dying father and my beautiful children, Jordan and Cole. I love them with every "fiber of my being." This work is also dedicated to the woman I love and think about, literally, every day of my life. Although I made the mistake of a lifetime and pushed her out of my life, she is - and always will be - my inspiration, my "kindred spirit", and my "Anne of Green Gables." Lord willing, I pray that someday we will be together again - only this time forever.

## ACKNOWLEDGEMENTS

I would like to express my gratitude toward many individuals who have contributed to this research. I acknowledge Dr. Harry Dorn, my research advisor, with whom many enlightening metallofullerene discussions took place. His advice and wisdom (sometimes followed) was an asset throughout my graduate studies.

From our research group, Paul Burbank, an undergraduate chemistry major, has been a vital link to the success of this project. From the automated system to the manual collection of fractions, his assistance is the most appreciated. Others who have contributed are Ziqi Sun and John Bailey.

From the Biochemistry department, a hearty acknowledgement is extended toward Kim Harich for his mass spectral services. His rapid turnaround of samples and mass spectra is very much appreciated. Kim did many favors for us throughout this research, and his "extra mile" approach is not forgotten.

From Analytical Services, Tom Glass provided insight into the computer programming of the HPLC-EPR apparatus. From the Glass Shop, several glass flow cells and hundreds of EPR tubes were cheerfully and promptly made by this competent staff. From the Electronics Shop, Larry Jackson and Jim Coulter repaired our EPR spectrometer when necessary. Finally, acknowledgement is extended to Don

Bethune, Mattanjah de Vries, Bob Johnson, and others at their research facility in California (IBM, Almaden) who provided financial support, arc-vaporized metallofullerene soot (raw extract), and mass spectral characterization of selected samples. This relationship between our Virginia Tech research group and IBM was the epitome of a symbiotic relationship at its finest - the way science should be done.

## TABLE OF CONTENTS

ABSTRACT.....	ii
DEDICATION.....	iii
ACKNOWLEDGEMENTS.....	iv
TABLE OF CONTENTS.....	vi
LIST OF FIGURES.....	xii
LIST OF TABLES.....	xx
CHAPTER 1: INTRODUCTION.....	1
1.1 Metallofullerenes.....	1
1.2 Detection.....	2
1.3 Research Problem.....	3
1.4 Research Objectives.....	4

CHAPTER 2: HISTORICAL BACKGROUND.....	6
2.1 Empty-cage Fullerenes ( $C_{2n}$ ).....	6
2.11 Discovery.....	6
2.12 Structure.....	7
2.13 Chromatography and Isolation.....	8
2.2 Metallofullerenes ( $A_m@C_{2n}$ ).....	11
2.21 Discovery.....	11
2.22 Nomenclature.....	11
2.23 Applications.....	12
2.24 Chromatographic Overview.....	13
2.25 Polystyrene Separations.....	15
2.26 Buckyclutcher Separations.....	16
2.27 TPP Separations.....	18
2.28 Buckyprep Separations.....	18
2.29 Isolation.....	19
2.3 HPLC-EPR.....	21
2.31 Historical.....	21
2.32 Advantages.....	21
2.33 Disadvantages.....	23

2.4 Goal and Justification.....	24
CHAPTER 3: EXPERIMENTAL.....	25
3.1 Metallofullerene Samples.....	25
3.11 Production.....	25
3.12 Extraction.....	26
3.13 Mobile Phase.....	27
3.14 Chromatographic Equipment.....	28
3.2 Instrumentation.....	29
3.21 HPLC-EPR Apparatus.....	29
3.22 Automated Apparatus.....	32
3.23 Mass Spectrometry.....	32
3.24 Two-Stage Chromatographic Systems.....	33
3.241 Polystyrene/Buckyclutcher System.....	33
3.242 Buckyclutcher/TPP and Buckyclutcher/PBB system.....	34
CHAPTER 4: RESULTS AND DISCUSSION.....	35
4.1 Metallofullerene ( $A_m@C_{2n}$ ) Separations.....	35
4.11 $Sc_m@C_{2n}$ .....	35



4.12	$Y_m@C_{2n}$ .....	69
4.13	$La_m@C_{2n}$ .....	79
4.14	$Er_m@C_{2n}$ .....	86
4.2	Improved Separation Methodology.....	94
4.21	PBB Column ( $Sc_m@C_{2n}$ ).....	94
4.3	Automated Separations.....	105
4.31	$Er_m@C_{2n}$ .....	107
4.4	Empty-cage ( $C_{2n}$ ) Separations.....	110
4.5	Trends in $A_m@C_{2n}$ Separations.....	121
CHAPTER 5: FUTURE DEVELOPMENTS.....		133
5.1	Summary.....	133
5.2	Concluding Remarks.....	135
5.3	Fullerene Related Materials.....	137
REFERENCES.....		139
APPENDIX I: $C_{2n}$ mass (table).....		166
APPENDIX II: $Sc_m@C_{2n}$ mass (table).....		167

APPENDIX III: $Y_m@C_{2n}$ mass (table).....	168
APPENDIX IV: $La_m@C_{2n}$ mass (table).....	169
APPENDIX V: $Er_m@C_{2n}$ mass (table).....	170
VITA.....	171

## LIST OF FIGURES

- Figure 2.1 Summary of the four most common stationary phases in metallofullerene separations.....17
- Figure 3.1 Block diagram of the on-line HPLC-EPR apparatus. C1 and C2 are the separating chromatographic columns.....30
- Figure 4.1 (a) Initial polystyrene pass of  $Sc_m@C_{2n}$  raw extract: HPLC-UV trace (340 nm), 5 mL injected (10-15 mg), 1.0 mL/min, and 80:20 toluene/decalin. (b) on-line HPLC-EPR profile, 9.55 GHz, 2.25 min/file, 4 scans/file, and 20 s/sweep....36
- Figure 4.2 HPLC-UV trace for  $Sc_m@C_{2n}$  separations in which the EPR active fraction is recovered and re-injected. The first through fourth polystyrene passes are represented by (a) - (d), respectively. Flow rate 1 mL/min, UV 340 nm detection. and the EPR active fraction is denoted as the hatched region (30 - 37 min.).....38
- Figure 4.3 (a) HPLC-UV trace (340 nm) for the fifth polystyrene pass of the  $Sc_3@C_{82}$  EPR active fraction, 410  $\mu$ L injection, 1.0 mL/min, and 80:20 toluene/decalin. (b) On-line HPLC-EPR profile, 4 scans/file, 9.55 GHz, and 20 s/sweep.....39
- Figure 4.4 Off-line, negative-ion CI mass spectrum for the fourth polystyrene pass  $Sc_3@C_{82}$  EPR active fraction. The "\*" indicates calibration peaks for the standard Ultramark 1621.....41
- Figure 4.5 (a) HPLC-UV trace (340 nm) of the EPR active  $Sc_3@C_{82}$  fraction after five polystyrene passes, 250  $\mu$ L detection, Buckyclutcher column, 2.1 mL/min, 80:20 toluene/decalin, EPR active region is peak #6. (b) On-line HPLC-EPR profile, 3 scans/file, 9.55 GHz, and 20 s/sweep.....43

Figure 4.6	Off-line EPR spectra of purified peak #6 ( $\text{Sc}_3@C_{82}$ ) in decalin. (a) 9.63 GHz, 500 s/sweep, one scan, and 25 °C. (b) 9.63 GHz, 500 s/sweep, one scan, and -70 °C.....	45
Figure 4.7	HPLC-UV chromatogram, 10 $\mu\text{L}$ of purified peak #6 ( $\text{Sc}_3@C_{82}$ ), Buckyclutcher column, 340 nm detection, and 2.1 mL/min of 80:20 toluene/decalin.....	46
Figure 4.8a	(a) Analytical HPLC-UV trace (peak #0), Buckyclutcher column, 2.1 mL/min of 80:20 toluene/decalin, and 340 nm detection. (b) off-line negative-ion chemical ionization mass spectrum of above using Ultramark 1621 as the calibration standard.....	47
Figure 4.8b	(a) Analytical HPLC-UV trace (peak #1), Buckyclutcher column, 2.1 mL/min of 80:20 toluene/decalin, and 340 nm detection. (b) off-line negative-ion chemical ionization mass spectrum of above using Ultramark 1621 as the calibration standard.....	48
Figure 4.8c	(a) Analytical HPLC-UV trace (peak #2), Buckyclutcher column, 2.1 mL/min of 80:20 toluene/decalin, and 340 nm detection. (b) off-line negative-ion chemical ionization mass spectrum of above using Ultramark 1621 as the calibration standard.....	49
Figure 4.8d	(a) Analytical HPLC-UV trace (peak #3), Buckyclutcher column, 2.1 mL/min of 80:20 toluene/decalin, and 340 nm detection. (b) off-line negative-ion chemical ionization mass spectrum of above using Ultramark 1621 as the calibration standard.....	50
Figure 4.8e	(a) Analytical HPLC-UV trace (peak #4), Buckyclutcher column, 2.1 mL/min of 80:20 toluene/decalin, and 340 nm detection. (b) off-line negative-ion chemical ionization mass spectrum of above using Ultramark 1621 as the calibration standard.....	51

Figure 4.8f	(a) Analytical HPLC-UV trace (peak #5), Buckyclutcher column, 2.1 mL/min of 80:20 toluene/decalin, and 340 nm detection. (b) off-line negative-ion chemical ionization mass spectrum of above using Ultramark 1621 as the calibration standard.....	52
Figure 4.8g	(a) Analytical HPLC-UV trace (peak #6), Buckyclutcher column, 2.1 mL/min of 80:20 toluene/decalin, and 340 nm detection. (b) off-line negative-ion chemical ionization mass spectrum of above using Ultramark 1621 as the calibration standard.....	53
Figure 4.8h	(a) Analytical HPLC-UV trace (peak #7), Buckyclutcher column, 2.1 mL/min of 80:20 toluene/decalin, and 340 nm detection. (b) off-line negative-ion chemical ionization mass spectrum of above using Ultramark 1621 as the calibration standard.....	54
Figure 4.8i	(a) Analytical HPLC-UV trace (peak #8), Buckyclutcher column, 2.1 mL/min of 80:20 toluene/decalin, and 340 nm detection. (b) off-line negative-ion chemical ionization mass spectrum of above using Ultramark 1621 as the calibration standard.....	55
Figure 4.8j	(a) Analytical HPLC-UV trace (peak #9.1 series), Buckyclutcher column, 2.1 mL/min of 80:20 toluene/decalin, and 340 nm detection. (b) off-line negative-ion chemical ionization mass spectrum of above using Ultramark 1621 as the calibration standard.....	56
Figure 4.8k	(a) Analytical HPLC-UV trace (peak #9.2 series), Buckyclutcher column, 2.1 mL/min of 80:20 toluene/decalin, and 340 nm detection. (b) off-line negative-ion chemical ionization mass spectrum of above using Ultramark 1621 as the calibration standard.....	57

Figure 4.8l	(a) Analytical HPLC-UV trace (peak #9.3 series), Buckyclutcher column, 2.1 mL/min of 80:20 toluene/decalin, and 340 nm detection. (b) off-line negative-ion chemical ionization mass spectrum of above using Ultramark 1621 as the calibration standard. (c) off-line EPR spectrum of above, 44 scans, 9.64 GHz, sweep width 140 g, and 200 s/sweep. Sample was "freeze-thaw" degassed in decalin.....	58
Figure 4.8m	(a) Analytical HPLC-UV trace (peak #9.4 series), Buckyclutcher column, 2.1 mL/min of 80:20 toluene/decalin, and 340 nm detection. (b) off-line negative-ion chemical ionization mass spectrum of above using Ultramark 1621 as the calibration standard.....	59
Figure 4.9	Off-line EPR spectrum of $Sc_m@C_{2n}$ raw extract to be injected for Buckyclutcher separations. Spectrum is taken under high modulation, saturation, and rapid sweep operating conditions (see Experimental), 20 s/sweep, 4 scans/file, sweep width 150 g, and 9.55 GHz.....	63
Figure 4.10	On-line HPLC-EPR experiment: (a) HPLC-UV trace following a 20 mg injection of $Sc_m@C_{2n}$ raw extract, Buckyclutcher column, 340 nm detection, and 2.0 mL/min, of 80:20 toluene/decalin. (b) on-line HPLC-EPR profile of above, 3 scans/file, 20 s/sweep, 9.55 GHz, and alternate files are shown.....	64
Figure 4.11	Off-line EPR spectra of collected $Sc_m@C_{2n}$ fractions (see Figure 4.10) centered at 17-20 min. and 20-26 min., respectively. (a) 17-20 min. fraction, sweep width 100 g, 100 s/sweep, 4 scans/file, 9.63 GHz, and the solvent is decalin. (b) #20-26 min. $Sc_m@C_{2n}$ fraction, sweep width 150 g, 100 s/scan, 9.63 GHz, in decalin.....	66
Figure 4.12	HPLC-UV trace, (second Buckyclutcher pass), 450 $\mu$ L of the 20-26 min. $Sc_m@C_{2n}$ EPR active fraction, 2.0 mL/min, 80:20 toluene/decalin, and 340 nm detection.....	67

Figure 4.13	Off-line EPR spectra corresponding to the experiment from Figure 4.12. (a) Sc@C <sub>82</sub> fraction, sweep width 100 g, 100 s/scan, 4 scans/file, 9.63 GHz, in decalin. (b) Sc <sub>3</sub> @C <sub>82</sub> fraction, sweep width 150 g, 100 s/scan, 4 scans/file, 9.63 GHz, in decalin.....	68
Figure 4.14	(a) HPLC-UV trace of Y <sub>m</sub> @C <sub>2n</sub> raw extract, first polystyrene pass, 1.0 mL/min, 80:20 toluene/decalin, 8 mg injected, and 340 nm detection. (b) on-line HPLC-EPR spectra, sweep width 130 g, 4 scans/file, and 20 s/sweep. The broad singlet was observed due to low resolution conditions (see Experimental).....	70
Figure 4.15	HPLC-UV chromatograms for Y <sub>m</sub> @C <sub>2n</sub> polystyrene injections, 2.0 mL/min, 80:20 toluene/decalin, and 340 nm detection. HPLC profiles represent (a) a first polystyrene pass, (b) a third polystyrene pass, and (c) a fifth polystyrene re-injection of the collected EPR active Y <sub>m</sub> @C <sub>2n</sub> fraction.....	73
Figure 4.16	Off-line negative-ion mass spectrum of the final, collected Y <sub>m</sub> @C <sub>2n</sub> EPR active fraction (fifth polystyrene pass). The calibration standard Ultramark 1621 is used.....	74
Figure 4.17	(a) HPLC-UV trace (340 nm), Buckyclutcher column, 2.0 mL/min of 80:20 toluene/decalin, and 250 μL injection of the Y <sub>m</sub> @C <sub>2n</sub> EPR active fraction obtained from the final polystyrene pass. (b) on-line HPLC-EPR profile, 9.56 GHz, 3 scans/file, and 20 s/scan. Alternate files are not shown.....	76
Figure 4.18	(a) Analytical HPLC-UV trace for isolated Y <sub>m</sub> @C <sub>82</sub> peak #5 (EPR active region), Buckyclutcher column, 2.0 mL/min, and 340 nm detection. (b) off-line negative ion mass spectrum of peak #5.....	78
Figure 4.19	(a) HPLC-UV trace of 10 mg La <sub>m</sub> @C <sub>2n</sub> raw extract, first polystyrene pass, 1.0 mL/min, 80:20 toluene/decalin, and 340 nm detection. (b) on-line HPLC-EPR profile, 4 scans/file, 20 s/scan, sweep width 130 g, and 9.55 GHz.....	80

Figure 4.20	HPLC-UV trace representing the recovery and re-injection of the EPR active $\text{La}_m@C_{2n}$ fraction: (a) first polystyrene pass, (b) third polystyrene pass, and (c) fifth polystyrene pass. Chromatographic conditions: 1.0 mL/min, 80:20 toluene/decalin, and 340 nm detection.....	81
Figure 4.21	HPLC-UV trace of the fifth polystyrene pass, 1.0 mL/min, 80:20 toluene/decalin, 340 nm detection, and 200 $\mu\text{L}$ of $\text{La}_m@C_{2n}$ sample. (b) on-line HPLC-EPR profile, 2 scans/file, 20 s/sweep, sweep width 130 g, and 9.55 GHz.....	82
Figure 4.22	Fifth polystyrene pass, $\text{La}_m@C_{2n}$ EPR active fraction on the Buckyclutcher column: (a) 110 $\mu\text{L}$ injection, 2.0 mL/min, 80:20 toluene/decalin, and 340 nm detection. (b) on-line HPLC-EPR profile, 2 scans/file, 20 s/sweep, sweep width 130 g, and 9.55 GHz.....	84
Figure 4.23	LD-TOF mass spectrum of isolated $\text{La}_m@C_{2n}$ fraction #0. (mass spectrum courtesy of IBM, Almaden).....	85
Figure 4.24	LD-TOF mass spectrum of $\text{Er}_m@C_{2n}$ raw extract. (mass spectrum courtesy of IBM, Almaden).....	87
Figure 4.25	HPLC-UV trace of $\text{Er}_m@C_{2n}$ raw extract, Buckyclutcher column, 200 $\mu\text{L}$ injection, 1.2 mL/min, 80:20 toluene/decalin, and 354 nm UV detection.....	89
Figure 4.26	HPLC-UV trace of $\text{Er}_2@C_{82}$ isomers I, II, and III. Chromatographic conditions: Two Buckyclutcher columns in series, 1.55 mL/min, 80:20 toluene/decalin, and 340 nm UV detection.....	90
Figure 4.27	HPLC-UV chromatogram for an $\text{Er}_2@C_{2n}$ (isomer III fraction), sample obtained from initial Buckyclutcher separations. Chromatographic conditions: TPP column, 1.0 mL/min $\text{CS}_2$ , and 340 nm UV detection.....	91



- Figure 4.28 (a) HPLC-UV analytical trace for isolated  $\text{Er}_2@\text{C}_{82}$  (isomer III), Buckyclutcher columns, 1.0 mL/min, 80:20 toluene/decalin, and 340 nm detection. (b) LD-TOF mass spectrum of above (courtesy of IBM, Almaden).....93
- Figure 4.29 Isolated  $\text{Er}@\text{C}_{82}$  sample obtained after Buckyclutcher and TPP column separations. (a) HPLC-UV analytical trace, Buckyclutcher columns, 1.0 mL/min, 80:20 toluene/decalin, and 340 nm UV detection. (b) negative-ion chemical ionization mass spectrum of above using Ultramark 1621 as the calibration standard.....95
- Figure 4.30 Isolated  $\text{Er}_2@\text{C}_{92}$  sample obtained after Buckyclutcher and TPP column separations. (a) HPLC-UV analytical trace, Buckyclutcher columns, 1.0 mL/min, 80:20 toluene/decalin, and 340 nm UV detection. (b) negative-ion chemical ionization mass spectrum of above using Ultramark 1621 as the calibration standard.....96
- Figure 4.31 (a) HPLC-UV analytical trace of PBB fraction 4.B,  $\text{CS}_2$  mobile phase, 380 nm UV detection, PBB column, and 2.0 mL/min. (b) HPLC-UV analytical trace of the final purified  $\text{Sc}_4@\text{C}_{82}$  sample, Buckyclutcher column, 2.0 mL/min, 380 nm UV detection, and 80:20 toluene/decalin mobile phase. (c) negative-ion chemical ionization mass spectrum of the above final purified  $\text{Sc}_4@\text{C}_{82}$  sample using Ultramark 1621 as the calibration standard..... 103
- Figure 4.32 Negative-ion chemical ionization mass spectrum for the  $\text{Sc}_4@\text{C}_{82}$  sample using Ultramark 1621 as the calibration standard. Obtained under optimal high resolution mass spectral condition, this mass spectrum was used for analyzing predicted isotope distribution patterns for  $\text{Sc}_4@\text{C}_{82}$ ..... 104

Figure 4.33	(a) HPLC-UV analytical trace for purified Sc <sub>2</sub> @C <sub>74</sub> , PBB column 2.0 mL/min, carbon disulfide mobile phase, and 380 nm UV detection. This sample was previously separated using the Buckyclutcher column and injected into the PBB column for final purification. (b) <sup>45</sup> Sc NMR spectrum for the above purified Sc <sub>2</sub> @C <sub>74</sub> sample obtained under ambient conditions suggesting that the two Sc atoms are equivalent on the NMR time scale. Under these conditions, ScCl <sub>3</sub> would have a chemical shift of 114 ppm.....	106
Figure 4.34	Automated HPLC apparatus: Load and separation columns are C1, C2 and C3, C4, respectively. The manual valve is an optional feature (details in ref. 173).....	108
Figure 4.35	(a) Automated sequence of Er <sub>m</sub> @C <sub>2n</sub> injections. Chromatographic conditions: first Buckyclutcher pass, 1.0 mL/min, 80:20 toluene/decalin, and 340 nm detection. (b) Re-injection of the Er <sub>2</sub> @C <sub>82</sub> fraction into the automated apparatus. Chromatographic conditions: second Buckyclutcher pass, 1.0 mL/min, 80:20 toluene/decalin, and 340 UV nm detection. The dominant peak corresponds to Er <sub>2</sub> @C <sub>82</sub> (isomer III).....	109
Figure 4.36	Automated sequence of the Er <sub>2</sub> @C <sub>82</sub> fraction (isomer III) obtained after two Buckyclutcher passes yielded a single, symmetric peak. Chromatographic conditions: TPP column, 1.0 mL/min, carbon disulfide, and 340 nm UV detection.....	112
Figure 4.37	HPLC-UV chromatograms for a typical polystyrene separation. Chromatographic conditions: second polystyrene pass of the Y <sub>m</sub> @C <sub>2n</sub> fraction, 1.0 mL/min, 80:20 toluene/decalin, and 340 nm UV detection.....	114
Figure 4.38a	Analytical HPLC-UV trace of an isolated C <sub>82</sub> fraction, Buckyclutcher column, 1.0 mL/min, 80:20 toluene/decalin, and 340 nm UV detection.....	115

Figure 4.38b	Analytical HPLC-UV trace of an isolated C <sub>84</sub> fraction, Buckyclutcher column, 1.0 mL/min, 80:20 toluene/decalin, and 340 nm UV detection.....	116
Figure 4.38c	Analytical HPLC-UV trace of an isolated C <sub>86</sub> fraction, Buckyclutcher column, 1.0 mL/min, 80:20 toluene/decalin, and 340 nm UV detection.....	117
Figure 4.38d	Analytical HPLC-UV trace of an isolated C <sub>88</sub> fraction, Buckyclutcher column, 1.0 mL/min, 80:20 toluene/decalin, and 340 nm UV detection.....	118
Figure 4.38e	Analytical HPLC-UV trace of an isolated C <sub>90</sub> fraction, Buckyclutcher column, 1.0 mL/min, 80:20 toluene/decalin, and 340 nm UV detection.....	119
Figure 4.38f	Analytical HPLC-UV trace of an isolated C <sub>92</sub> fraction, Buckyclutcher column, 1.0 mL/min, 80:20 toluene/decalin, and 340 nm UV detection.....	120
Figure 4.39	Plot of chromatographic capacity factor ( $\log k'$ ) versus cage size (number of carbon atoms), ● polystyrene column ◆ Buckyclutcher column, and 80:20 toluene/decalin mobile phase. (a) is an expanded inset from (b).....	122
Figure 4.40	Plots of chromatographic capacity factor ( $\log k'$ ) versus the hyperfine coupling constant, $a$ , for (a) Buckyclutcher and (b) polystyrene separations, respectively. The mobile phase is 80:20 toluene/decalin.....	127
Figure 4.41	(a) mass spectrum of a Y <sub>3</sub> @C <sub>82</sub> - containing Buckyclutcher fraction. (b) Predicted hyperfine value for Y <sub>3</sub> @C <sub>82</sub> using a plot of $\log k'$ versus hyperfine coupling constant.....	132

## LIST OF TABLES

Table 4.1	Summary of Sc <sub>m</sub> @C <sub>2n</sub> fractions obtained from the Buckyclutcher column.....	61
Table 4.2	Composition of Sc <sub>m</sub> @C <sub>2n</sub> fraction (#2 Buckyclutcher series) from PBB chromatographic column.....	98
Table 4.3	Composition of Sc <sub>m</sub> @C <sub>2n</sub> fraction (#3 Buckyclutcher series) from PBB chromatographic column.....	99
Table 4.4	Composition of Sc <sub>m</sub> @C <sub>2n</sub> fraction (#4 Buckyclutcher series) from PBB chromatographic column.....	100
Table 4.5	Composition of Sc <sub>m</sub> @C <sub>2n</sub> fraction (#5 Buckyclutcher series) from PBB chromatographic column.....	101
Appx. I	Empty-cage C <sub>2n</sub> mass (table).....	166
Appx. II	Sc <sub>m</sub> @C <sub>2n</sub> mass (table).....	167
Appx. III	Y <sub>m</sub> @C <sub>2n</sub> mass (table).....	168
Appx. IV	La <sub>m</sub> @C <sub>2n</sub> mass (table).....	169
Appx. V	Er <sub>m</sub> @C <sub>2n</sub> mass (table).....	170

## CHAPTER 1: INTRODUCTION

### 1.1 Metallofullerenes

Historically, graphite and diamond were the only known allotropes of carbon. Recently, however, a third form of carbon has been discovered.<sup>1</sup> Specifically, the fullerenes<sup>1-133</sup> ( $C_{2n}$ ,  $n \geq 30$ ) consist of fused, five- and six-membered rings in an all-carbon framework to form a class of hollow spherical/ovoid species. Following their discovery, numerous experiments exploring the reactivity<sup>91-112</sup> and characterization<sup>33-37,113-133</sup> (e.g. EPR<sup>113-129</sup>, NMR<sup>33-37,130-133</sup>) of fullerenes quickly ensued. The structures of several purified fullerenes (e.g.  $C_{60}$ ,  $C_{70}$ ) have only recently been elucidated.<sup>33-37</sup>

The encapsulation of a metal atom(s) inside these vacant empty-cage fullerenes has produced an intriguing class of compounds<sup>134-211</sup> whose chemical and structural properties remain uncertain. These metallofullerenes<sup>134-211</sup> ( $A_m@C_{2n}$ ;  $A=Sc, Y, La$ ;  $m=1-3$ ;  $n=30-60$ ) are of interest due to their predicted applications as superconductors,<sup>160</sup> catalysts,<sup>175</sup> non-linear optical devices,<sup>175</sup> and in biological systems.<sup>2-4</sup>

However, their successful isolation and characterization were initially unsuccessful due to their low abundance<sup>134,144-146,155,162</sup> (<1% of raw extract) and

uncertain stability in aerobic environments.<sup>137,174</sup> Efforts to separate these  $A_m@C_{2n}$  species from empty-cage fullerenes have focused primarily on chromatographic methods. Production from the usual electric arc-burning synthesis yields at least 30 to 50 distinct  $A_m@C_{2n}$  and fullerene species with unique variations in the number of carbons, the number of structural isomers, and the number of encapsulated metal atoms. For these reasons, one can readily envision the difficulty of developing a successful separation protocol which would be selective enough to yield a purified  $A_m@C_{2n}$  species starting from this complex mixture.

## 1.2 Detection

Since those  $A_m@C_{2n}$  species with an odd number of encapsulated atoms ( $m = 1, 3$ ) are "EPR active,"<sup>137,140,142,143,145-147,151,152,156,158,160,164,166,169,173,174,176,177,179,181,182</sup> the implementation of an on-line HPLC-EPR approach would permit selective monitoring of these compounds. Since conventional chromatographic detection (e.g. UV) is typically unable to distinguish between  $A_m@C_{2n}$  and empty-cage fullerenes, the necessity for more selective detection would be beneficial. This becomes especially important as chromatographic conditions and selection of stationary phases are optimized. With an on-line EPR approach, the eluting metallofullerenes can be

separated in a controlled anaerobic environment, and any air-sensitive  $A_m@C_{2n}$  compounds would not be compromised. Furthermore, accurate chromatographic retention times for these EPR active metallofullerenes can be readily established by observation of the on-line HPLC-EPR spectra as a function of time.

This ability to continually monitor EPR active metallofullerene species has permitted the development of successful purification methodologies in our laboratory. Briefly, the EPR active metallofullerenes,  $Sc@C_{82}$ ,  $Sc_3@C_{82}$ ,  $Y@C_{82}$ , and  $La@C_{82}$ , have been selectively monitored with on-line HPLC-EPR detection<sup>174</sup> for an initial separation of the metallofullerene fraction from the abundant empty-cage fullerenes utilizing a combination of polystyrene columns. This preparative "clean-up" procedure has been followed by HPLC-EPR detection of these species employing a more selective column [e.g.  $\pi$ -acidic stationary phase<sup>5</sup> (Buckyclutcher)] for their final stages of purification. With this methodology, the concomitant isolation of both empty-cage fullerenes and diamagnetic metallofullerenes (e.g.  $Sc_2@C_{2n}$ ) has also been achieved in this research.

### 1.3 Research Problem

When this research began, the field of metallofullerene science was in its early

stages. There was no methodology to obtain isolated metallofullerene samples. Instead, there was a complex and intimidating mixture of at least 30 to 50 unique fullerene and metallofullerene species in a typical initial raw extract. There were no columns available that were manufactured specifically for fullerene separations. In fact, it was debatable whether or not chromatographic methods could succeed at all in providing purified metallofullerene samples. It was already difficult to obtain milligram quantities of the empty-cage  $C_{60}$  and  $C_{70}$  fullerenes, which were highly abundant species (>90%) in the raw extract.

#### 1.4 Research Objectives

The primary objective of this research was to develop a methodology to obtain a purified metallofullerene sample(s). Since it was an arbitrary decision regarding which metallofullerene to isolate, the initial decisions focused on the paramagnetic  $A_m@C_{2n}$  species. The logic being that an on-line EPR approach would be selective for only one or two compounds whereas the majority of species ( $C_{2n}$  and  $A_2@C_{2n}$  - diamagnetic) present in the initial raw extract would not be detected. Since the HPLC-EPR approach had not yet been extended toward metallofullerene separations, a secondary objective was to demonstrate its feasibility and potential impact on



metallofullerene separations. In this regard, the HPLC-EPR approach would later become invaluable in developing a successful purification methodology.

## CHAPTER 2: HISTORICAL BACKGROUND

### 2.1 Empty-cage Fullerenes (C<sub>2n</sub>)

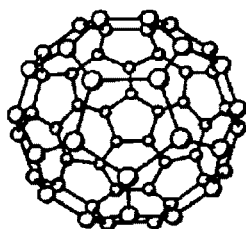
#### 2.11 Discovery

Named after Buckminster Fuller (famous architect of the geodesic dome), the presence of empty-cage fullerenes was first proposed in 1985 by Kroto et al.<sup>1</sup> According to landmark mass spectral data,<sup>1</sup> a series of peaks separated by 24 mass units was obtained. A striking feature of this mass spectrum was a dominant peak at  $m/z = 720$  that was noticeably more intense relative to other surrounding peaks. An assignment to a highly symmetrical icosahedral empty-cage C<sub>60</sub> species was made, and the field of fullerene science was born. At this stage, however, production of the fullerene species was limited to the microgram to nanogram level.

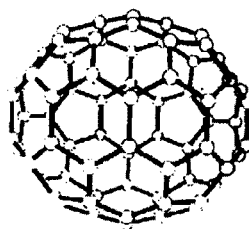
It was not until 1990 that Krätschmer et al.<sup>6</sup> developed a method to produce fullerenes in *macroscopic* quantities. In this procedure, graphite rods were "burned" in an electric-arc synthesis.<sup>6</sup> Although some of the resulting soot was insoluble material, a significant portion of the extract contained C<sub>60</sub>, C<sub>70</sub>, C<sub>84</sub>, etc. in milligram quantities.

## 2.12 Structure

The structure for any of the fullerenes was not elucidated until the early 1990's. In general, the fullerenes<sup>1-133</sup> consist of fused five- and six-membered rings in a hollow spherical/ovoid all-carbon framework as demonstrated below.



**C<sub>60</sub>**



**C<sub>70</sub>**

According to the "isolated pentagon rule",<sup>212-214</sup> two pentagon rings can not be located adjacent to each other. Instead, pentagons are bordered by hexagon rings to preserve this isolated pentagon rule. Using this rule, one of the smallest possible structures that can be formed is the C<sub>60</sub> fullerene. This species was predicted to possess a truncated icosohedral symmetry. If this highly symmetrical assignment was correct,

then its  $^{13}\text{C}$  NMR spectrum would be predicted to have only one signal - despite having sixty carbon atoms in its structure.

### 2.13 Chromatography and Isolation

The initial attempts to obtain purified fullerene samples have focused on chromatographic methods.<sup>33-36</sup> In 1990, Taylor<sup>33</sup> and Ajie<sup>34</sup> successfully isolated  $\text{C}_{60}$  by alumina chromatography. Since obtaining macroscopic amounts (mg level) of  $\text{C}_{60}$  was difficult in these early stages of development, it was fortunate that only one NMR signal was predicted. Had there been 20 to 60 expected signals, this early NMR experiment likely would have failed at this time. Nevertheless, in 1990 Taylor,<sup>33</sup> Johnson,<sup>34a</sup> and Ajie<sup>34b</sup> successfully obtained a  $^{13}\text{C}$  NMR spectrum for  $\text{C}_{60}$ . Experimentally, the spectrum contained only one signal (142.68 ppm) and was consistent with earlier theoretical predictions. With these data, the highly symmetrical icosahedral structure was confirmed. Few molecules are known to possess this unusual type of symmetry.

Other empty-cage fullerenes have subsequently been isolated.<sup>33,34</sup> The  $\text{C}_{70}$  species was also chromatographically isolated in 1990 by Taylor<sup>33</sup> and Ajie.<sup>34</sup> Subsequent  $^{13}\text{C}$  NMR characterization revealed that  $\text{C}_{70}$  possessed five distinct signals corresponding

to a  $D_{5h}$  cage symmetry. Shortly thereafter, the empty-cage  $C_{76}$  species ( $D_2$  symmetry) was isolated and characterized.<sup>7,8</sup>

Early isolation and NMR studies<sup>7,8,11,12</sup> on  $C_{78}$  and higher mass fullerenes have been (and still are to some extent) hampered due to the existence of structural isomers of various cage symmetries. For example, the  $C_{78}$  fullerene actually possesses two isomers of  $C_{2v}$  and  $D_3$  symmetries.<sup>8,14</sup> Each of these cage symmetries would correspond to different NMR spectra. Typically, the smaller cage sizes possess a higher symmetry and fewer NMR lines. However, purified  $C_{78}$  samples had to be obtained before any NMR characterization could be performed. Chromatographically, finding a stationary phase that was selective enough to distinguish between these two  $C_{78}$  isomers would be extremely difficult. Nevertheless in 1991, Diederich et al.<sup>8</sup> successfully isolated these two  $C_{78}$  isomers. Subsequent  $^{13}C$  NMR data confirmed the previously theoretical symmetries - ( $D_3$ ; 13 lines) and ( $C_{2v}$ ; 21 lines).

For the fullerene species (e.g.  $C_{60}$ ,  $C_{70}$ ,  $C_{76}$ ,  $C_{78}$ ,  $C_{84}$  etc.), increasing the number of carbon atoms in the outer-cage generally results in decreasing the symmetry of the molecule. This often results in multiple structural isomers. This feature results in NMR spectra which can easily consist of 30 to 84 lines per structural isomer. With NMR samples of multiple isomers, the spectra often become more complex. In

addition, the number of expected NMR lines is directly proportional to the amount of sample that is necessary. Thus, higher mass empty-cage fullerenes of lower symmetry ( $C_{82}$  -  $C_{110}$ ) would require at least an order of magnitude more sample relative to  $C_{60}$ . Due to the unavailability of columns with sufficient resolving power, it is extremely difficult to obtain purified samples of individual cage symmetries for the  $C_{82}$  -  $C_{110}$  empty-cage fullerenes. For example, the empty-cage  $C_{82}$  fullerene is believed to possess at least three different structural isomers.<sup>12</sup> Although a  $C_{82}$  fraction has been isolated,<sup>12</sup> the resulting  $^{13}\text{C}$  NMR spectrum actually represents a composite mixture of these individual isomers co-added together in one NMR spectrum. Predicted  $C_{82}$  cage symmetries are  $C_2$ ,  $C_{2v}$ , and  $C_{3v}$ .<sup>12</sup> Ideally, one would like to have three sample vials - one for each  $C_{82}$  cage symmetry. However, a primary difficulty is finding a stationary phase with adequate selectivity to separate a  $C_{82}$  mixture into their three structural isomers. Since it is already difficult to locate a stationary phase that can resolve differences between structures consisting of similar size carbon cages (e.g.  $C_{86}$ ,  $C_{88}$ ), one can readily envision the challenge of separating multiple isomers of the same mass (e.g.  $C_{82}$ ).

## 2.2 Metallofullerenes ( $A_m@C_{2n}$ )

### 2.21 Discovery

As early as 1985, it was suggested<sup>1</sup> that metal atom(s) could be "trapped" or encapsulated inside these hollow empty-cage fullerenes. Shortly thereafter, confirmation of this notion was supported by mass spectral evidence. In 1985, Heath et al.<sup>215</sup> laser-vaporized a lanthanum-impregnated graphite rod and produced an extract containing lanthanum encapsulated fullerenes. As a result, a global scientific interest in the field of metallofullerene science rapidly ensued.

### 2.22 Nomenclature

The nomenclature presently adopted for the metallofullerenes is denoted by  $A_m@C_{2n}$ , where "A" represents which metal (e.g. Sc, Y, La, etc) is present. The lower-case "m" indicates the number of metal atoms "trapped" inside the empty-cage structures. The "@" symbol<sup>216</sup> denotes the position of the metal relative to the empty-cage surroundings. Specifically, the "@" symbol indicates that the metal is inside (endohedral) and encapsulated by the fullerene cage. In contrast, the absence of the

"@" symbol would represent a metal located outside (exohedral) of the fullerene cage. Finally, the "2n" term represents the number of carbon atoms in the fullerene cage network. For example, a case where  $n = 30$  would be  $C_{60}$  (i.e. a cage with sixty carbon atoms). The numerical two in the "2n" term originates from the fact that only empty-cage fullerenes with an even carbon number (e.g.  $C_{90}$ ,  $C_{92}$ ,  $C_{94}$ , etc) are produced. Odd-numbered empty-cage species (e.g.  $C_{91}$ ,  $C_{93}$ ,  $C_{95}$ , etc) are not formed in the production process.

### 2.23 Applications

The presence of a metal(s) "trapped" inside of empty-cage fullerenes has generated considerable interest in the scientific community. Numerous properties and characteristics of this new class of compounds have been predicted.<sup>160,175</sup> Because several exohedral metallofullerenes<sup>217-242</sup> (e.g.  $K_3C_{60}$  - metal outside the fullerene cage) were proven to be superconducting,<sup>231-242</sup> it was believed that endohedral metallofullerenes could be superconducting as well.

Recent applications of empty-cage fullerenes have been in the pharmaceutical area.<sup>2-4</sup> Specifically, derivatized empty-cage fullerenes<sup>2-4</sup> have recently exhibited some activity against the AIDS virus. There are potentially other areas of biological



applications. The possibility of encapsulating radioactive species inside of fullerene cages could have a significant impact in cancer research. Metallofullerenes have also been predicted to be useful as possible non-linear optical devices.<sup>175</sup> It has also been suggested that metallofullerenes could be used as novel catalysts.<sup>175</sup>

## 2.24 Chromatographic Overview

Although first produced in nanogram quantities in 1985,<sup>215</sup> it was not until 1990<sup>6</sup> that a methodology to produce a metallofullerene extract in macroscopic amounts (mg) was developed. Research efforts to obtain purified metallofullerenes samples quickly ensued on the global level. Although some research groups had attempted non-chromatographic techniques (e.g. sublimation),<sup>163</sup> the majority of initial purification efforts involved liquid chromatographic methods.<sup>33-37,134,135,243-251</sup> This was not surprising since some foundational work had only recently been performed with the empty-cage separations<sup>33-37,134,135</sup> discussed *vide supra*. Note that at this time, chemists had just chromatographically isolated C<sub>60</sub> and C<sub>70</sub>.<sup>2,3</sup> Thus, there was some recently acquired experience regarding which type of column and mobile phase would produce the most favorable results.

In this regard, it was not surprising that initial efforts to obtain purified

metallofullerenes paralleled the earlier chromatographic methods which had permitted isolation of  $C_{60}$  and  $C_{70}$ . However, it was later realized that certain types of columns and mobile phases which achieved favorable results with empty-cage species were not necessarily the best choice for metallofullerene separations. For example, reversed-phase chromatography<sup>27</sup> readily separated the empty-cage fullerenes with excellent separation factors. However, the amount of sample that could be injected into reversed-phase columns was unsatisfactory. This poor sample throughput was due to the low solubility of fullerene material in reverse-phase type mobile phases (e.g. acetonitrile, water, etc). Even with toluene/acetonitrile mixtures of solvents, the amount of sample loadability was still inadequate for initial, preparative separations. Since the metallofullerenes are typically present at only <1% abundance in their stock,<sup>134,144-146,155,162</sup> reverse-phase<sup>27</sup> methods were not suited for the large sample throughput which was necessary for these initial, preparative clean-up procedures. In addition, there was evidence that certain metallofullerenes would either decompose or never elute from reverse-phase columns.

To achieve improved sample throughput, the metallofullerenes needed to be sufficiently soluble in the mobile phase. At this time, it was suggested that metallofullerene samples should be dissolved in normal-phase type solvents (e.g. aromatic hydrocarbons). However, traditional octadecyl ( $C_{18}$ ) normal-phase columns

with these solvents permitted little or no resolution. Injected fullerene material eluted as an unresolved bolus demonstrating a poor separation.

### 2.25 Polystyrene Separations

In June of 1993, it was believed that polystyrene separations might be successful. With polystyrene columns, it would still be possible to use solvents with a high solubility for fullerenes (carbon disulfide, toluene/decalin) with the widely available pore sizes of polystyrene columns. It was hoped that a successful separation would result based on a size-exclusion mechanism. In principle, it was an ideal response to the problem of solvent selection and resolving power of the stationary phase. With the polystyrene system, it would be possible to achieve high sample loadability since the fullerenes were very soluble in this mobile phase. Since the separating mechanism was predicted to be based on size exclusion, there were high expectations for success with polystyrene separations. Various manufacturers even began shifting sales efforts toward polystyrene columns for fullerene separations.

However, the actual experimental data were conflicting. Depending on the type of column and mobile phase, some research groups<sup>168,169</sup> did achieve a size-exclusion based polystyrene separation (i.e. C<sub>84</sub>, C<sub>70</sub>, then C<sub>60</sub>). Yet others achieved an

absorption-type separation<sup>32,173,174,246</sup> (i.e. elution of C<sub>60</sub>, C<sub>70</sub>, then C<sub>84</sub>). In these experiments, it was proposed that a weak  $\pi$ - $\pi$  interaction between the metallofullerene and polystyrene substrate was the dominant separation mechanism. Nevertheless, the polystyrene did permit a much higher sample throughput relative to reverse-phase separations. Because the separation factors were often poor with polystyrene columns, several "recovery and re-injection" steps were often necessary to obtain a metallofullerene-containing fraction. In fact, some polystyrene-based separations (manufacturers' brochures) were so poor that four or more columns had to be connected in series to achieve sufficient resolution for fraction collection. To improve the separation and avoid backpressure problems, low flow rates were often utilized. Under these conditions, some separations required over 10 hours for an injected sample to elute. Some common stationary phases utilized in fullerene and metallofullerene separations are presented in Figure 2.1.

### 2.26 Buckyclutcher Separations

Fortunately, a much more selective column became commercially available. Developed by Pirkle and Welch,<sup>5</sup> this silica gel-based stationary phase consisted of tripodal, tridentate di-nitrophenyl ligands capable of strong  $\pi$ - $\pi$  complexation

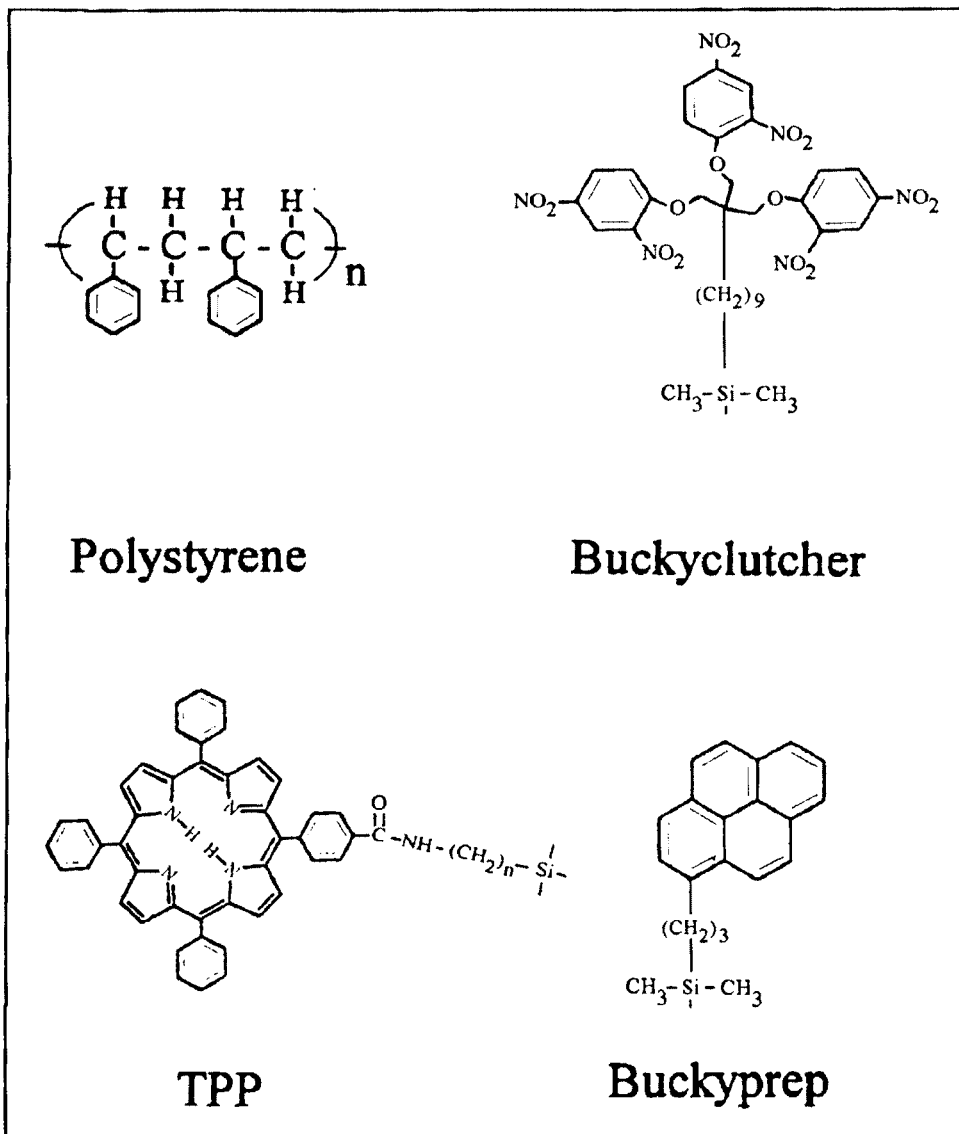


Figure 2.1 Summary of the four most common stationary phases in metallofullerene separations.

interactions with the metallofullerenes. With such a strong retention mechanism, the use of solvents with a high solubility for fullerenes could now be incorporated without sacrificing resolution. This feature permitted even larger sample throughput for preparative clean-up injections of initial raw extract. In addition, the improved selectivity later permitted the first isolation of purified metallofullerene samples.

### 2.27 TPP Separations

Other types of silica-gel based columns have now become commercially available. Historically, the silica-based tetraphenyl-porphyrin (TPP) based stationary phase had previously been utilized in the separation of aromatic compounds.<sup>252</sup> Shortly thereafter, this type of column was successfully extended for use in both fullerene separations<sup>248</sup> and metallofullerene separations.<sup>178,184</sup> For example, Savina et al.<sup>184</sup> utilized a binary solvent system (toluene/CS<sub>2</sub>) with this TPP column to obtain a purified La@C<sub>82</sub> sample.<sup>184</sup>

### 2.28 Buckyprep Separations

Recently, another highly selective silica gel-based column has been utilized in

metallofullerene separations. Historically, the pyrenyl-ethyl (PYE) based stationary phase had been utilized in the separation of aromatic compounds.<sup>254,255</sup> For this reason, the PYE column was also extended for use in fullerene and metallofullerene separations.<sup>182,187,188,190,191</sup> Similar to the Buckyclutcher, the pyrenyl-ethyl based column (PYE or "Buckyprep")<sup>182,187,188,190,191</sup> offers high selectivity, reduced solvent consumption, high sample loadability, and rapid separations. This is accomplished through a retention mechanism thought to consist of a combination of steric, dipolar, and  $\pi$ -electron interactions. This electron-accepting stationary phase also has the flexibility to be utilized for initial preparative clean-up procedures or in the final purification stages. Buckyprep columns have now been utilized in the isolation of  $\text{Sc}_3@\text{C}_{82}$ ,  $\text{La}@\text{C}_{82}$ ,  $\text{Gd}@\text{C}_{82}$ , and  $\text{Pr}@\text{C}_{82}$ .<sup>182,187,188,190,191</sup>

## 2.29 Isolation

To date, several research groups<sup>168-172,174-178,182-188,190,191</sup> have now obtained purified metallofullerene samples. The methodology has typically involved two types of chromatographic columns. These "two-stage" systems have involved a combination of any two of the previously mentioned columns. For example, an initial preparative clean-up step to remove empty-cage fullerenes will typically result in a

metallofullerene-containing fraction. However, this sample will often be contaminated with low levels of at least one co-eluting empty-cage fullerene. Through injection with a second type of column (e.g. Buckyclutcher), these contaminants will no longer co-elute with the desired metallofullerene. In this manner, a purified metallofullerene can often be obtained.

The development of purification methodologies for the metallofullerenes has resulted from a global scientific effort. Early pioneers in the chromatographic separation of metallofullerenes were headed by Shinohara,<sup>168,180,186,187</sup> Dorn,<sup>172-178</sup> and Kikuchi.<sup>169-171,183,185</sup> In summary, Shinohara et al.<sup>168,180,187</sup> have isolated Sc<sub>2</sub>@C<sub>74</sub>, Sc<sub>2</sub>@C<sub>84</sub>, Sc<sub>3</sub>@C<sub>82</sub>, Pr@C<sub>82</sub>. Dorn et al.<sup>172-178</sup> have isolated Sc<sub>2</sub>@C<sub>74</sub>, Sc<sub>2</sub>@C<sub>84</sub> (two isomers), Sc<sub>3</sub>@C<sub>82</sub>, La<sub>2</sub>@C<sub>72</sub>, Er@C<sub>82</sub>, Er<sub>2</sub>@C<sub>82</sub> (two isomers), and Er<sub>2</sub>@C<sub>92</sub>. Kikuchi et al.<sup>169,170,183</sup> have isolated La@C<sub>82</sub> and La<sub>2</sub>@C<sub>80</sub>. Yamamoto et al.<sup>188,190,191</sup> have obtained purified La@C<sub>82</sub>. Meyerhoff et al.<sup>184</sup> have also isolated La@C<sub>82</sub>. With all these different purification methodologies now published and available, other scientists should now be able to obtain even larger amounts of purified metallofullerene samples. Now that the pioneering research on metallofullerene separations has been performed, the next few years will likely represent a new era in the field of metallofullerene science. Namely, a plethora of long-awaited characterization experiments will be performed to discover what properties these new,



exciting molecules will exhibit.

## 2.3 HPLC-EPR

### 2.31 Historical

Historically, the monitoring of paramagnetic species as they are eluted from a chromatographic column has existed since 1975.<sup>256</sup> In a landmark paper, the on-line HPLC-EPR approach was demonstrated by Rokushika et al<sup>256</sup> with the separation of stable organic radicals. Since then, the HPLC-EPR approach has been utilized in the separation of metal complexes,<sup>257-260</sup> spin adducts,<sup>261-271</sup> and spin-trapped<sup>272-295</sup> species.

However, the HPLC-EPR technique had not been applied to the area of metallofullerenes. Therefore, a secondary objective of this research focused on utilizing HPLC-EPR as a technique to assist in the development of a separation methodology which would result in purified metallofullerene samples.

### 2.32 Advantages

There are several distinct advantages for selecting an on-line EPR approach versus

conventional UV detection alone. The primary advantage of on-line EPR detection of metallofullerene separations is the high specificity for metallofullerenes with an odd number of encapsulated metal atoms. Specifically, recent experiments<sup>137,140,142,143,145-147,151,152,156,158,160,164,166,169,173,174,176,177,179,181,182</sup> have demonstrated Sc@C<sub>82</sub>, Sc<sub>3</sub>@C<sub>82</sub>, Y@C<sub>82</sub>, and La@C<sub>82</sub> to be EPR active. As an example, a typical scandium raw extract represents a complex mixture of at least 30 empty-cage fullerenes as well as ~20 Sc<sub>m</sub>@C<sub>2n</sub> metallofullerene species differing in the number of encapsulated metal atoms, the number of structural isomers, and the number of carbons in the surrounding cage network. Experimentally, the empty-cage fullerenes and di-scandium species (Sc<sub>2</sub>@C<sub>2n</sub>) are essentially diamagnetic and therefore EPR silent. In contrast, the mono-metal Sc@C<sub>82</sub> and tri-metal Sc<sub>3</sub>@C<sub>82</sub> species are paramagnetic and EPR active. Therefore, the striking feature is that only two of the ~50 species in the initial raw extract would exhibit significant EPR activity. This represents a distinct advantage of on-line EPR detection. With this approach, it is possible to monitor a single metallofullerene species in the midst of an overwhelming abundance of all other fullerene and metallofullerene compounds. As chromatographic conditions (e.g. mobile phase, stationary phase, flow, etc.) are optimized, it is possible with on-line EPR detection to monitor the effect of these changes on a given separation. Since this is accomplished on-line, the extra time

involved in fraction collection, sample handling, and off-line characterization procedures can be avoided.

There are other advantages to the HPLC-EPR approach. With on-line EPR detection, accurate retention times for EPR active metallofullerenes can be conveniently determined without resorting to off-line techniques. Since the on-line technique is non-invasive, the recovery of valuable metallofullerene samples and coupling to other HPLC detectors is straightforward. Since the on-line EPR approach monitors the eluting metallofullerene species in a controlled *anaerobic environment*, the potential decomposition of air-sensitive metallofullerenes is not compromised, (Previous reports have demonstrated that some metallofullerene species are susceptible to decomposition upon exposure to air).<sup>137,134</sup>

### 2.33 Disadvantages

There are disadvantages to the on-line HPLC-EPR technique. Since the majority of species are diamagnetic, on-line EPR detection is not possible. Thus, on-line EPR experiments involving di-metal species ( $A_2@C_{2n}$ ) and empty-cage ( $C_{2n}$ ) fullerenes would not be useful. Another consideration is the sensitivity of the flow EPR experiment. In a typical  $A_m@C_{2n}$  stock solution, the concentration of paramagnetic

species in the EPR flow cell is estimated at only  $10^{-5}$  to  $10^{-6}$  M.

In addition, the extra "lag time" between the conventional UV detector and EPR flow cell must be accurately measured. This step is crucial in correlating EPR activity with a corresponding peak on the UV-generated chromatogram. For optimal fraction collection, the additional time from the EPR flow cell (detection) and the outlet must also be accurately determined for optimal fraction collection. In addition, band broadening occurs with the extra void volume originating from the on-line EPR flow cell and connecting tubing.

#### 2.4 Goal and Justification

At the time this research began, there was no protocol available for obtaining purified metallofullerene samples. Thus, our primary goal was to develop a chromatographic methodology which would permit purified metallofullerenes. Since these molecules were predicted to have many unique applications (see Introduction), there was a high demand for purified samples so that characterization experiments could be performed. In this regard, this research addresses and fulfills this need for obtaining purified metallofullerene samples.

## CHAPTER 3: EXPERIMENTAL

### 3.1 Metallofullerene Samples

#### 3.11 Production

All metallofullerene samples were produced by IBM and provided to our lab with the intent of developing a suitable chromatographic methodology for their isolation. Scandium, yttrium, lanthanum, and erbium metallofullerene-containing soot was produced in a JS-2000 fullerene generator under a He atmosphere. This electric-arc synthesis was similar to the Krätschmer-Huffman method.<sup>6</sup> Specifically, cored-carbon rods were impregnated with mixtures of graphite and either pure metal, metal oxide, or metal carbide. Previous experiments<sup>172,176,178</sup> suggested that the form in which the metal is introduced does not drastically affect the yield and product distribution. It should be noted that the ratio of metal to carbon atoms in these initial rods affects the amount of mono-, di-, and tri-metallofullerene species.<sup>172,176,178</sup> For example, a lower ratio of Sc metal to carbon atoms (1% Sc) will result in an improved yield of Sc@C<sub>82</sub> relative to Sc<sub>3</sub>@C<sub>82</sub>. In contrast, a higher ratio (3-5% Sc) will generate more Sc<sub>3</sub>@C<sub>82</sub> and reduced quantities of Sc@C<sub>82</sub>. Typical production

experiments yield only ~1%<sup>134,144-146,155,162</sup> metallofullerenes with the empty-cage fullerenes (~99%) dominating the soluble product distribution. The empty-cage C<sub>60</sub> is the dominant species followed by C<sub>70</sub> and C<sub>84</sub>.

### 3.12 Extraction

Once these cored rods are "burned", the resulting metallofullerene-containing soot must be extracted. This extraction step is critical since the choice of solvent and extraction methods dictate the amount of empty-cage and metallofullerene material that will be obtained from the soot. Empty-cage fullerenes are virtually insoluble in hexane, pentane, cyclohexane, acetonitrile, and water.<sup>29</sup> Solubility increases with solvents such as benzene, toluene, and decalin. Even higher solubilities are achieved with ortho-dichlorobenzene,  $\alpha$ -chloronaphthalene, and CS<sub>2</sub>. A detailed solubility study of the empty-cage C<sub>60</sub> fullerene has recently been published.<sup>29</sup> Although it is believed that the metallofullerenes possess similar solubilities as the empty-cage species, there has not been a corresponding detailed study of purified *metallofullerene* solubilities.

In our laboratory, metallofullerene soot was located in thimbles and extracted through Soxhlet and/or static techniques. Although CS<sub>2</sub> was the primary choice of

solvent, ortho-dichlorobenzene and toluene have also been employed. Following extraction, the solvents were evaporated - leaving a solid, black powder which was then weighed. Prior to chromatography, this initial raw extract was filtered over a home-built bed of glass wool, sand, and silica gel. This step was useful in preventing any remaining insoluble soot from possibly clogging the chromatographic tubing and columns. With the 80:20 toluene/decalin solvent, approximately 3 mg/mL would dissolve into the solution. Thus, the solubility of metallofullerenes in this stock solution limited the amount of material that could be separated in the initial clean-up procedure.

### 3.13 Mobile Phase

A 80% toluene (Fischer) / 20% decalin (Aldrich Chemical Co.) mixture was selected as the mobile phase for polystyrene and Buckyclutcher column separations. The decision to incorporate decalin was based on a previous study<sup>27</sup> in which decalin resulted in shorter retention times for higher molecular weight fullerenes (e.g. C<sub>100</sub> - C<sub>130</sub>). In addition, it was suspected that the metallofullerenes also had increased solubilities in decalin. Meanwhile, carbon disulfide was employed as the mobile phase for experiments with the TPP and PBB columns. Regardless of which mobile

phase was employed, all solvents were degassed by either bubbling N<sub>2</sub> gas and/or sonication. Removing dissolved O<sub>2</sub> was essential for preventing decomposition of any air-sensitive metallofullerenes (e.g. Sc@C<sub>82</sub>). In addition, on-line EPR spectra can often be obtained with higher resolution and an increased signal-to-noise ratio if the solvent is adequately degassed.

### 3.14 Chromatographic Equipment

This research focused primarily on four types of columns. The polystyrene separating columns (cross-linked) were connected in series with a Perkin-Elmer, 25 cm x 10 mm PL gel, 10 μm, 1000 Å column followed by a 25 cm x 10 mm PL gel, 5 μm, 5000 Å column. Typical chromatographic conditions for separations using the polystyrene columns were 1 ml./min of 80:20 toluene/decalin (UV detection, 340 nm). In addition, a more selective Trident-Tri-DNP HPLC column ("Buckyclutcher", 25 cm x 10 mm i.d., 5 μm gel, 100 Å, Regis Chemical, Morton Grove, IL, 60053, 1-800-323-8144) permitted sufficient resolution of individual fullerene and metallofullerene species. For this reason, the Buckyclutcher column was often utilized in final purification separations. A third type of column employed was a tetraphenyl-porphyrin derivatized silica-gel column ("TPP-RP" stationary phase, 10



$\mu\text{m}$  gel, 300 Å pore size, Fullesep column, 4.6 x 100 mm, Anspec, Ann Arbor MI, 48107, 1-800-521-1720). A fourth type of chromatographic column ("PBB," Cosmosil packed, 10 mm x 25 cm, 5  $\mu\text{m}$  gel, Phenomenex, Torrance, CA, 90501, 1-310-212-0555) utilized pentabromobenzyl ligands immobilized onto silica gel. The columns packed with a smaller size silica gel (i.e. 5  $\mu\text{m}$  gel) typically offered improved resolution. All chromatographic experiments utilized a Hitachi L-4000 UV detector and D-2500 Chromato-Integrator recorder with flow rates  $\sim$ 1 mL/min. Typically, the 80:20 toluene/decalin solvent system was employed for all separations except for the PBB and TPP columns. These columns employed  $\text{CS}_2$  as the mobile phase.

## 3.2 Instrumentation

### 3.21 HPLC-EPR Apparatus

For on-line HPLC-EPR experiments, an IBM 200D-SRC EPR spectrometer was placed immediately after the UV detector in the chromatographic flow stream. A simplified diagram of the HPLC-EPR apparatus is illustrated in Figure 3.1. The selection of EPR operating parameters (e.g. attenuation, time constant, sweep time,

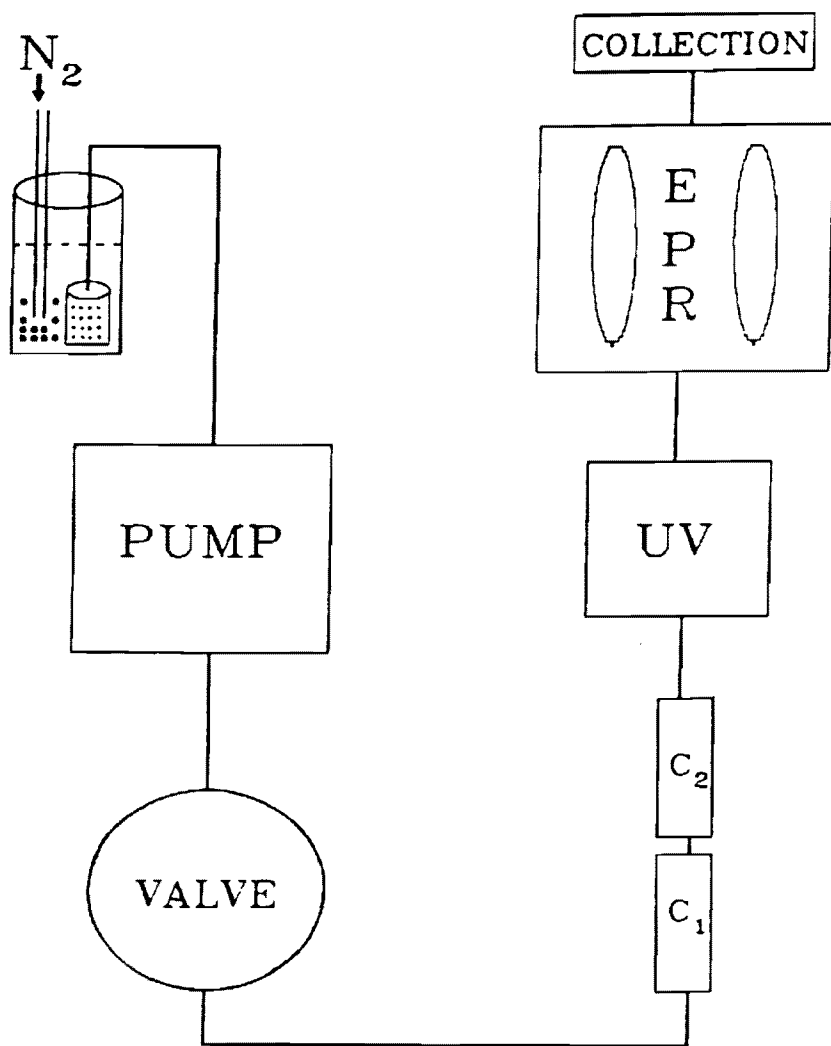


Figure 3.1 Block diagram of the on-line HPLC-EPR apparatus.  $C_1$  and  $C_2$  are the separating chromatographic columns.

gain, and modulation) were optimized for the flow experiment. Since the paramagnetic metallofullerenes were present in such low abundance (<0.05 % in the raw extract), resolution in the EPR spectra was sacrificed at the expense of obtaining an increased signal-to-noise ratio. Specific EPR conditions included a high modulation amplitude (1.0 - 1.5 gauss), high microwave power (~10 mW), and a rapid sweep of the magnetic field at a rate of 4 - 7 gauss per second. Under these conditions, an expected doublet with a small hyperfine coupling constant (0.4-0.9 g) would appear as a "broadened singlet." During the course of this research, Wilson et al<sup>195</sup> also attempted on-line EPR detection for a Y@C<sub>82</sub> sample. Using a fixed field and frequency (i.e. no EPR spectral resolution), they obtained EPR activity as a function of time.

Microwave irradiation was provided by a Bruker microwave bridge operating at 9.54 GHz. The detection volume of the home-built EPR glass flow cell was measured at 250  $\mu$ L. For on-line HPLC-EPR experiments, this flow cell was located in the front side of a dual TE<sub>102</sub> microwave cavity. PEEK tubing (0.010-in. i.d., Upchurch Sci.) connected chromatographic eluents to the EPR flow cell. For on-line experiments, 20 second magnetic field sweeps with a spectral window of 90 to 130 gauss were typical. An ASPECT 2000 computer permitted storage of subsequent on-line EPR spectra. Signal averaging of 2 to 4 scans/file provided "stacked plots" of

EPR spectra versus elution time. Each file corresponded to 1 - 3 minute segments of time.

### 3.21 Automated Apparatus

See Automated Section (Results and Discussion).

### 3.23 Mass Spectrometry

For off-line characterization of fractions, several different types of mass spectrometers were utilized. The majority of mass spectral data were obtained from a VG 7070E-HF mass spectrometer (VG Analytical, Manchester, UK). This apparatus could perform either positive-ion or negative-ion chemical ionization. Specifically, metallofullerene samples were injected onto a DCI probe filament. The current was ramped from 0 to 1 A at a rate of 0.05 A/sec to evaporate and desorb the sample. Methane was selected as the reagent gas.

Other spectra were obtained from a laser desorption-time of flight (LD-TOF) mass spectrometer located at IBM. In addition, fast atom bombardment (FAB) spectra have also been obtained from a VG Quattro mass spectrometer.

### 3.24 Two-Stage Chromatographic Systems

Separations involving only one type of column will not generally result in purified metallofullerene samples. This is due to the co-elution of the underlying, high-mass empty-cage fullerenes - which elute as a homologous series across the  $A_m@C_{2n}$  fractions. For these reasons, we have developed in this research several two-stage systems which have permitted purified metallofullerene samples.

#### 3.241 Polystyrene/Buckyclutcher System

Metallofullerene raw extracts (i.e.  $Sc_m@C_{2n}$ ,  $Y_m@C_{2n}$ , and  $La_m@C_{2n}$ ) were injected into the polystyrene columns as a first step to remove the dominant  $C_{60}$ - $C_{84}$  fullerenes. Due to the poor selectivity for these polystyrene columns, four to five "recovery and re-injection" steps of the  $A_m@C_{2n}$  fraction were necessary. This sample obtained from the polystyrene separations (now enriched in  $A_m@C_{2n}$ ) was further separated by the selective Buckyclutcher column into 10 to 15 additional peaks. Collection of these regions resulted in the isolation of individual metallofullerene samples with various levels of purity.

### 3.242 Buckyclutcher/TPP and Buckyclutcher/PBB Systems

Because five polystyrene re-injections were often necessary to remove the  $C_{60}$  -  $C_{84}$  fullerenes, this process became tedious and time-consuming. With increased sample loadability and improved selectivity, the Buckyclutcher column quickly replaced the polystyrene columns for the initial preparative injections. Raw metallofullerene extract was separated in an initial Buckyclutcher pass for removal of  $C_{60}$  -  $C_{84}$ . Re-injection into the Buckyclutcher column would permit 10 to 15 single homogeneous peaks. However, to remove the underlying  $C_{90}$  -  $C_{116}$  impurities, a second column (TPP or PBB column) was employed. These stationary phases would readily separate these higher-mass empty-cage contaminants from the metallofullerenes. In this manner, purified metallofullerene samples were obtained.

## CHAPTER 4: RESULTS AND DISCUSSION

### 4.1 Metallofullerene Separations

#### 4.11 Sc<sub>m</sub>@C<sub>2n</sub>

A stock solution (~3 mg/mL) containing Sc<sub>m</sub>@C<sub>2n</sub> and empty-cage fullerenes was prepared for injection into two polystyrene columns connected in series. The production of this metallofullerene sample was optimized for an improved yield of Sc<sub>3</sub>@C<sub>82</sub> relative to Sc@C<sub>82</sub>. With negligible quantities of Sc@C<sub>2n</sub>, only Sc<sub>3</sub>@C<sub>2n</sub> species would result in an EPR signal. The empty-cages and Sc<sub>2</sub>@C<sub>2n</sub> compounds are diamagnetic and therefore EPR-silent.

Figure 4.1 represents a typical chromatogram for an initial, clean-up injection with the polystyrene columns. At 15 milligrams of injected material, this chromatogram suggests the column is overloaded with no useful separation in the UV domain. However, on-line EPR spectra reveals that the "tailing region" of the chromatographic peak contains the paramagnetic Sc<sub>3</sub>@C<sub>82</sub>. The majority of the peak area (~90 %) consists of C<sub>60</sub>, C<sub>70</sub>, C<sub>84</sub>. Although a smaller injection would permit improved resolution, this large amount of injected sample represents a satisfactory compromise between resolution and sample throughput. Note that of the 22 lines expected (I =

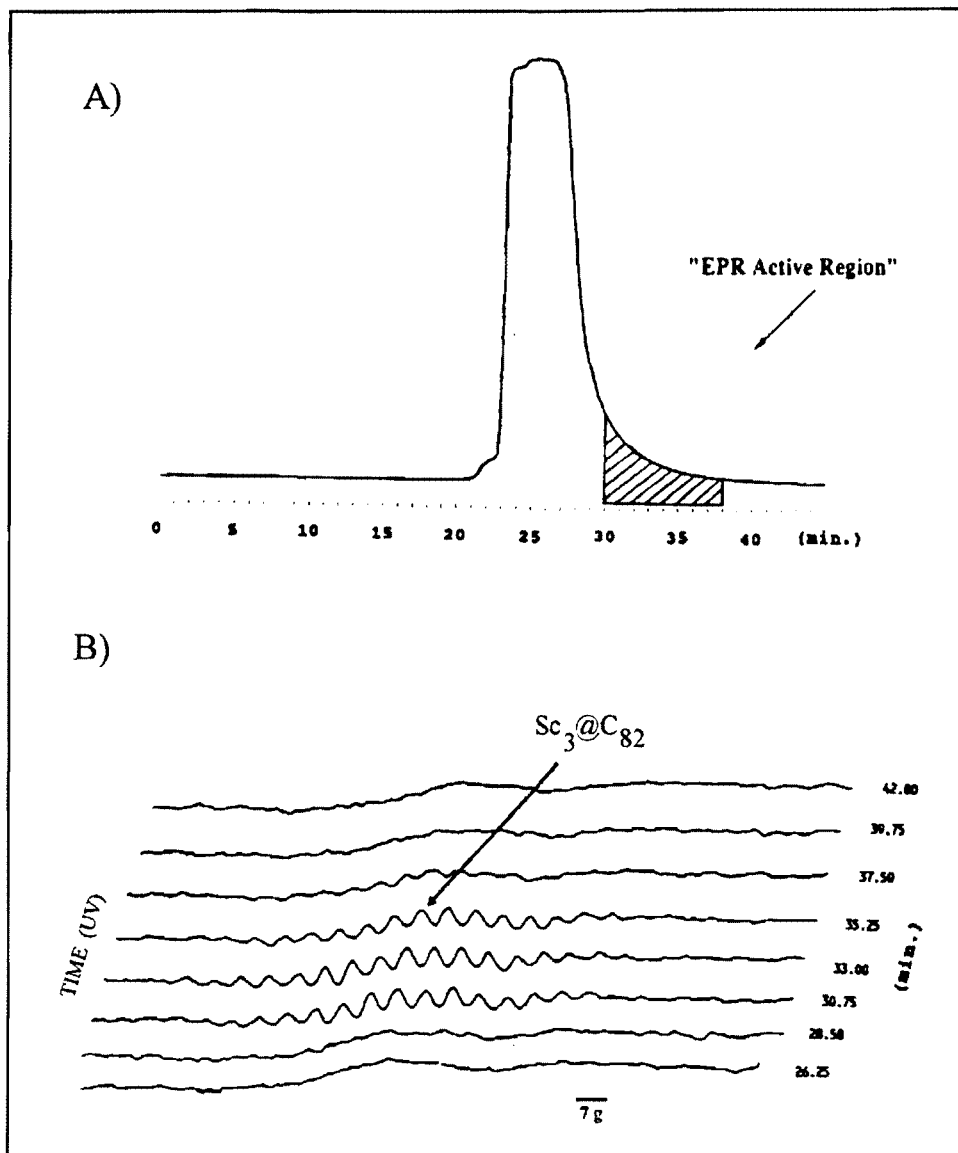


Figure 4.1 (a) Initial polystyrene pass of  $Sc_m@C_{2n}$  raw extract: HPLC-UV trace (340 nm), 5 mL injected (10-15 mg), 1.0 mL/min, and 80:20 toluene/decalin. (b) on-line HPLC-EPR profile, 9.55 GHz, 2.25 min/file, 4 scans/file, and 20 s/sweep.



7/2; 3 equivalent Sc nuclei) for  $\text{Sc}_3@C_{82}$ , only ~17 can be observed under these EPR conditions which were optimized for an improved signal-to-noise ratio (oversaturation; see Experimental).

A fraction corresponding to this EPR-active region was collected for subsequent, off-line mass spectral analysis. At this stage, the purity of this metallofullerene fraction was unknown. Although  $\text{Sc}_3@C_{82}$  was in this fraction, it was not known whether additional metallofullerenes and/or empty-cages contaminants were also present. To address these considerations, negative-ion mass spectral data were obtained. The results indicated that  $C_{60}$ ,  $C_{70}$ , and significant amounts of higher-mass empty-cages ( $C_{84}$ - $C_{120}$ ) were still present with the  $\text{Sc}_3@C_{82}$  and at least ten other  $\text{Sc}_2@C_{2n}$  species. Each re-injection of this EPR-active fraction into the polystyrene columns removed increasing quantities of the empty-cages  $C_{60}$ - $C_{92}$ . For this reason, a total of four re-injections of the EPR-active fraction was performed. The chromatograms of the 1<sup>st</sup>, 2<sup>nd</sup>, 3<sup>rd</sup>, and 4<sup>th</sup> polystyrene passes are presented in Figure 4.2. For the fifth and final polystyrene pass, the chromatogram and corresponding on-line EPR spectra are presented in Figure 4.3. Through retention time data, this chromatogram indicates that  $C_{60}$ ,  $C_{70}$ , and  $C_{84}$  have been removed from the EPR-active fraction. Furthermore, the ability of the HPLC-EPR technique to selectively "monitor" a metallofullerene from a starting stock to a final, collected fraction was

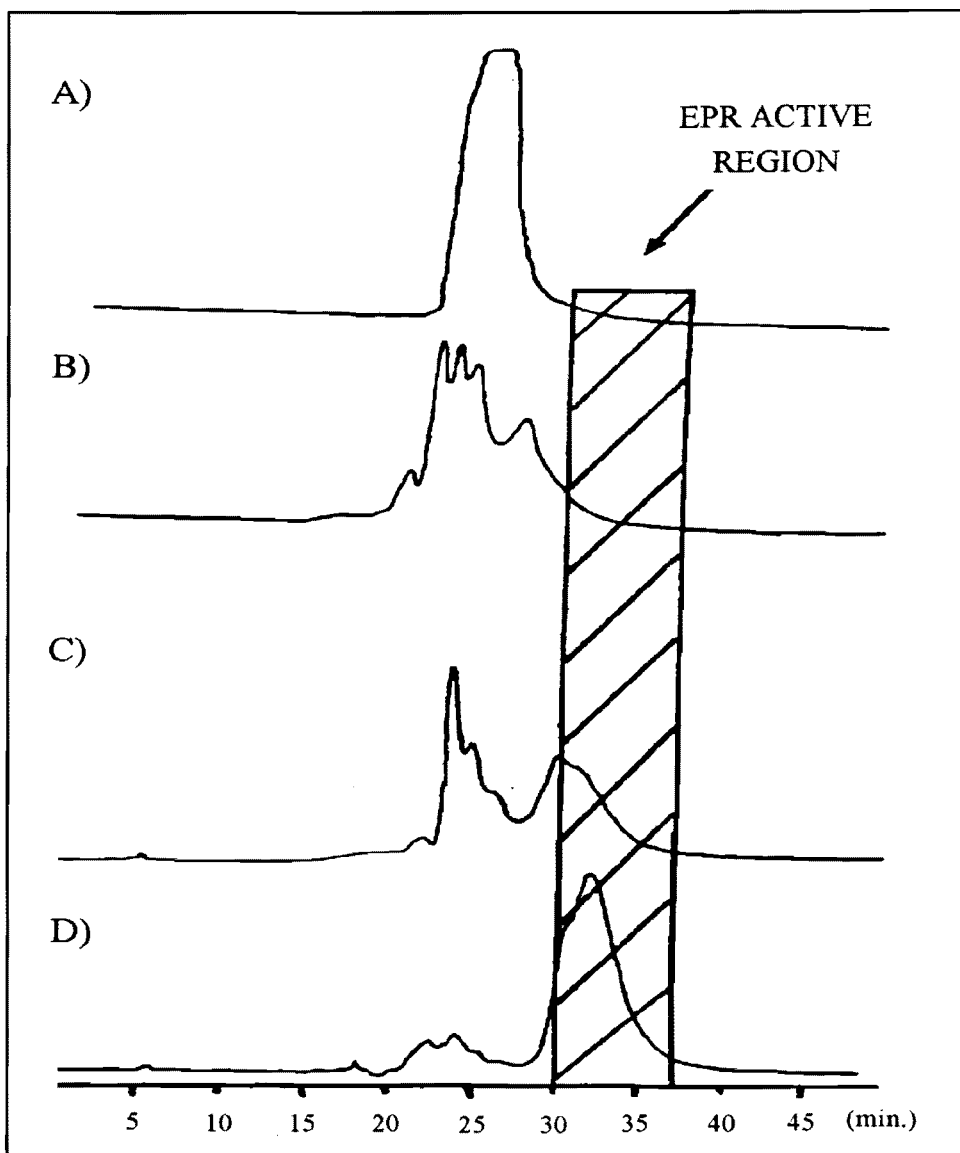


Figure 4.2 HPLC-UV trace for  $Sc_m@C_{2n}$  separations in which the EPR active fraction is recovered and re-injected. The first through fourth polystyrene passes are represented by (a) - (d), respectively. Flow rate 1 mL/min, UV 340 nm detection, and the EPR active fraction is denoted as the hatched region (30 - 37 min.).

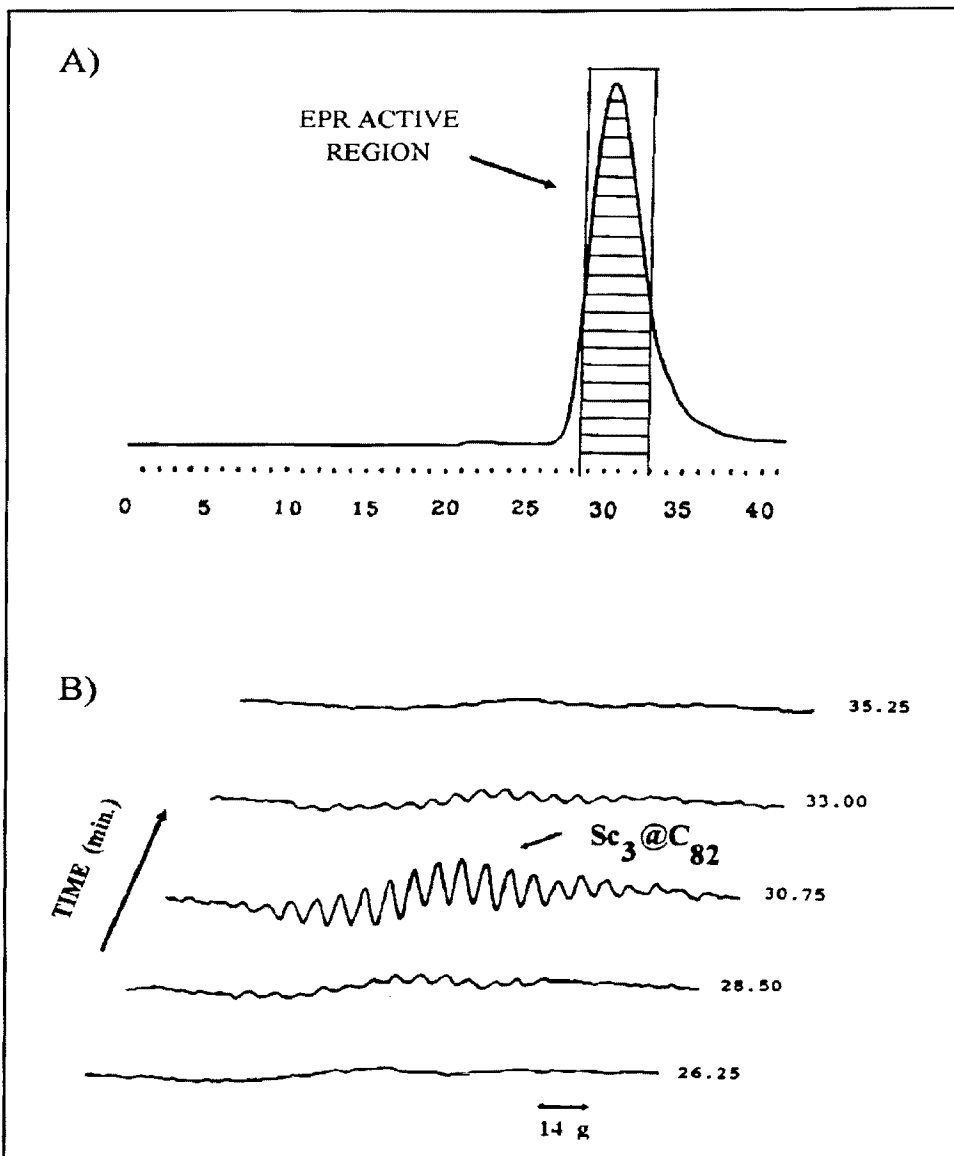


Figure 4.3 (a) HPLC-UV trace (340 nm) for the fifth polystyrene pass of the  $\text{Sc}_3@C_{82}$  EPR active fraction, 410  $\mu\text{L}$  injection, 1.0 mL/min, and 80:20 toluene/decalin. (b) On-line HPLC-EPR profile, 4 scans/file, 9.55 GHz, and 20 s/sweep.

demonstrated for the first time. Note the surprisingly large signal-to-noise ratio for the  $\text{Sc}_3@C_{82}$  fraction flowing through the small 250  $\mu\text{L}$  EPR flow cell.

Unfortunately, the composition of this final EPR-active fraction was not purified  $\text{Sc}_3@C_{82}$ . Instead, a metallofullerene-enriched sample had been obtained. Nevertheless, the composition of this fraction represented a "turning point" in developing the metallofullerene separation process since this sample contained virtually all metallofullerenes and negligible amounts of the higher-mass empty-cage fullerenes. For the first time, a methodology had been developed to remove  $C_{60}$ - $C_{92}$  from an initial extract and eventually obtain a mixture of metallofullerenes. The negative-ion mass spectrum of this final EPR-active fraction is shown in Figure 4.4.  $\text{Sc}@C_{82}$  is not observed since it was a low-abundant compound in the starting stock. A series of di-scandium  $\text{Sc}_2@C_{74}$  -  $\text{Sc}_2@C_{102}$  metallofullerenes is readily observed in the mass spectrum. The paramagnetic  $\text{Sc}_3@C_{82}$  ( $m/z = 1119$ ) species is also relatively abundant in this sample. Only small amounts of extremely high molecular weight empty-cage fullerenes contaminated the fraction. It should be noted that since all  $\text{Sc}_2@C_{2n}$  species had a similar retention time on the polystyrene columns relative to the EPR-active  $\text{Sc}_3@C_{82}$ , it was possible to obtain a sample that contained only metallofullerenes. Ironically, the poor selectivity of the polystyrene columns for individual metallofullerenes was beneficial since the metallofullerenes co-eluted with

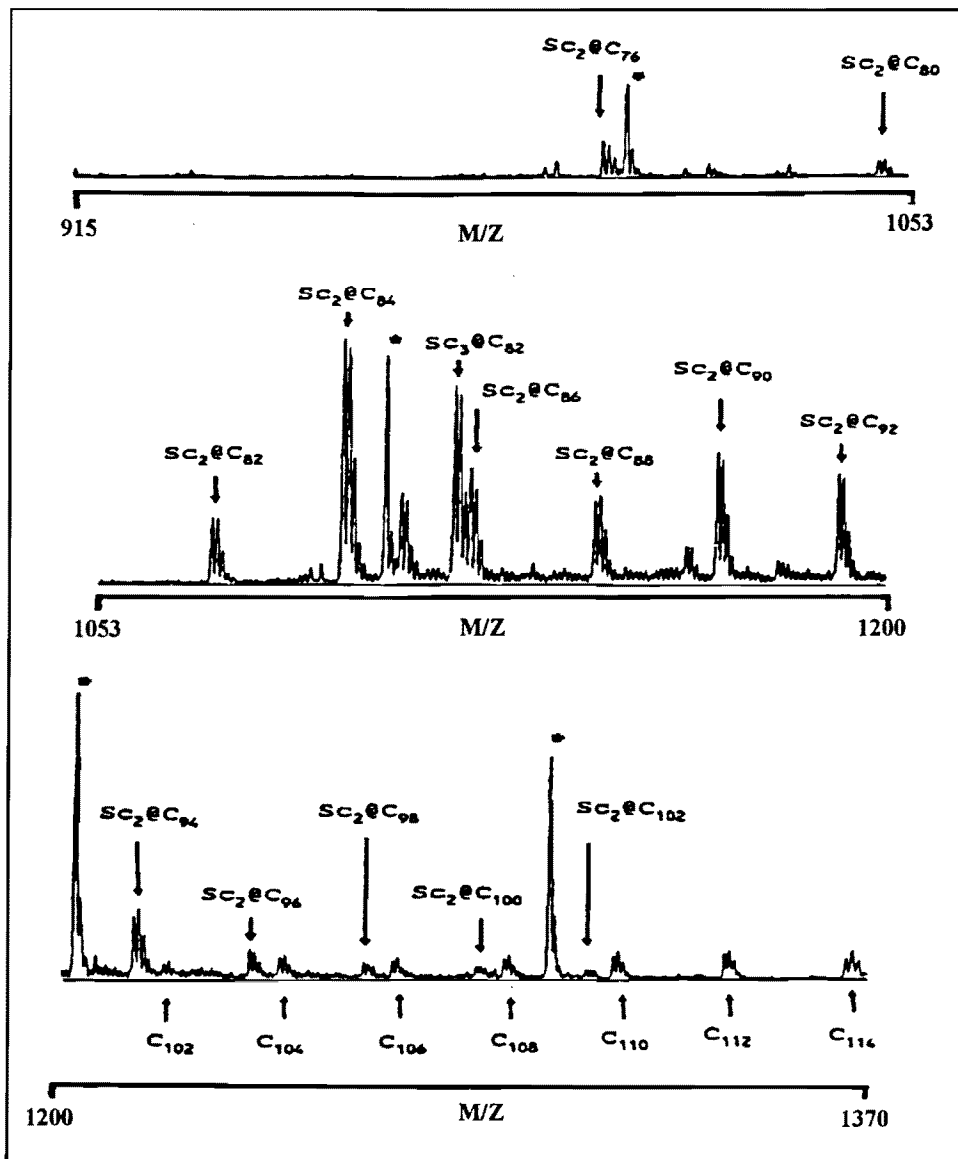


Figure 4.4 Off-line, negative-ion CI mass spectrum for the fourth polystyrene pass  $Sc_3@C_{82}$  EPR active fraction. The "\*" indicates calibration peaks for the standard Ultramark 1621.

each other.

In summary, the polystyrene technique was tedious and cumbersome since at least four to five polystyrene re-injections were necessary to effectively remove large quantities of the lower-mass empty-cage fullerenes. On the other hand, a valuable sample containing only metallofullerenes could eventually be obtained.

At this time, it was realized that the polystyrene column did not have sufficient resolving power to further separate this mixture of metallofullerenes. Fortunately, a column (Buckyclutcher), which claimed effective separations of fullerene compounds, became available. Developed by Welch and Pirkle,<sup>5</sup> this stationary phase consisted of tripodal (2,4-dinitrophenyl) ligands which possessed increased  $\pi$ - $\pi$  complexation interactions with the metallofullerene family.

For this reason, the EPR-active metallofullerene fraction was separated with this selective column for the final purification stages. A typical chromatogram following a typical 500  $\mu$ L injection is presented in Figure 4.5a. Since many peaks were observed, ten arbitrary fractions were collected for subsequent off-line EPR and mass spectral characterization. The corresponding on-line EPR activity for this injection is shown in Figure 4.5b. Although the signal-to-noise ratio is poor, a partial EPR spectrum of  $\text{Sc}_3@C_{82}$  can be observed. Note that the maximum EPR activity corresponds to peak #6 on the chromatogram. As further confirmation to  $\text{Sc}_3@C_{82}$ ,

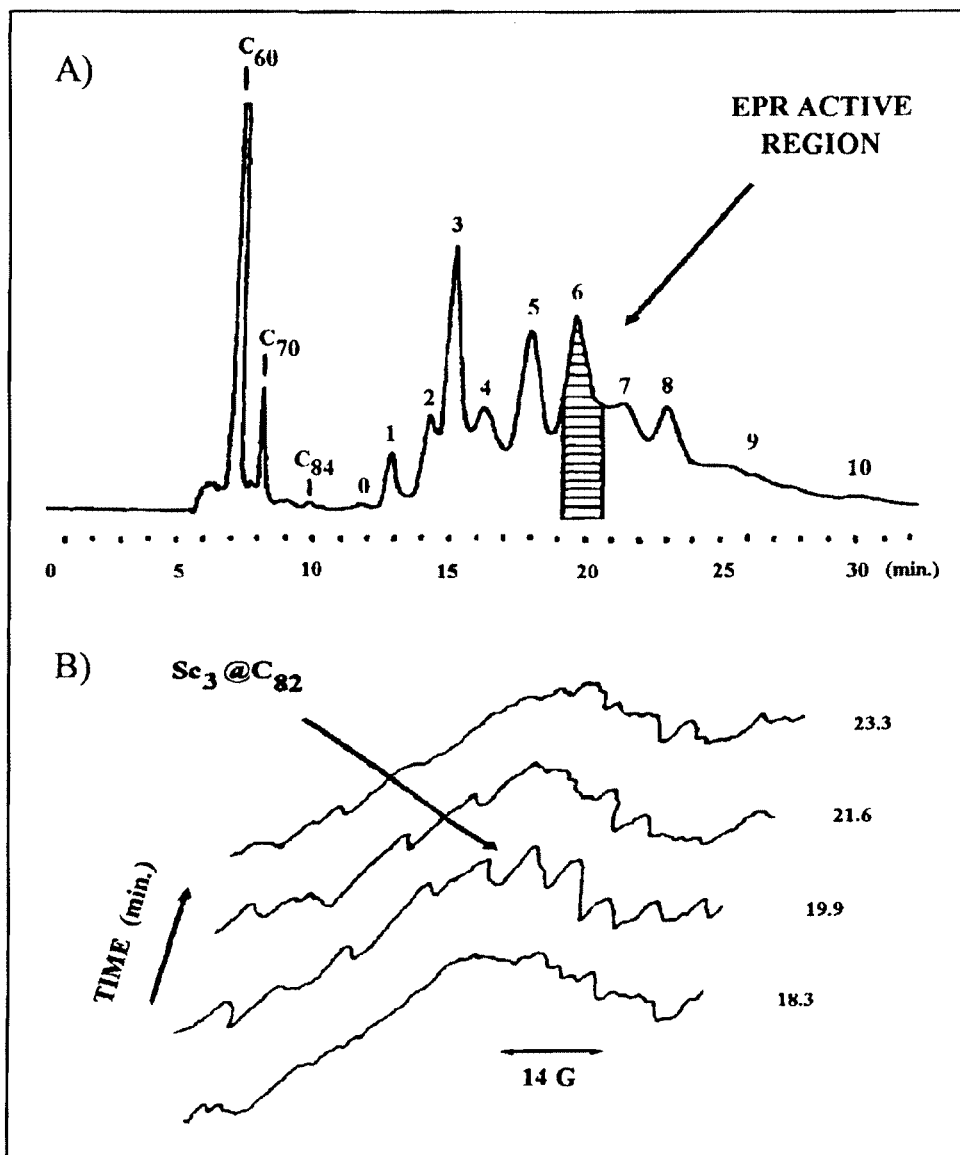


Figure 4.5 (a) HPLC-UV trace (340 nm) of the EPR active  $Sc_3@C_{82}$  fraction after five polystyrene passes, 250  $\mu$ L detection, Buckyclutcher column, 2.1 mL/min, 80:20 toluene/decalin, EPR active region is peak #6. (b) On-line HPLC-EPR profile, 3 scans/file, 9.55 GHz, and 20 s/sweep.

fraction #6 was evaporated, concentrated, and degassed for subsequent high resolution, off-line EPR characterization. After a number of collection and re-injections of fraction #6, a purified  $\text{Sc}_3@C_{82}$  sample of > 90% purity was obtained. The expected 22-line pattern is easily observed as indicated by its EPR spectrum (Figure 4.6). An analytical injection of this sample and corresponding negative-ion mass spectrum are presented in Figure 4.7.

It should be noted that an isolated  $\text{Sc}_3@C_{82}$  sample was sent to IBM for further EPR characterization. In that study,<sup>177</sup> EPR spectra were taken at temperatures ranging from 77 °K to 333 °K. According to linewidth analysis, it was possible to monitor the dynamics of the  $\text{Sc}_3$  trimer inside the  $C_{82}$  fullerene cage network. The data suggest that the Sc atoms of the  $\text{Sc}_3$  trimer reorient rapidly inside the  $C_{82}$  surrounding cage network. At 200 K, a reorientational energy barrier for the Sc ions was determined to be 28 meV with a correlation time of  $5 \times 10^{-9}$  s.

Peak #6 was not the only fraction that was isolated. Specifically, fractions #0-9 were also collected and re-injected until single, homogeneous peaks for each fraction were obtained. The analytical traces and corresponding mass spectra are presented in Figure 4.8a through Figure 4.8m. A mass spectrum for each of these samples was then obtained to ascertain their purity. Although symmetrical, single peaks were observed in the chromatograms, not all samples were pure and were contaminated



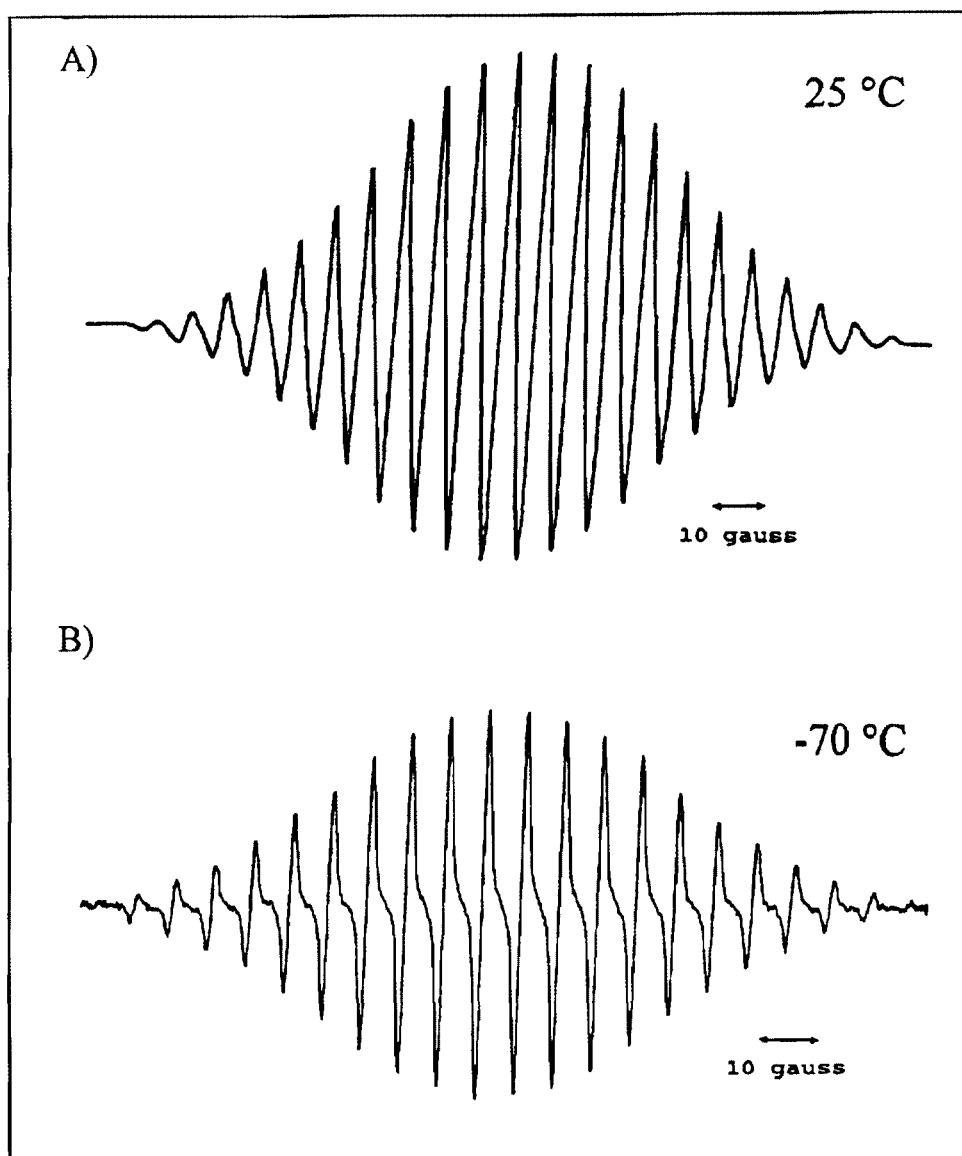


Figure 4.6 Off-line EPR spectra of purified peak #6 ( $\text{Sc}_3@C_{82}$ ) in decalin. (a) 9.63 GHz, 500 s/sweep, one scan, and 25 °C. (b) 9.63 GHz, 500 s/sweep, one scan, and -70 °C.

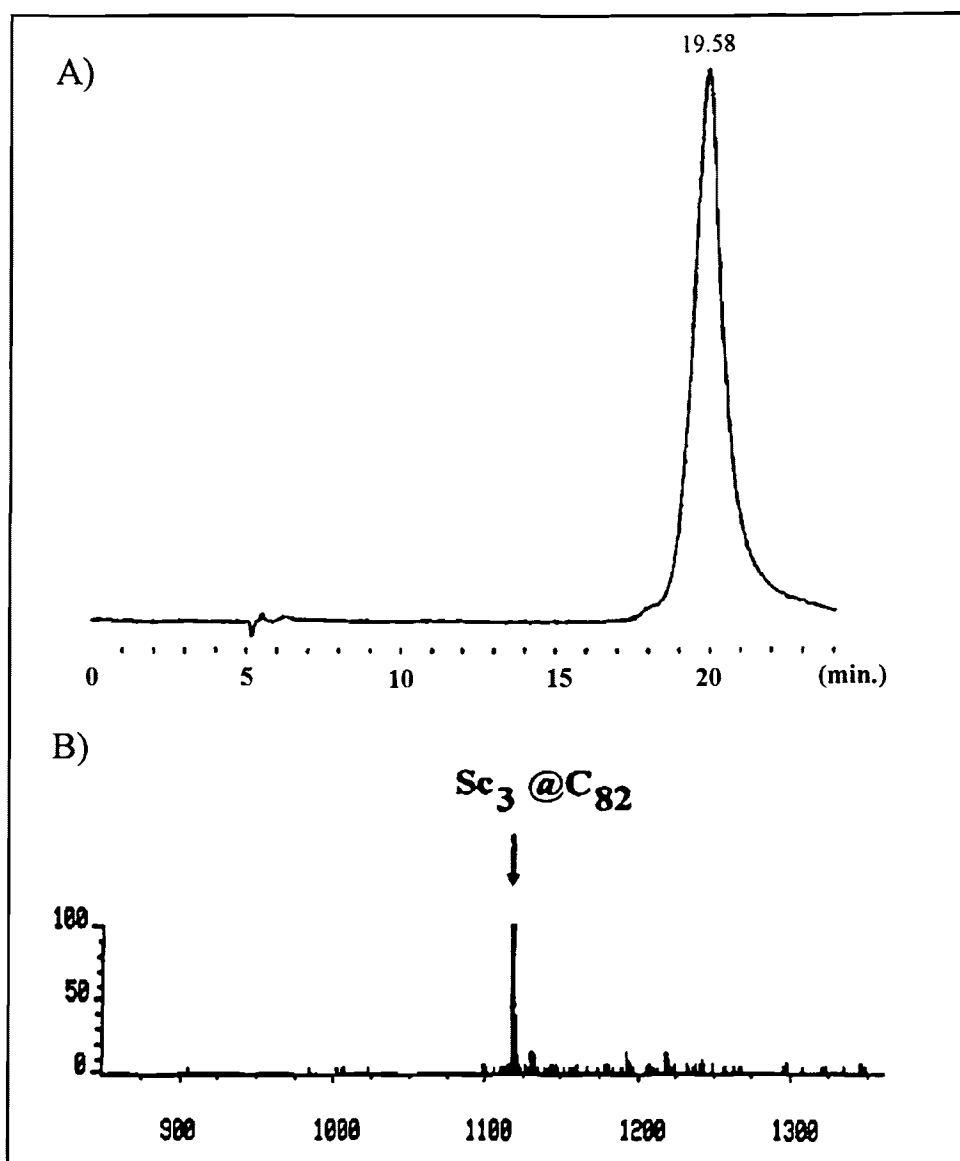


Figure 4.7 HPLC-UV chromatogram, 10  $\mu$ L of purified peak #6 ( $\text{Sc}_3\text{@C}_{82}$ ), Buckyclutcher column, 340 nm detection, and 2.1 mL/min of 80:20 toluene/decalin.

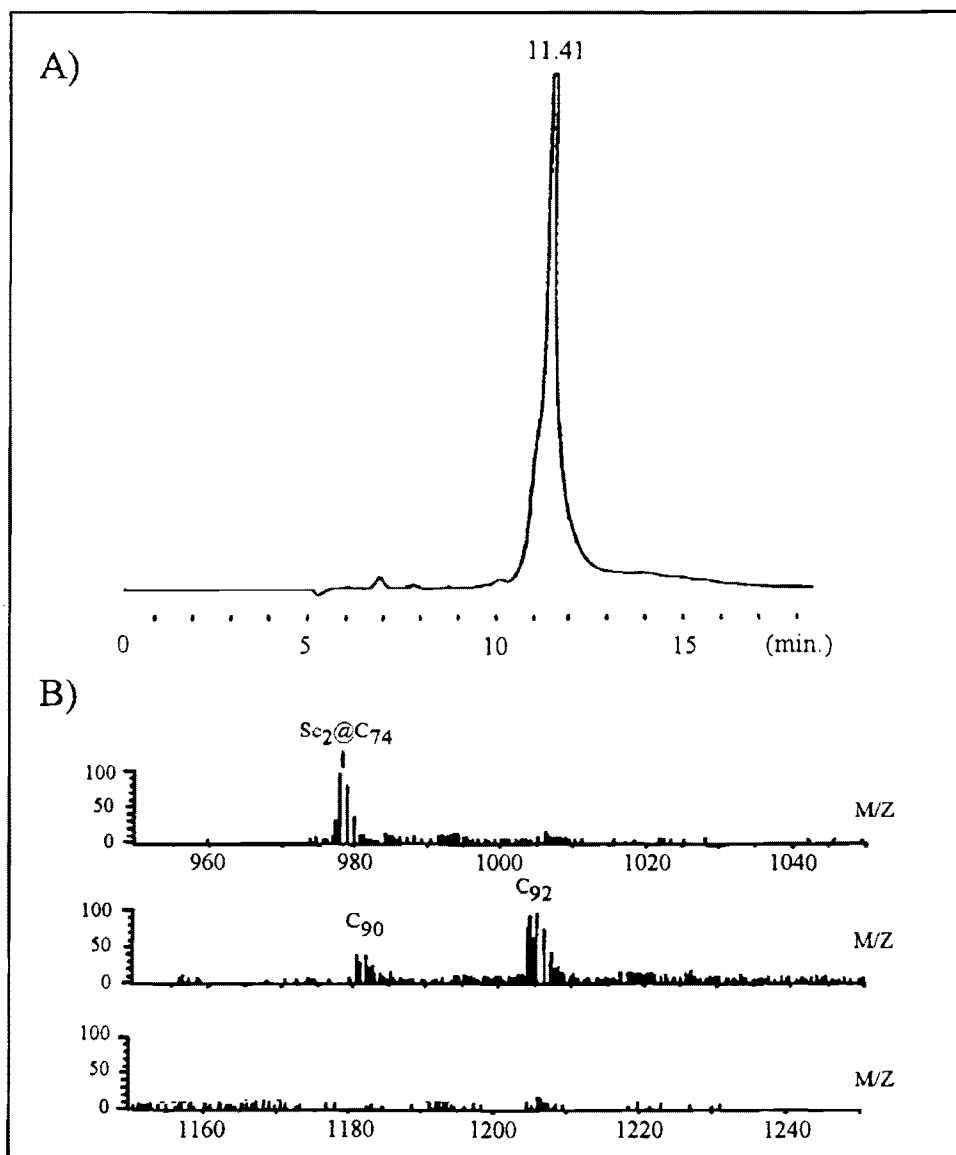


Figure 4.8a (a) Analytical HPLC-UV trace (*peak #0*), Buckyclutcher column, 2.1 mL/min of 80:20 toluene/decalin, and 340 nm detection. (b) off-line negative-ion chemical ionization mass spectrum of above using Ultramark 1621 as the calibration standard.

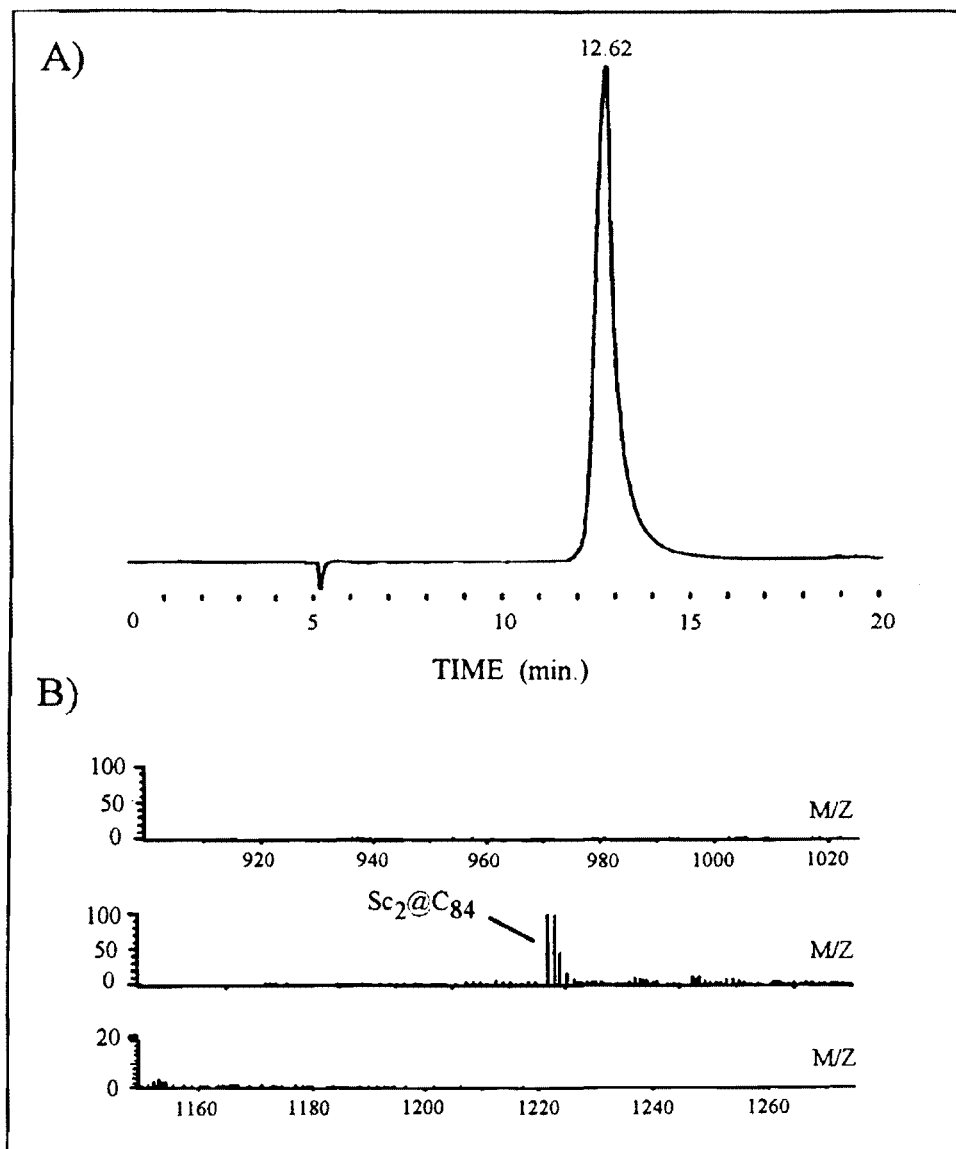


Figure 4.8b (a) Analytical HPLC-UV trace (*peak #1*), Buckyclutcher column, 2.1 mL/min of 80:20 toluene/decalin, and 340 nm detection. (b) off-line negative-ion chemical ionization mass spectrum of above using Ultramark 1621 as the calibration standard.

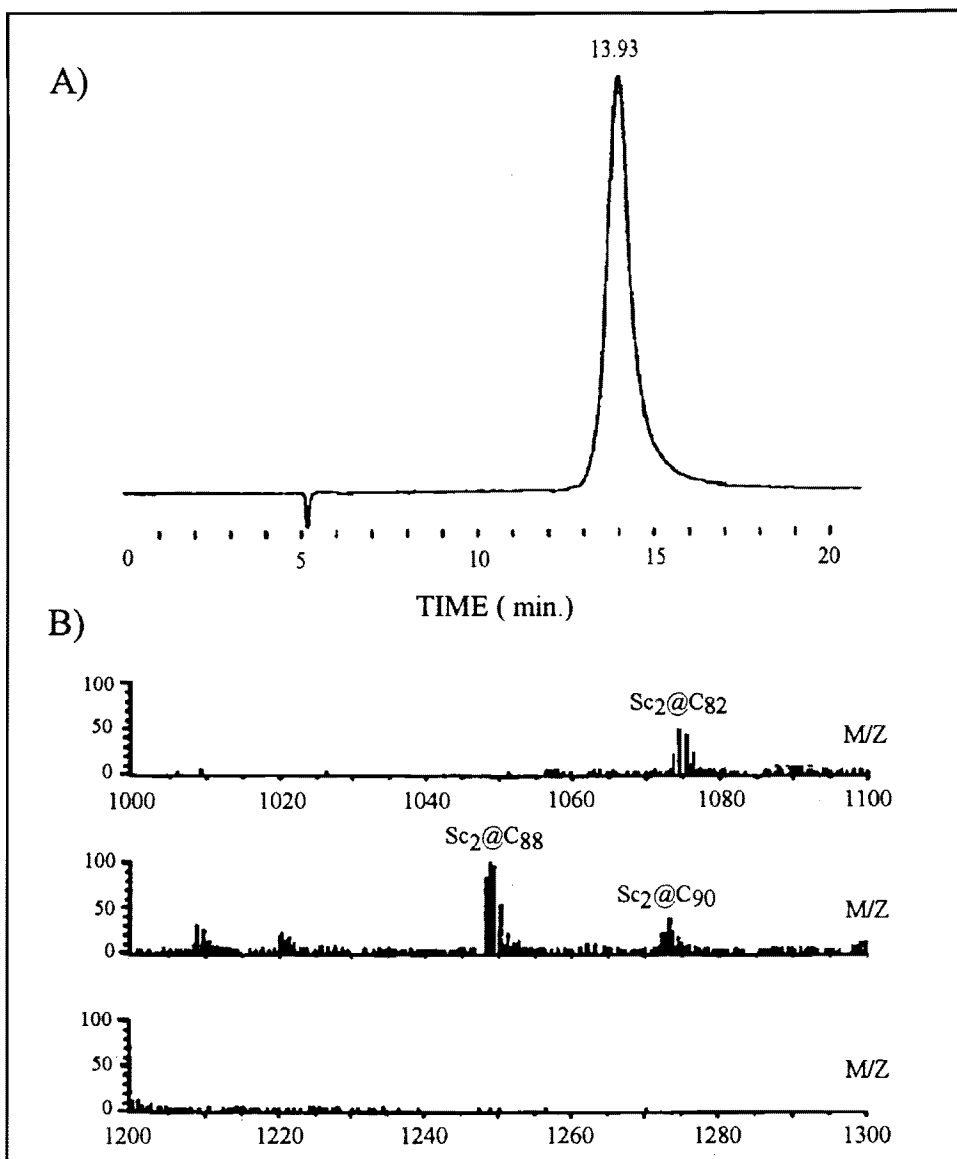


Figure 4.8c (a) Analytical HPLC-UV trace (*peak #2*), Buckyclutcher column, 2.1 mL/min of 80:20 toluene/decalin, and 340 nm detection. (b) off-line negative-ion chemical ionization mass spectrum of above using Ultramark 1621 as the calibration standard.

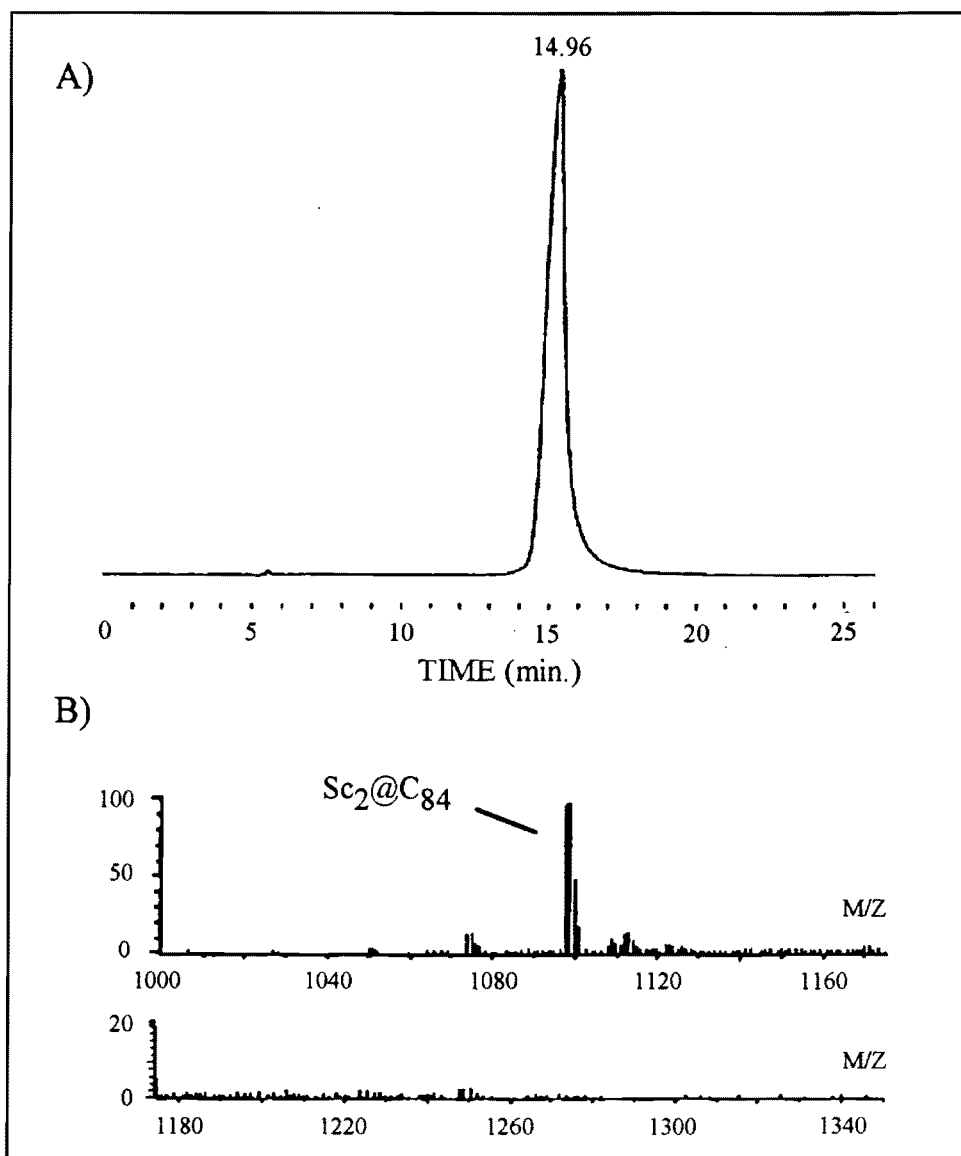


Figure 4.8d (a) Analytical HPLC-UV trace (*peak #3*), Buckyclutcher column, 2.1 mL/min of 80:20 toluene/decalin, and 340 nm detection. (b) off-line negative-ion chemical ionization mass spectrum of above using Ultramark 1621 as the calibration standard.

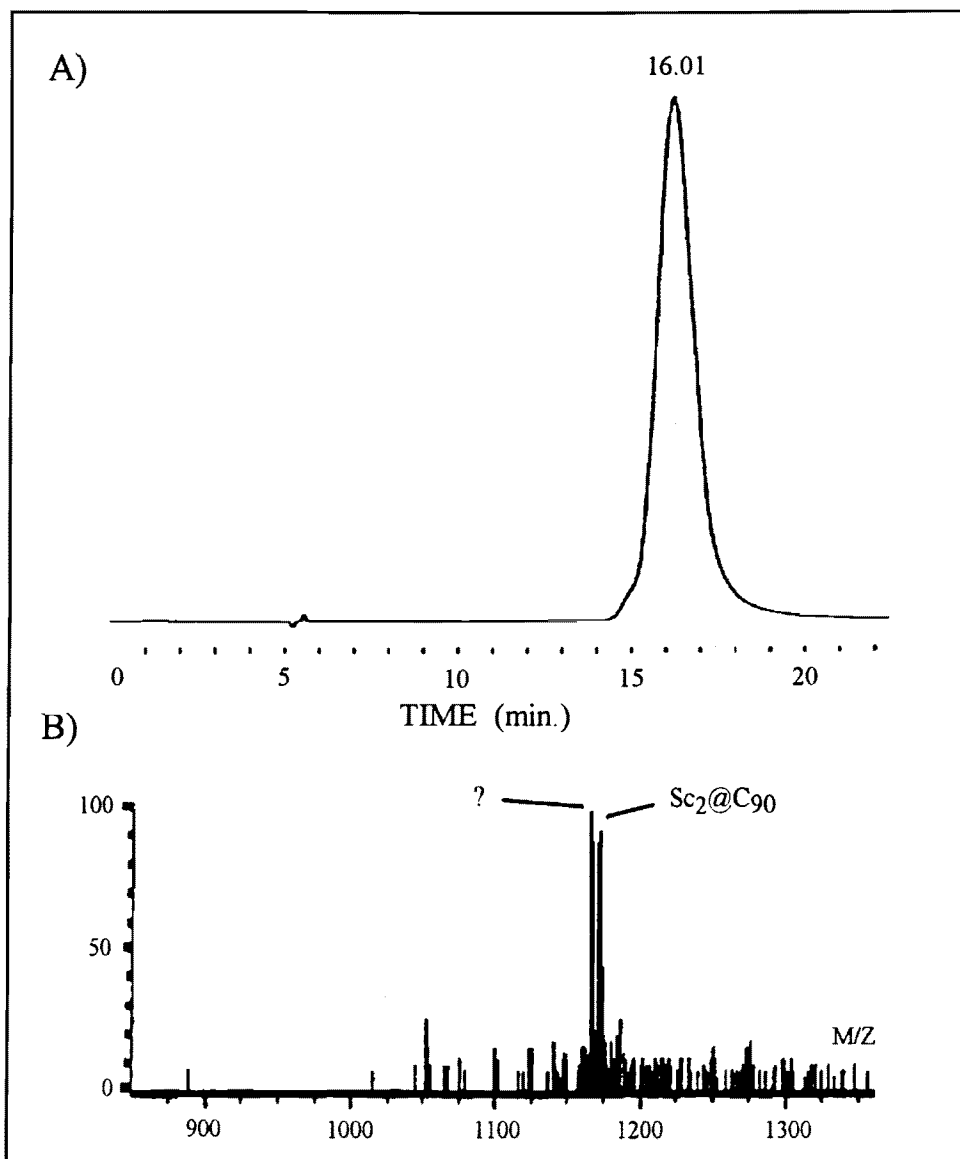


Figure 4.8e (a) Analytical HPLC-UV trace (peak #4), Buckyclutcher column, 2.1 mL/min of 80:20 toluene/decalin, and 340 nm detection. (b) off-line negative-ion chemical ionization mass spectrum of above using Ultramark 1621 as the calibration standard.

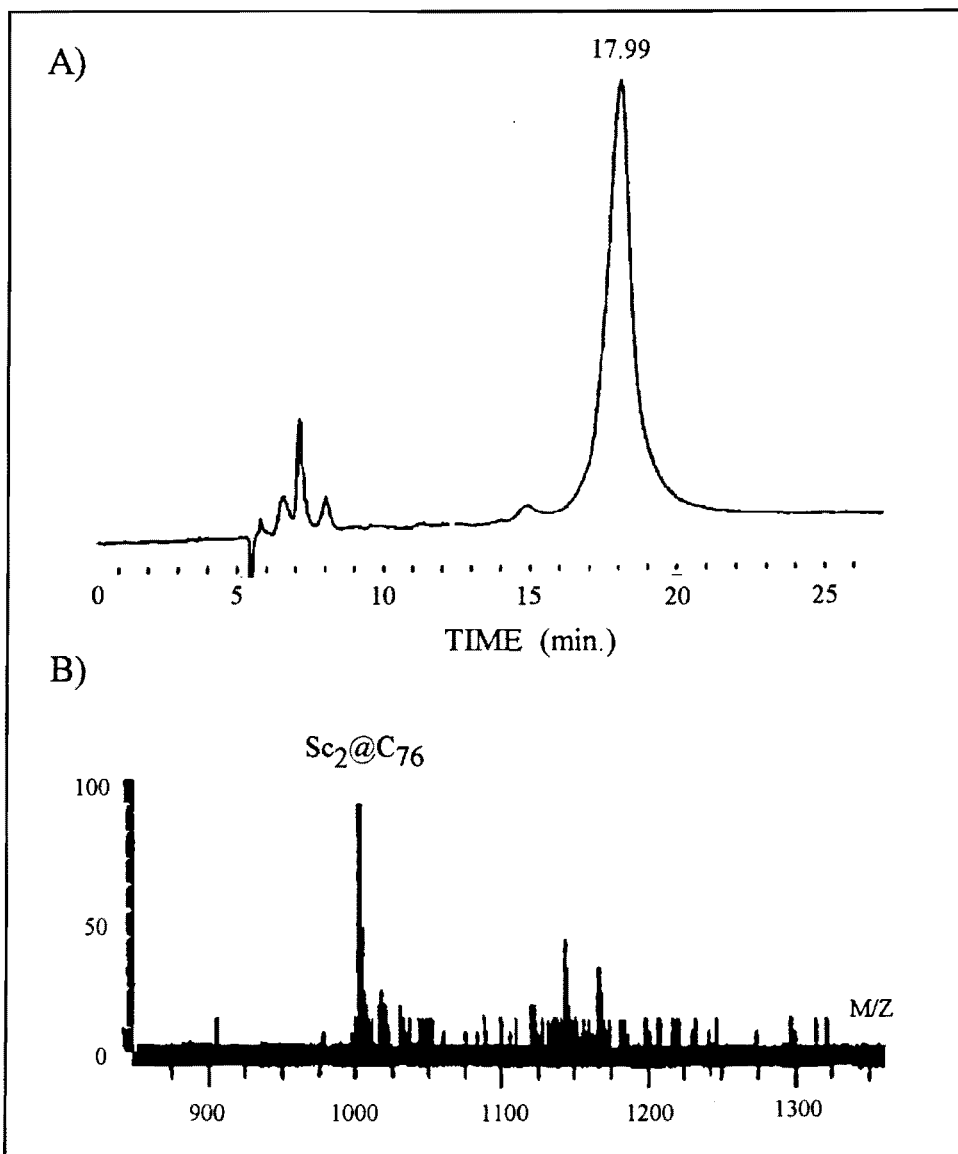


Figure 4.8f (a) Analytical HPLC-UV trace (*peak #5*), Buckyclutcher column, 2.1 mL/min of 80:20 toluene/decalin, and 340 nm detection. (b) off-line negative-ion chemical ionization mass spectrum of above using Ultramark 1621 as the calibration standard.



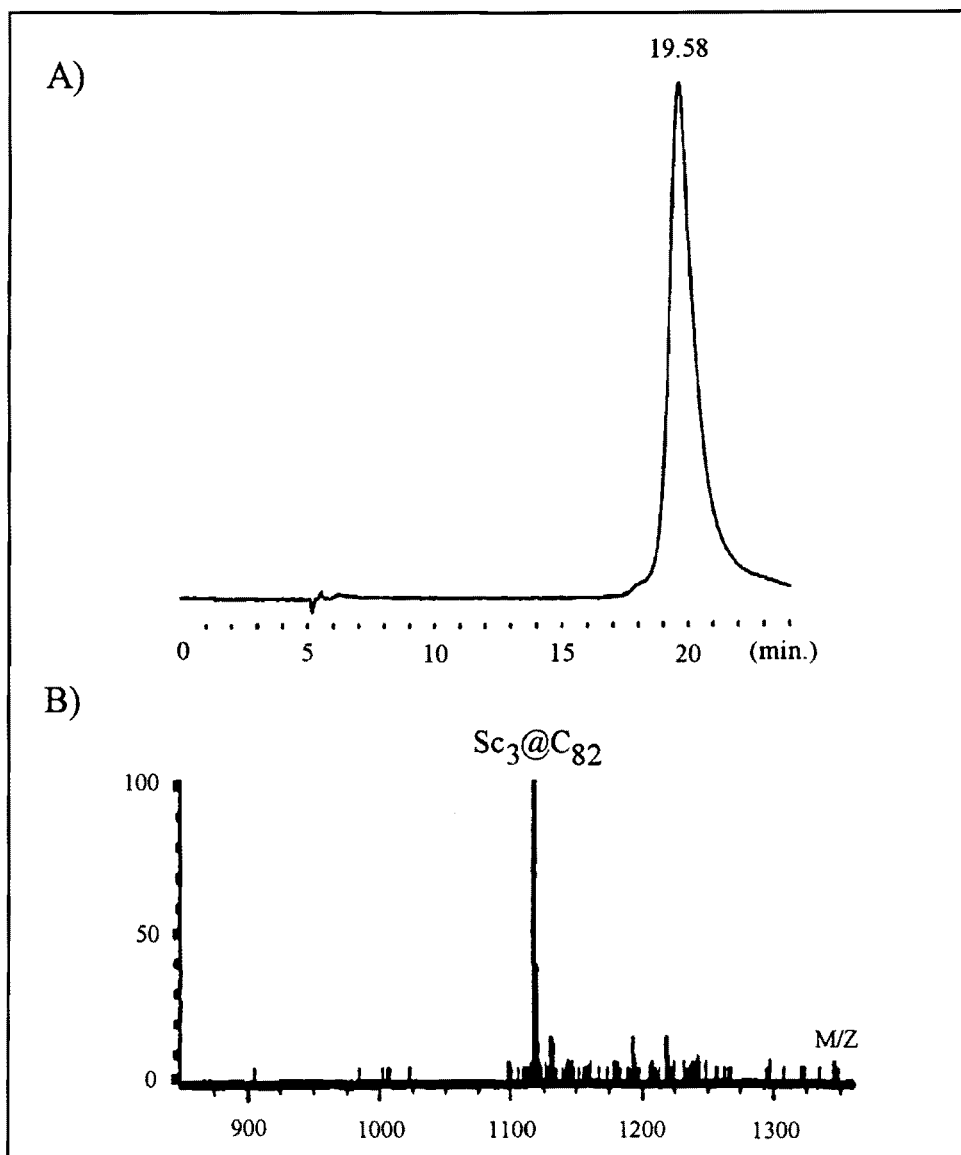


Figure 4.8g (a) Analytical HPLC-UV trace (*peak #6*), Buckyclutcher column, 2.1 mL/min of 80:20 toluene/decalin, and 340 nm detection. (b) off-line negative-ion chemical ionization mass spectrum of above using Ultramark 1621 as the calibration standard.

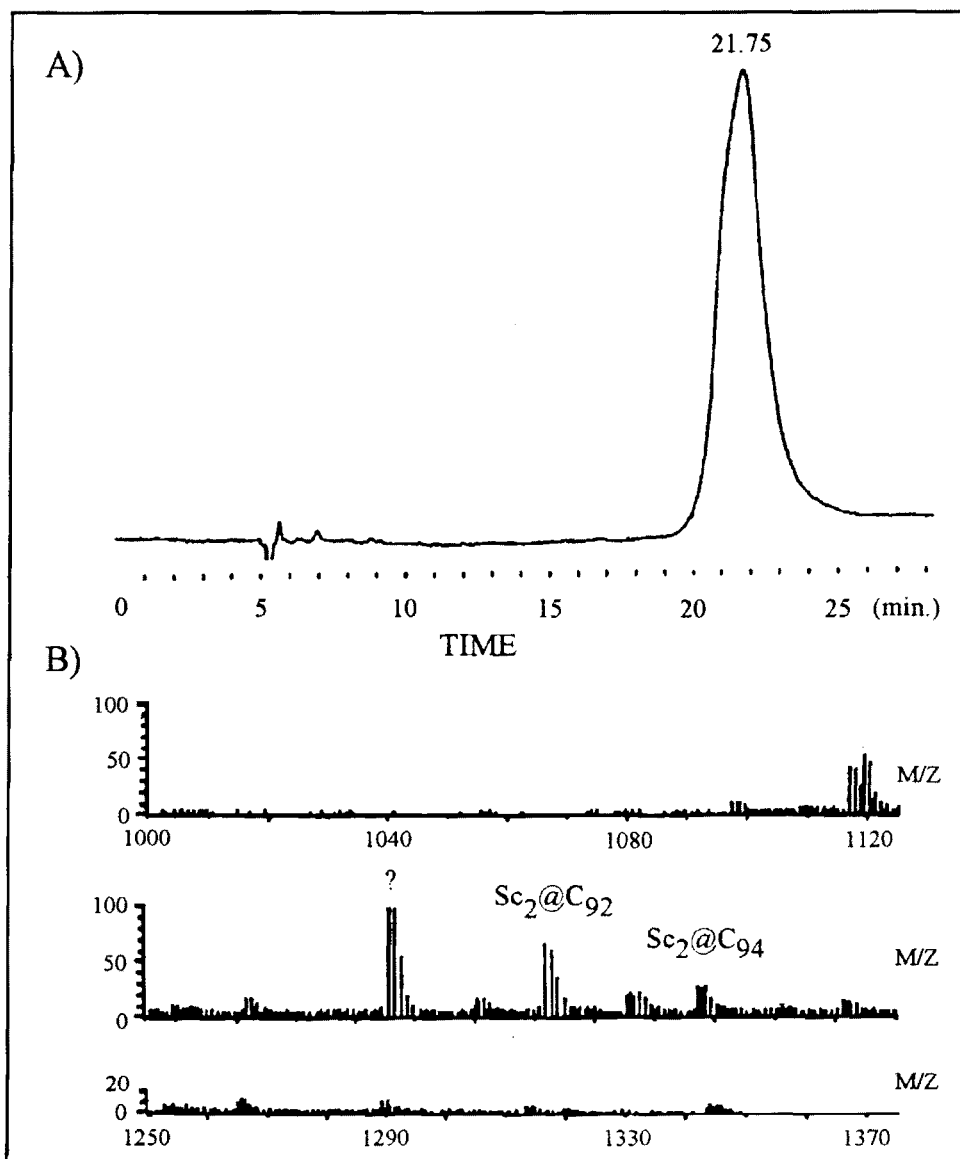


Figure 4.8h (a) Analytical HPLC-UV trace (*peak #7*), Buckyclutcher column, 2.1 mL/min of 80:20 toluene/decalin, and 340 nm detection. (b) off-line negative-ion chemical ionization mass spectrum of above using Ultramark 1621 as the calibration standard.

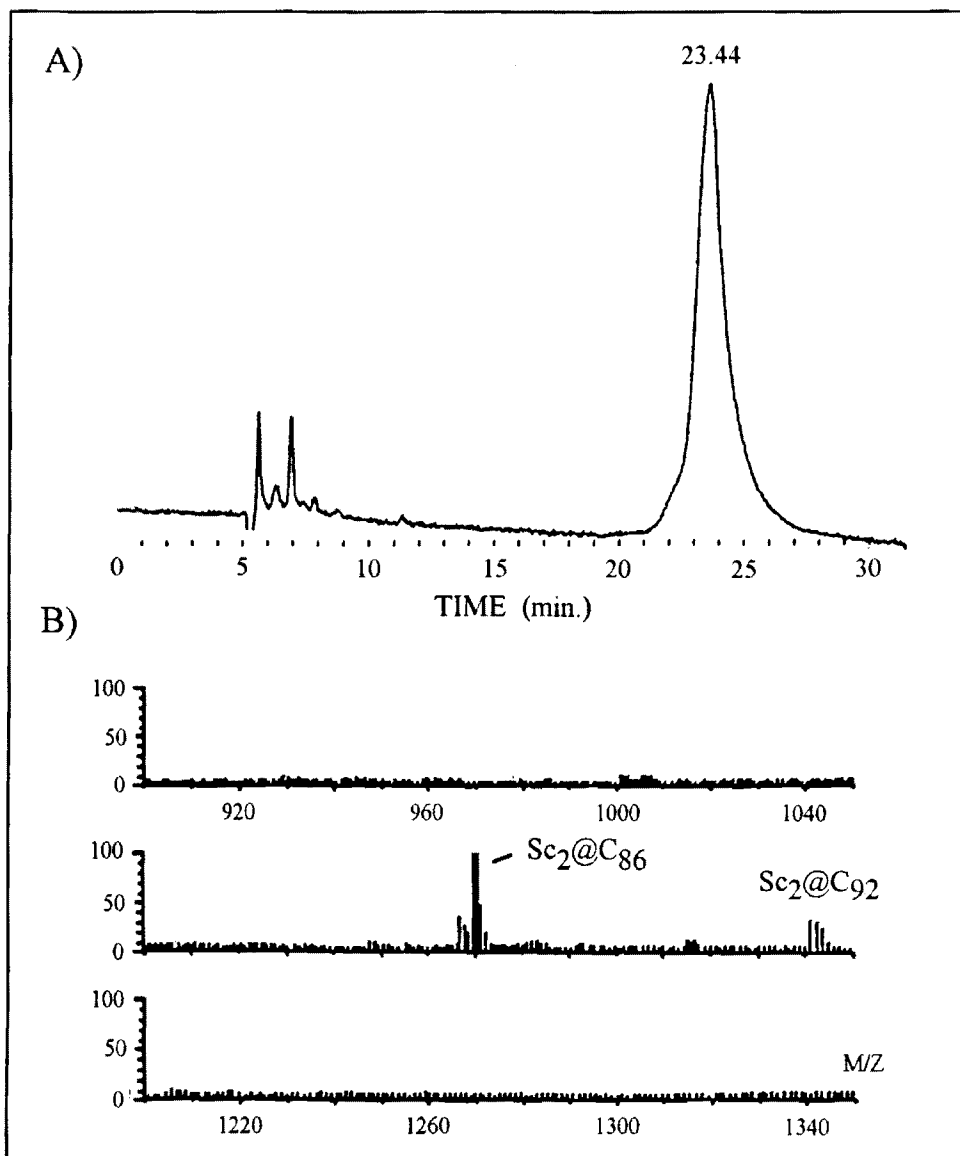


Figure 4.8i (a) Analytical HPLC-UV trace (peak #8), Buckyclutcher column, 2.1 mL/min of 80:20 toluene/decalin, and 340 nm detection. (b) off-line negative-ion chemical ionization mass spectrum of above using Ultramark 1621 as the calibration standard.

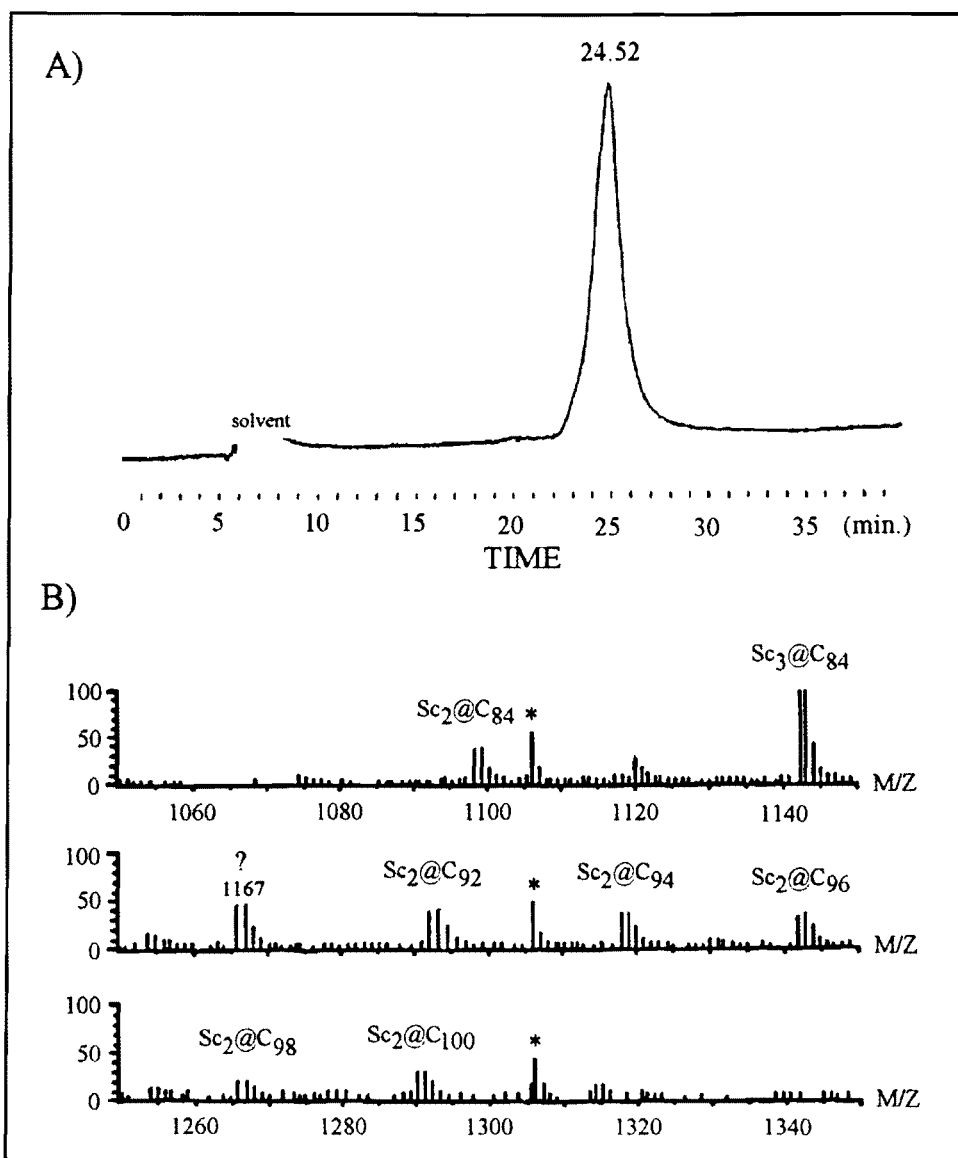


Figure 4.8j (a) Analytical HPLC-UV trace (*peak #9.1 series*), Buckyclutcher column, 2.1 mL/min of 80:20 toluene/decalin, and 340 nm detection. (b) off-line negative-ion chemical ionization mass spectrum of above using Ultramark 1621 as the calibration standard.

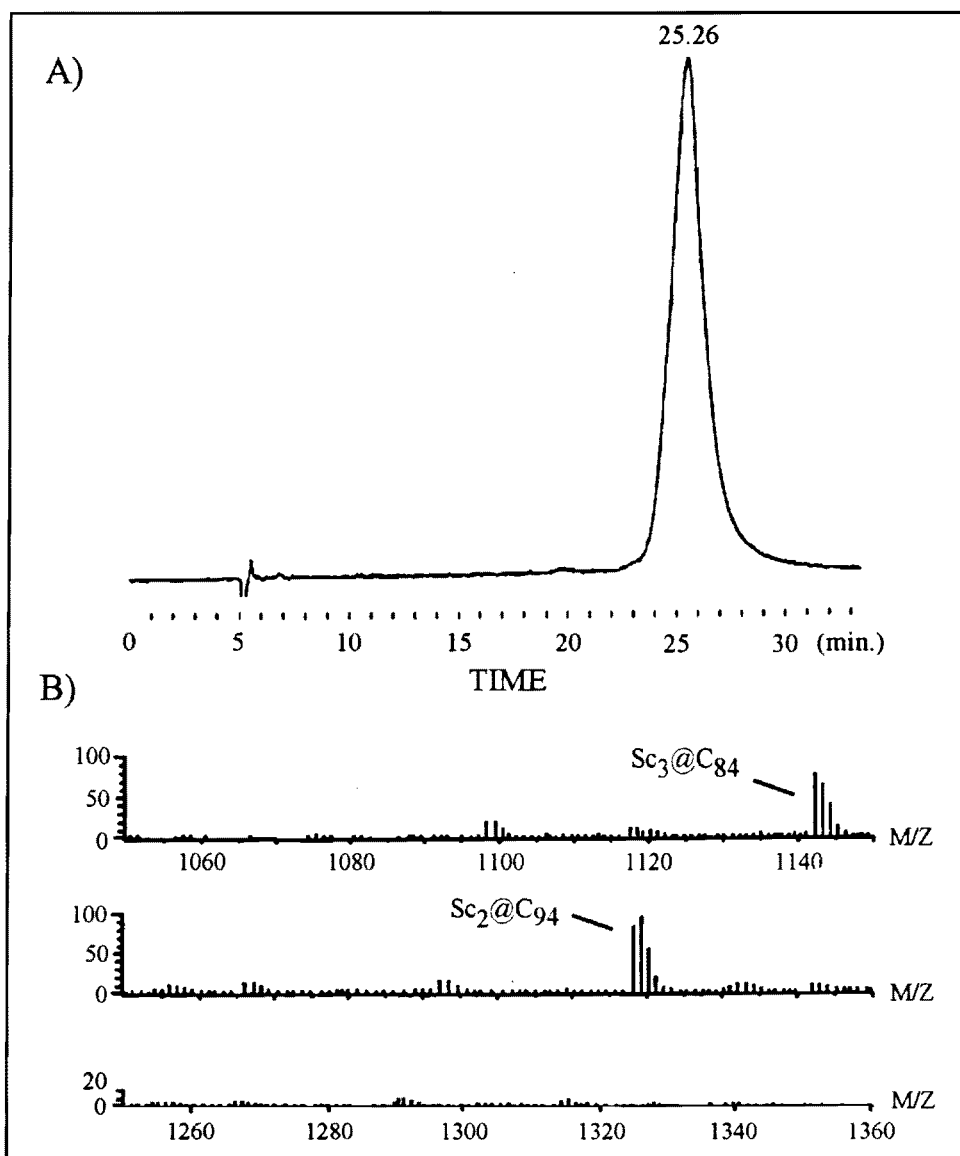


Figure 4.8k (a) Analytical HPLC-UV trace (*peak #9.2 series*), Buckyclutcher column, 2.1 mL/min of 80:20 toluene/decalin, and 340 nm detection. (b) off-line negative-ion chemical ionization mass spectrum of above using Ultramark 1621 as the calibration standard.

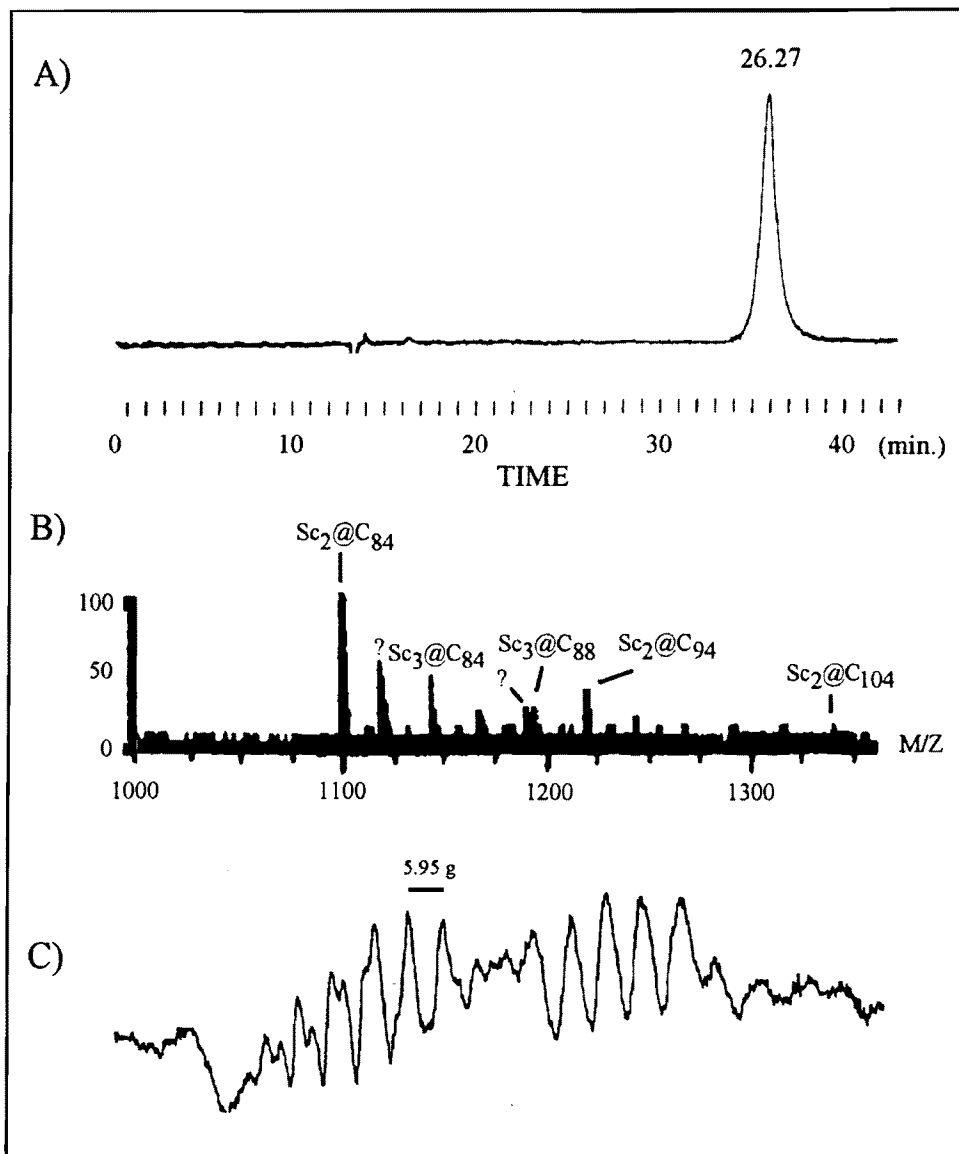


Figure 4.81 (a) Analytical HPLC-UV trace (*peak #9.3 series*), Buckyclutcher column, 2.1 mL/min of 80:20 toluene/decalin, and 340 nm detection. (b) off-line negative-ion chemical ionization mass spectrum of above using Ultramark 1621 as the calibration standard. (c) off-line EPR spectrum of above, 44 scans, 9.64 GHz, sweep width 140 g, and 200 s/sweep. Sample was "freeze-thaw" degassed in decalin.

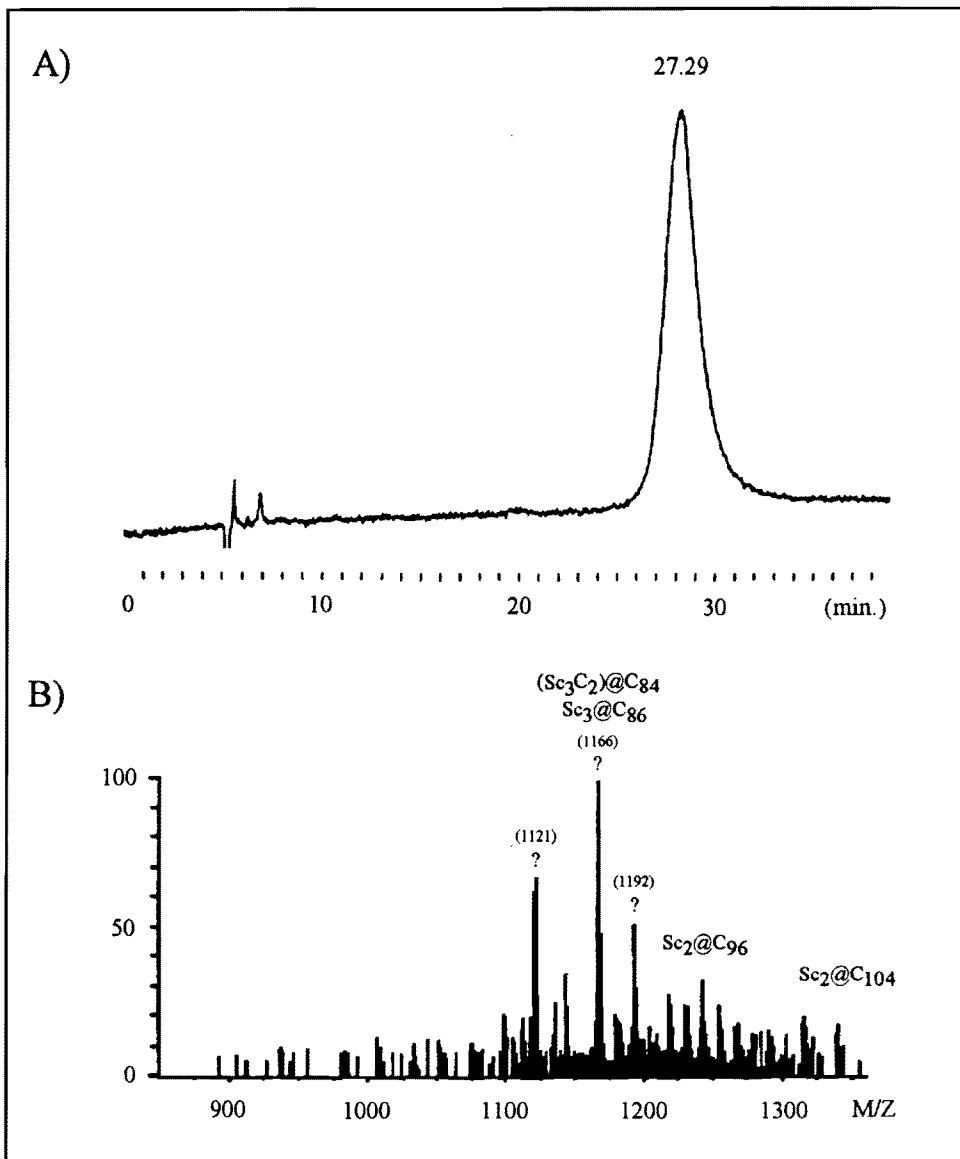


Figure 4.8m (a) Analytical HPLC-UV trace (*peak #9.4 series*), Buckyclutcher column, 2.1 mL/min of 80:20 toluene/decalin, and 340 nm detection. (b) off-line negative-ion chemical ionization mass spectrum of above using Ultramark 1621 as the calibration standard.

with other co-eluting metallofullerenes. Nevertheless, several purified samples were obtained. For the first time, we had isolated  $\text{Sc}_2@C_{74}$  (#0, ~40% purity),  $\text{Sc}_2@C_{84}$  (isomer I, ~95% purity; isomer II, ~85% purity), and  $\text{Sc}_3@C_{82}$  (#6, ~90% purity). The composition of  $\text{Sc}_m@C_{2n}$  fractions # 0-9 are summarized in Table 4.1.

As noted above, two isomers of the  $\text{Sc}_2@C_{84}$  metallofullerene were chromatographically isolated. These two purified samples were characterized by our collaborating IBM research lab utilizing energy dispersive X-ray spectroscopy (EDS) and high resolution tunneling electron microscopy (TEM). Results of these experiments have recently been published in *Nature*.<sup>175</sup> Specifically, it was found that  $\text{Sc}_2@C_{84}$  (isomer from fraction 3) molecules are packed in a hexagonal-close-packed (hcp) structure. The ratio of lattice constants  $c/a = 1.63$  is comparable to the value expected for ideal-sphere packing. The spacing between individual  $\text{Sc}_2@C_{84}$  molecules was 11.2 Å, a distance comparable to the empty-cage  $C_{84}$  fullerene.

Although a significant amount of final metallofullerene samples were obtained (~1 mg), several questions regarding the "missing"  $\text{Sc}@C_{82}$  metallofullerene remained largely unanswered. It was uncertain when or if  $\text{Sc}@C_{82}$  would elute from the Buckyclutcher column. Since the  $\text{Sc}_m@C_{2n}$  separations (#0-9) mentioned *vide supra* involved negligible amounts of  $\text{Sc}@C_{82}$  in the initial, starting stock solution, this species was not found in the final collected  $\text{Sc}_m@C_{2n}$  fractions (#0-9). For this



TABLE 4.1

Composition of  $Sc_m@C_{2n}$  Fractions  
Buckyclutcher column

$Sc_m@C_{2n}$ Fraction	Dominant $A_m@C_{2n}$	Next Dominant $A_m@C_{2n}$	Least Dominant $A_m@C_{2n}$
#0	$Sc_2@C_{74}$		
#1	$Sc_2@C_{84}$		
#2	$Sc_2@C_{88}$	$Sc_2@C_{82}$	$Sc_2@C_{90}$
#3	$Sc_2@C_{84}$		
#4	$Sc_2@C_{90}$		
#5	$Sc_2@C_{76}$		
#6	$Sc_3@C_{82}$		
#7	$Sc_2@C_{92}$	$Sc_2@C_{94}$	
#8	$Sc_2@C_{86}$		
#9.1	$Sc_3@C_{84}$	$Sc_2@C_{84}$	$Sc_2@C_{92} - Sc_2@C_{100}$
#9.2	$Sc_2@C_{94}$	$Sc_3@C_{84}$	
#9.3	$Sc_2@C_{84}$	$Sc_3@C_{84}$	$Sc_2@C_{94}$
#9.4	$(Sc_3C_2)@C_{84} ?$ or $Sc_3@C_{86} ?$	$Sc_2@C_{96} - Sc_2@C_{104}$	

reason, a new  $\text{Sc}_m@C_{2n}$  extract was prepared with a smaller, initial Sc/C metal loading ratio in the hope that the  $\text{Sc}@C_{82}$  concentration would increase. An off-line EPR spectrum of this stock solution is given in Figure 4.9. In this spectrum, the octet of the  $\text{Sc}@C_{82}$  species is distorted by the 22-line pattern expected for  $\text{Sc}_3@C_{82}$ . In addition, these signals are also distorted due to excessive microwave power (saturation) conditions of the EPR spectrometer. Although these operating conditions distort the off-line spectra, they provide the on-line HPLC-EPR experiment with a higher signal-to-noise ratio.

Since the EPR detection limits for a flowing  $\text{Sc}@C_{82}$  sample were unknown, a large amount of starting extract (5 mL) was injected into the HPLC-EPR apparatus. Although the Buckyclatcher was overloaded, there was a sufficient quantity of  $\text{Sc}@C_{82}$  in the EPR flow cell for observation. Although the on-line EPR spectra are distorted, the entire, expected octet for  $\text{Sc}@C_{82}$  can be observed at 19 minutes as presented in Figure 4.10. In contrast, ~16 of the 22 expected lines of  $\text{Sc}_3@C_{82}$  are observed at 23 minutes.

This on-line data was valuable. First, it established that  $\text{Sc}@C_{82}$  could potentially be isolated by chromatography. Before, it was unknown whether  $\text{Sc}@C_{82}$  was permanently retained on the column or possessed such a long retention time that its elution profile was too broad for efficient collection. In addition, the on-line data

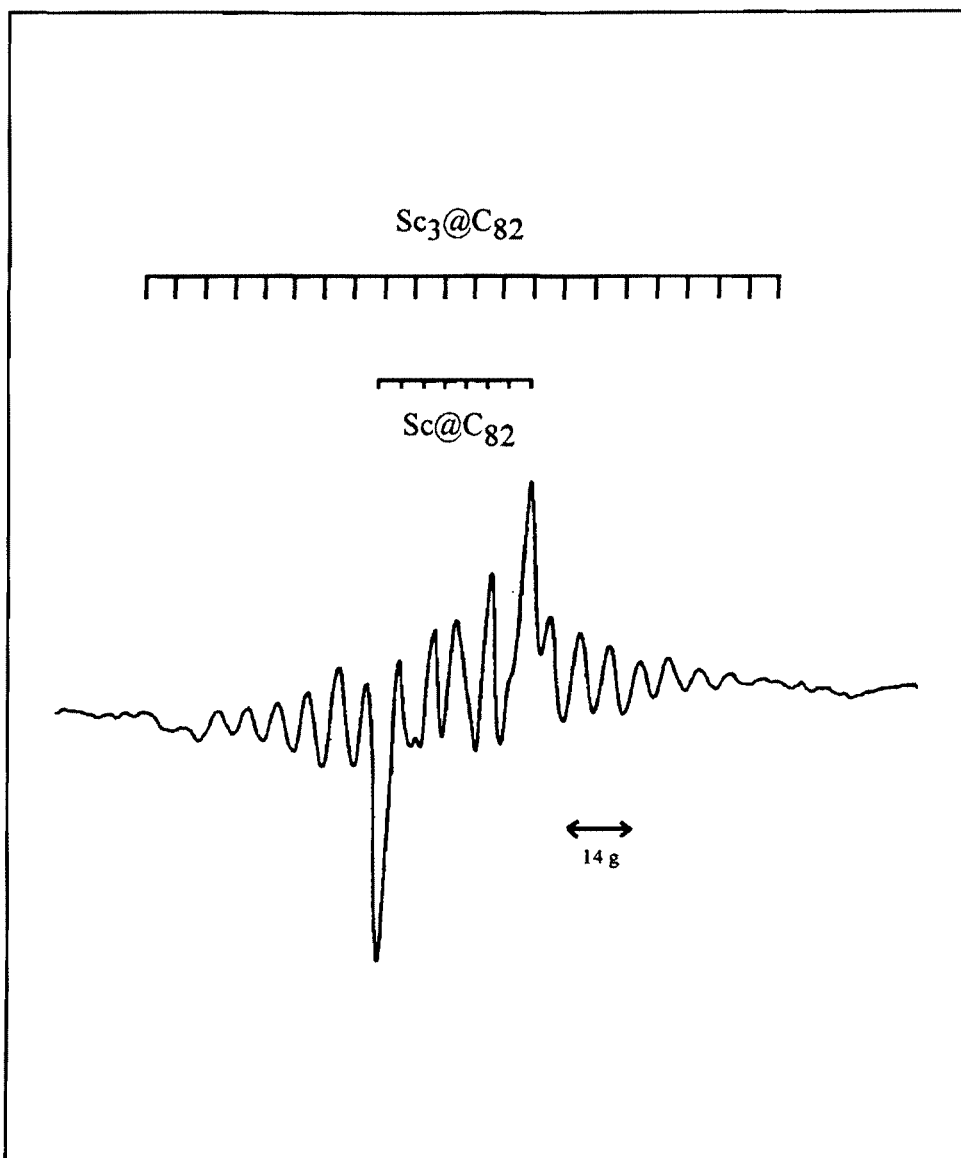


Figure 4.9 Off-line EPR spectrum of  $Sc_m@C_{2n}$  raw extract to be injected for Buckyclutcher separations. Spectrum is taken under high modulation, saturation, and rapid sweep operating conditions (see Experimental), 20 s/sweep, 4 scans/file, sweep width 150 g, and 9.55 GHz.

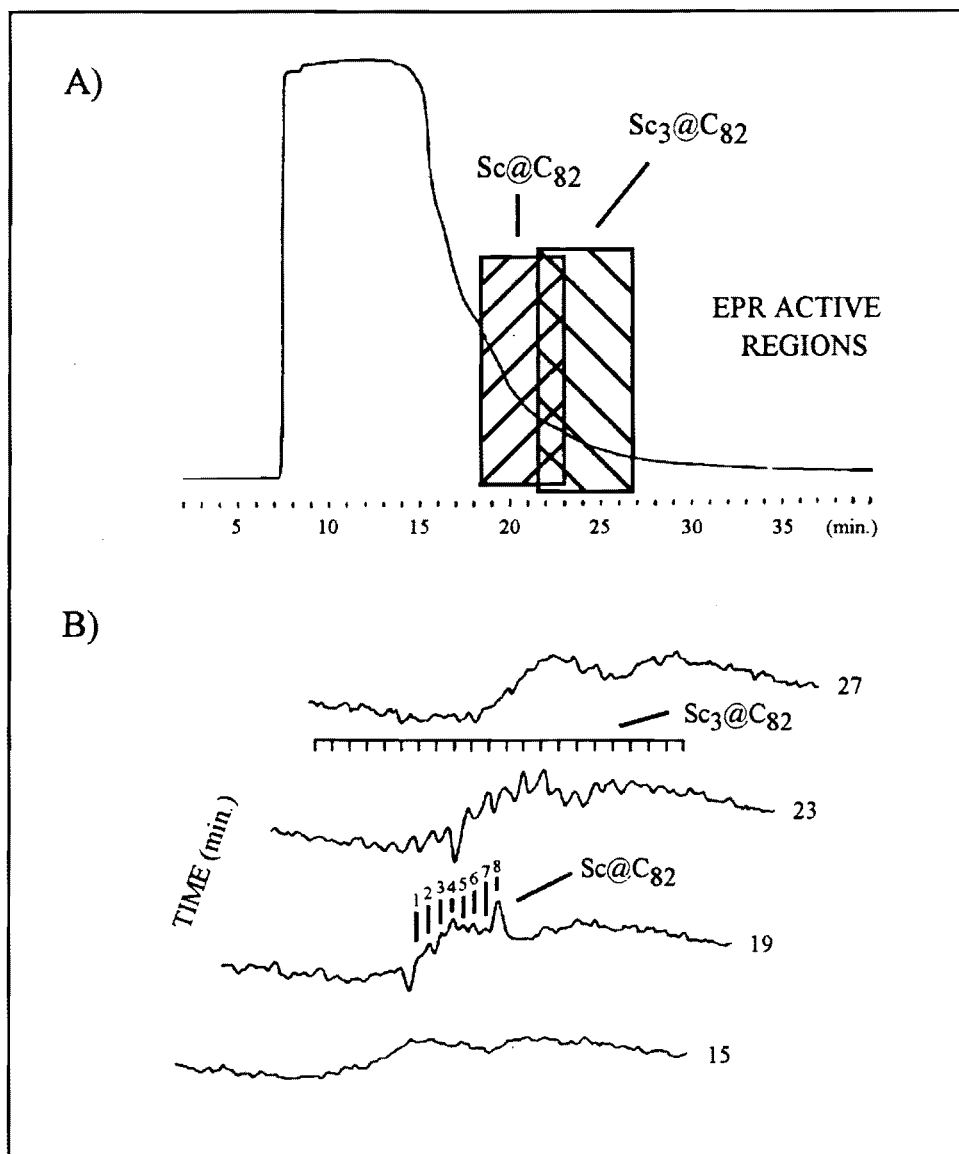


Figure 4.10 On-line HPLC-EPR experiment: (a) HPLC-UV trace following a 20 mg injection of  $Sc_m@C_{2n}$  raw extract, Buckyclutcher column, 340 nm detection, and 2.0 mL/min, of 80:20 toluene/decalin. (b) on-line HPLC-EPR profile of above, 3 scans/file, 20 s/sweep, 9.55 GHz, and alternate files are shown.

readily established the elution order of  $\text{Sc}@C_{82}$  before  $\text{Sc}_3@C_{82}$  without the need for off-line analysis. The monitoring of potentially unstable species (e.g.  $\text{Sc}@C_{82}$ ) is a distinct advantage of the on-line HPLC-EPR approach. Although off-line EPR characterization (Figure 4.11) and mass spectral data were obtained to corroborate the on-line EPR data, there were potential risks of utilizing off-line techniques alone. Before the on-line EPR data, it was uncertain if  $\text{Sc}@C_{82}$  eluted from the column but decomposed during the off-line sample handling. Whereas the di-metal  $\text{Sc}_2@C_{2n}$  and tri-metal  $\text{Sc}_3@C_{2n}$  compounds appeared to be stable, the monometal  $\text{Sc}@C_{2n}$  species was previously suspected to undergo irreversible aerobic oxidation.

Re-injection of this  $\text{Sc}_1@C_{2n}/\text{Sc}_3@C_{2n}$  EPR-active fraction into the Buckyclutcher indicated resolvable peaks in the chromatogram (Figure 4.12). In an experiment to ascertain which peaks were due to  $\text{Sc}@C_{82}$  and  $\text{Sc}_3@C_{82}$ , the on-line HPLC-EPR apparatus was not utilized. In this manner, the lag time between UV detection and manual fraction collection was reduced to a few seconds and more accurate peak assignments and retention times could therefore be made. The off-line EPR spectra for these corresponding fractions are presented in Figure 4.13. Based on EPR and mass spectral data, the regions at 18.8 minutes and 20.8 minutes were assigned to  $\text{Sc}@C_{82}$  and  $\text{Sc}_3@C_{82}$ , respectively.

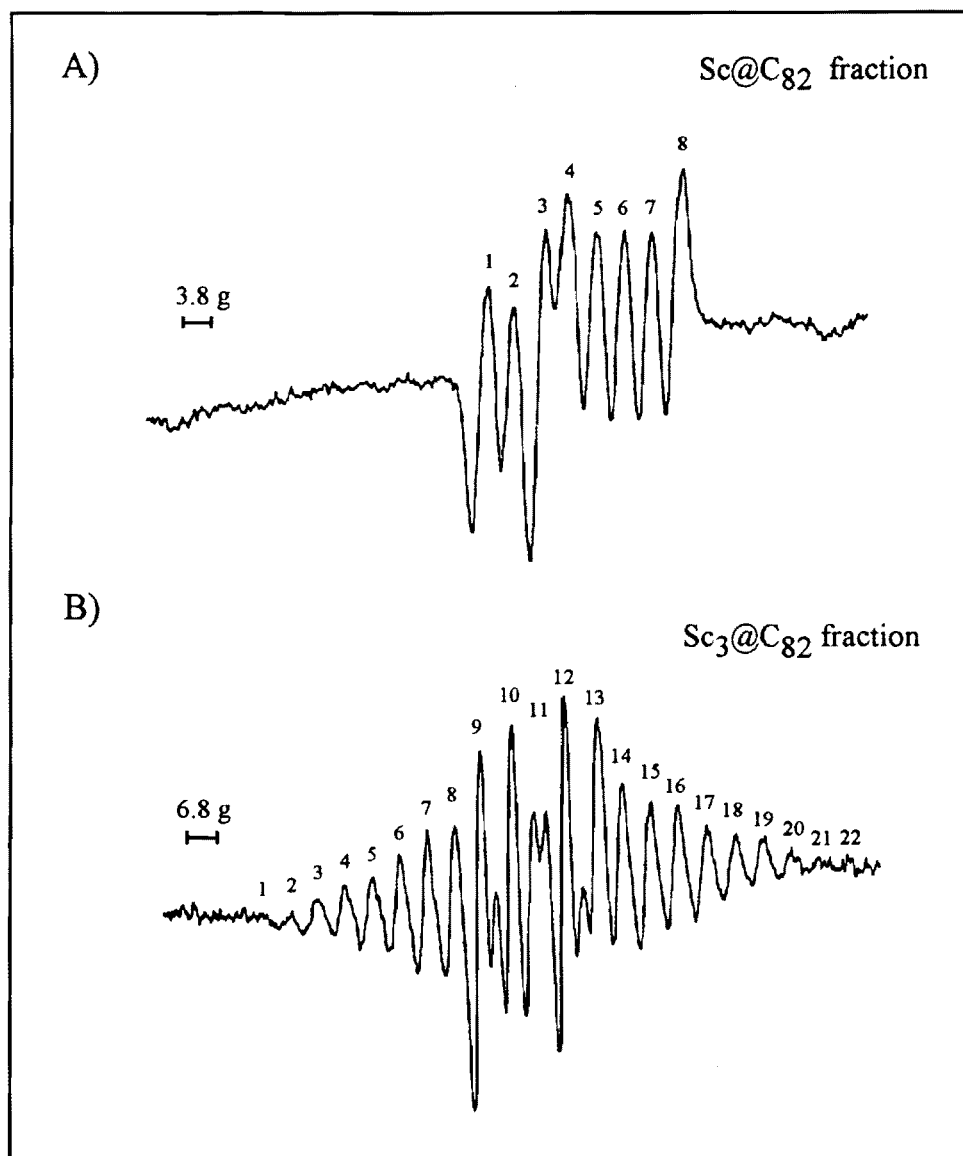


Figure 4.11 Off-line EPR spectra of collected Sc<sub>m</sub>@C<sub>2n</sub> fractions (see Figure 4.10) centered at 17-20 min. and 20-26 min., respectively. (a) 17-20 min. fraction, sweep width 100 g, 100 s/sweep, 4 scans/file, 9.63 GHz, and the solvent is decalin. (b) #20-26 min. Sc<sub>m</sub>@C<sub>2n</sub> fraction, sweep width 150 g, 100 s/scan, 9.63 GHz, in decalin.

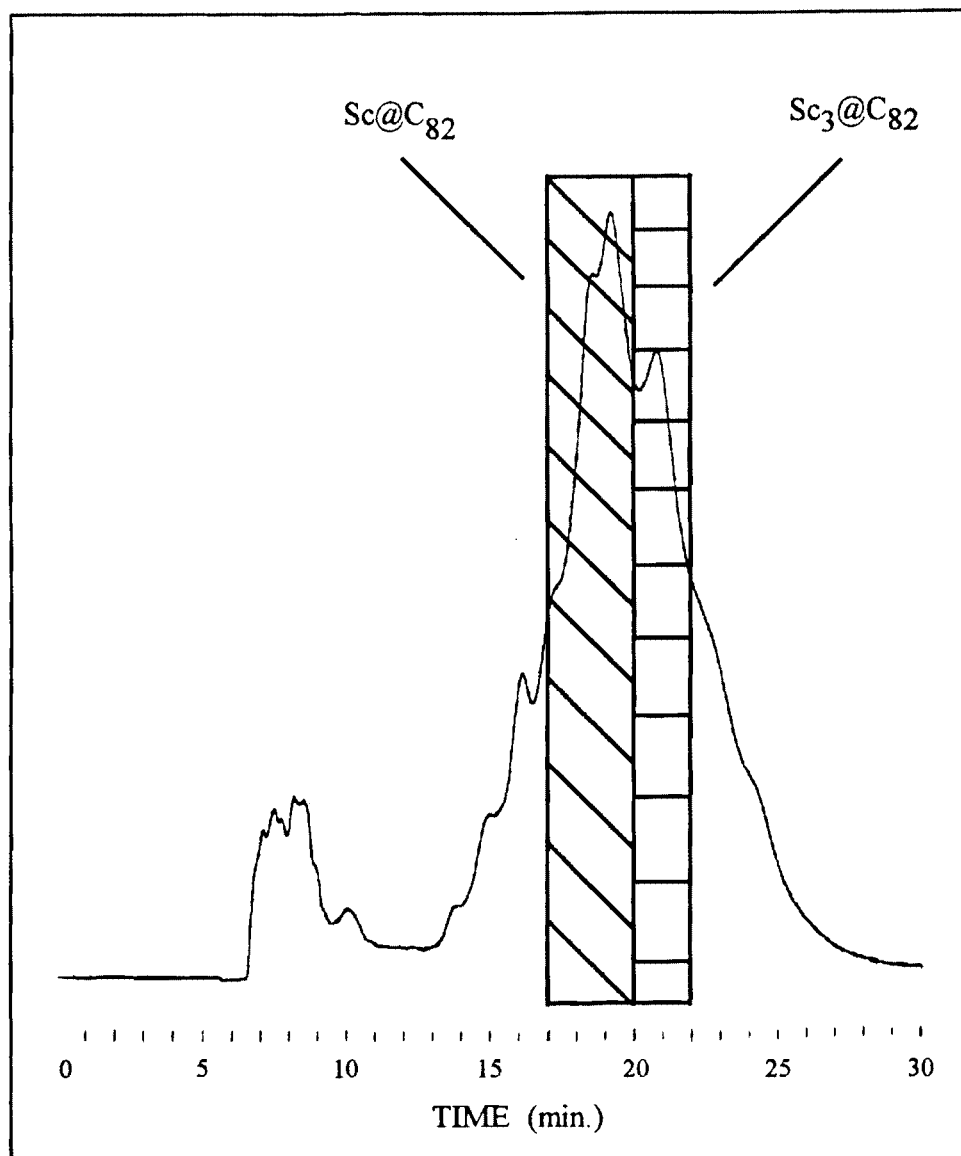


Figure 4.12 HPLC-UV trace, (second Buckyclutcher pass), 450  $\mu\text{L}$  of the 20-26 min.  $\text{Sc}_m\text{@C}_{2n}$  EPR active fraction, 2.0 mL/min, 80:20 toluene/decalin, and 340 nm detection.

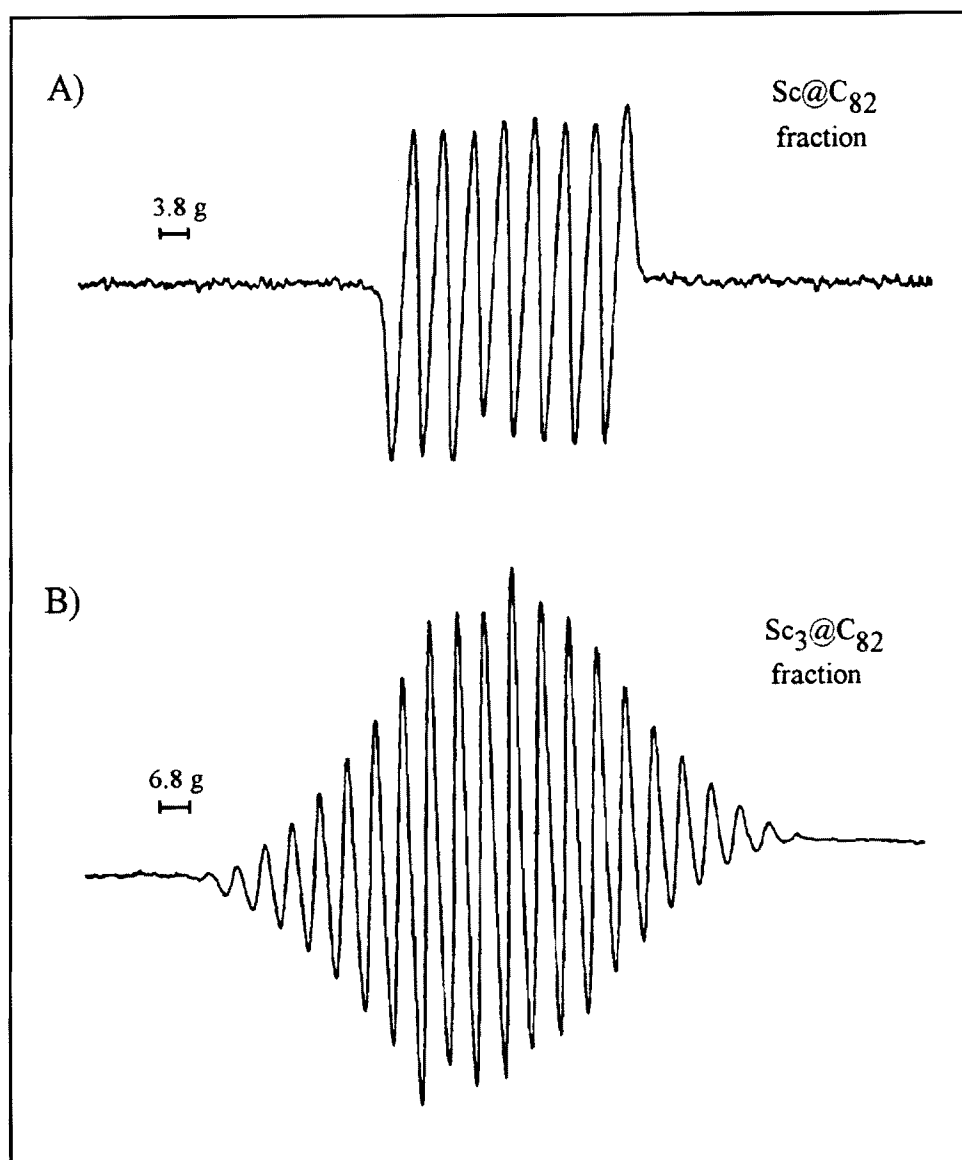


Figure 4.13 Off-line EPR spectra corresponding to the experiment from Figure 4.12. (a)  $\text{Sc@C}_{82}$  fraction, sweep width 100 g, 100 s/scan, 4 scans/file, 9.63 GHz, in decalin. (b)  $\text{Sc}_3\text{@C}_{82}$  fraction, sweep width 150 g, 100 s/scan, 4 scans/file, 9.63 GHz, in decalin.



#### 4.12 $Y_m@C_{2n}$

Because  $Y_m@C_{2n}$  species were desired for  $^{89}Y$  NMR and dynamic nuclear polarization (DNP) experiments, research efforts also focused on separations involving yttrium metallofullerenes. Since a typical starting yttrium stock solution contains only <1% metallofullerenes, a large amount of  $Y_m@C_{2n}$  raw extract (~8 mg) was injected into the two polystyrene columns (Figure 4.14). To ensure a sufficient quantity of  $Y@C_{82}$  and exceed the detection limits in the flow HPLC-EPR experiment, this high sample loading was employed. Note that the toluene/decalin solvent system permits a relatively high solubility of  $Y_m@C_{2n}$  extract. Therefore, a large sample throughput is possible. In contrast, the fullerenes and metallofullerenes are virtually insoluble in typical reverse-phase solvents (e.g. acetonitrile, water, ether, etc).

Following injection, the UV chromatogram (Figure 4.14a) provides little worthwhile information other than indicating an overloaded column. It is not obvious where any of the metallofullerenes elute relative to the abundant empty-cage fullerenes. Although a lack of chromatographic resolution is indicated in the HPLC-UV trace, the on-line EPR dimension (Figure 4.14b) clearly demonstrates that a significant initial separation of  $Y@C_{82}$  relative to the empty-cage fullerenes has

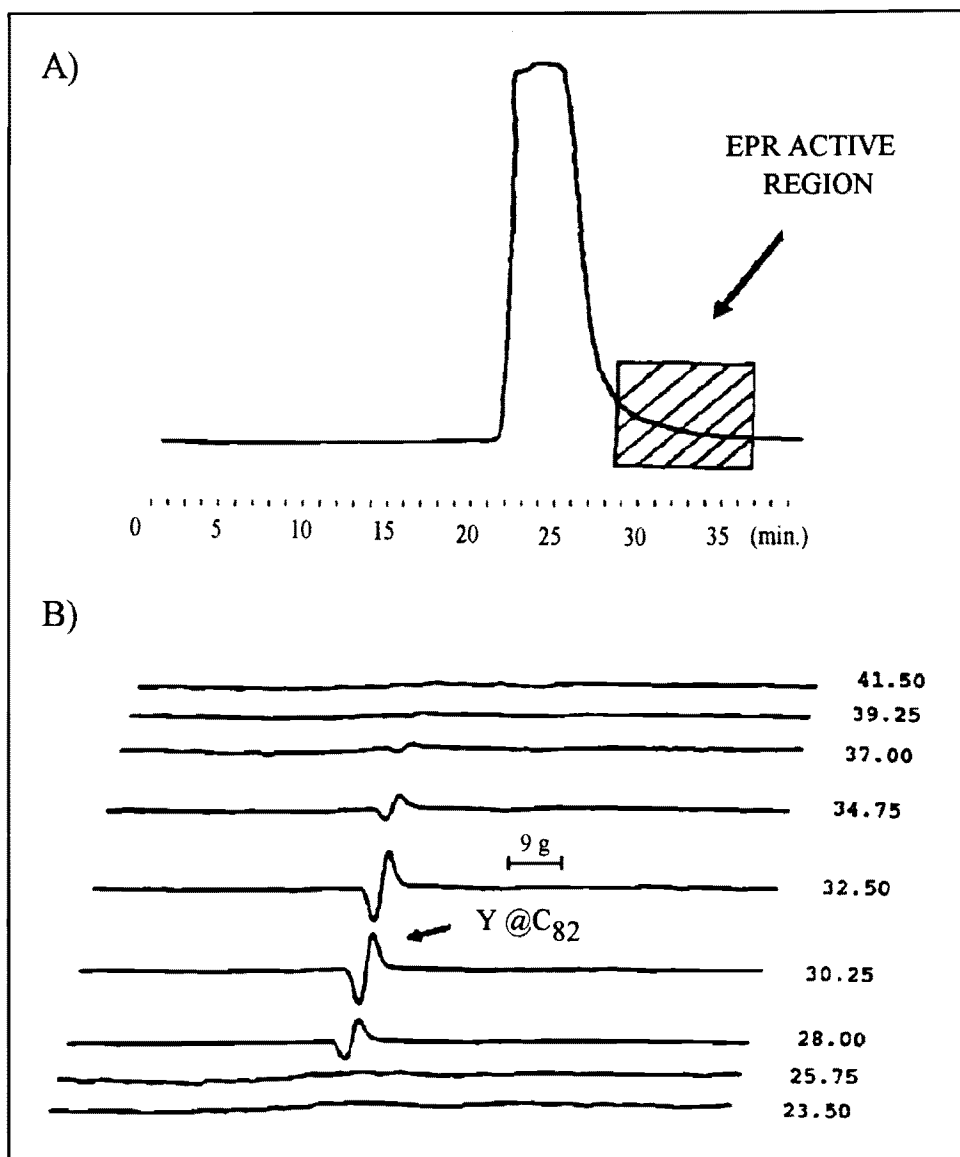


Figure 4.14 (a) HPLC-UV trace of  $Y_m@C_{2n}$  raw extract, first polystyrene pass, 1.0 mL/min, 80:20 toluene/decalin, 8 mg injected, and 340 nm detection. (b) on-line HPLC-EPR spectra, sweep width 130 g, 4 scans/file, and 20 s/sweep. The broad singlet was observed due to low resolution conditions (see Experimental).

occurred. Specifically, an EPR-active chromatographic region from 28 to 37 minutes has been established for  $Y@C_{82}$  as denoted by the cross-hatched region. The extremely small area under the curve is also consistent with a low (<1%) abundance of the  $Y_m@C_{2n}$  species in the initial stock solution. For comparison, the dominant peak (unshaded region) consists of the empty-cages  $C_{60} - C_{92}$  with retention times ranging from 23 - 29 minutes, respectively. Since true size exclusion chromatography (SEC) is not observed, these large differences in retention times (5 - 10 min) between the empty-cage  $C_{60}$  region and  $Y@C_{82}$  have been attributed to weak " $\pi$ - $\pi$ " interactions of the  $Y_m@C_{2n}$  species with the polystyrene substrate.

At this point, the EPR active region (tailing portion of the UV trace) was not resolved from the empty-cage fullerenes. Thus a sequence of "recovery and re-injection" steps for this  $Y@C_{82}$  fraction was performed to improve the separation. Following two initial polystyrene passes, mass spectral data of the EPR active fraction indicated the presence of  $Y@C_{82}$  in addition to the di-yttrium metallofullerenes ( $Y_2@C_{80} - Y_2@C_{104}$ ) and empty-cage fullerenes  $C_{60} - C_{120}$ . The composition of the pre- and post-regions to the EPR active fraction was determined. Mass spectra of these samples indicated the presence of only empty-cage fullerenes of various molecular masses. Thus, it was established the entire yttrium metallofullerene profile eluted in the same fraction as  $Y@C_{82}$ . In this manner,

monitoring the paramagnetic  $Y@C_{82}$  species served as a "marker" for the overall metallofullerene region.

In an effort to further remove tailing empty-cage fullerenes from the EPR active fraction, five polystyrene passes were necessary. A summary of the 1st - 5th polystyrene passes is presented in Figure 4.15. The composition of the EPR active fraction after the fifth polystyrene pass is indicated in Figure 4.16. Although most of the lower mass empty-cage  $C_{60}$  -  $C_{92}$  fullerenes have been removed, there are still significant quantities of higher mass  $C_{98}$  -  $C_{106}$  empty-cage fullerenes. Nevertheless, this sample is composed primarily of yttrium metallofullerenes. Specifically, the mono-metal  $Y@C_{82}$  and di-metal species ( $Y_2@C_{80}$  -  $Y_2@C_{98}$ ) are present. The large number of  $Y_2@C_{2n}$  species indicated that the isolation of individual, purified metallofullerenes would be difficult. In contrast to the  $Sc_m@C_{2n}$  separations, there is no corresponding mass spectral evidence for  $Y_2@C_{74}$ ,  $Y_2@C_{76}$ , or the tri-metal  $Y_3@C_{82}$ . Although this  $Y_m@C_{2n}$  "enriched" EPR active fraction could have been further separated with the Buckyclutcher column (analogous to the scandium case), the small amount of sample remaining after five polystyrene passes prevented further purification efforts.

A second objective of the  $Y_m@C_{2n}$  separation process was to establish the retention time of  $Y@C_{82}$  with the Buckyclutcher column. Since the corresponding  $Sc@C_{82}$

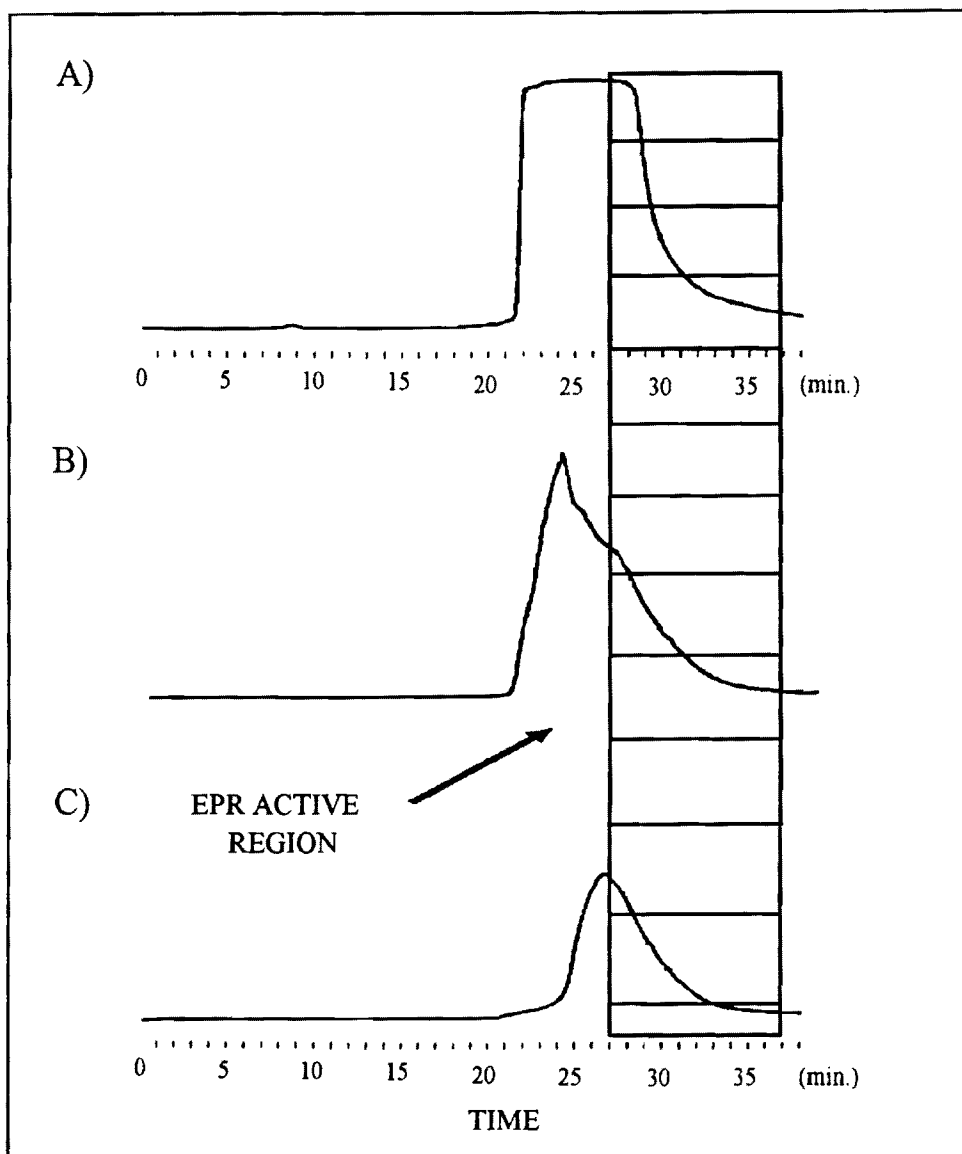


Figure 4.15 HPLC-UV chromatograms for  $Y_m@C_{2n}$  polystyrene injections, 2.0 mL/min, 80:20 toluene/decalin, and 340 nm detection. HPLC profiles represent (a) a first polystyrene pass, (b) a third polystyrene pass, and (c) a fifth polystyrene re-injection of the collected EPR active  $Y_m@C_{2n}$  fraction.

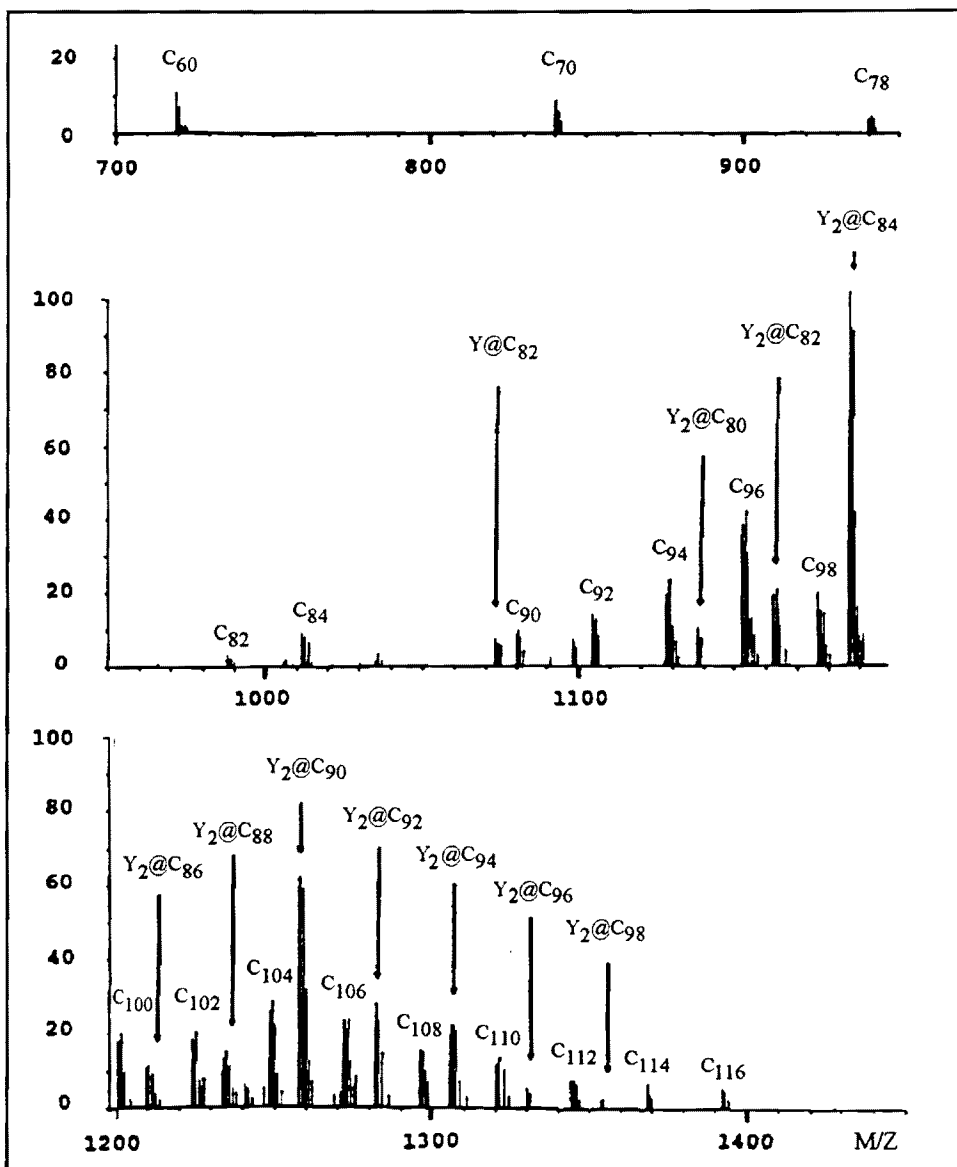


Figure 4.16 Off-line negative-ion mass spectrum of the final, collected  $Y_m@C_{2n}$  EPR active fraction (fifth polystyrene pass). The calibration standard Ultramark 1621 is used.

analog was susceptible to decomposition, it was believed that  $Y@C_{82}$  would also be difficult to monitor. Thus, an effort to perform any experiments with minimal sample handling and time was made. Injection of  $Y_m@C_{2n}$  extract directly into the Buckyclutcher would not permit an accurate retention time due to such a large injection volume and subsequent column overloading. An excessive amount of injected material and corresponding sample volume would be necessary to ensure sufficient  $Y@C_{82}$  in the EPR flow cell. Column overloading and inaccurate retention times would have resulted. Thus, it was necessary to perform at least two polystyrene passes to remove a portion of the abundant empty-cage fullerenes. Although five polystyrene passes would have removed even more empty-cage species, the additional time and sample handling would likely have been detrimental to preventing decomposition. For this reason, only two polystyrene clean-up passes of the EPR active region were performed.

Next, 500  $\mu$ L of this  $Y@C_{82}$  - concentrated sample was injected into the Buckyclutcher. The UV trace (Figure 4.17a) reveals at least 15 distinct peaks, and it is not possible to determine which one corresponds to  $Y@C_{82}$  with conventional UV detection alone. However, the on-line EPR profile (Figure 4.17b) clearly indicates the presence of  $Y@C_{82}$  at 17.3 minutes. It should be emphasized that on-line HPLC-EPR identified fraction #5 as containing  $Y@C_{82}$  without the necessity of

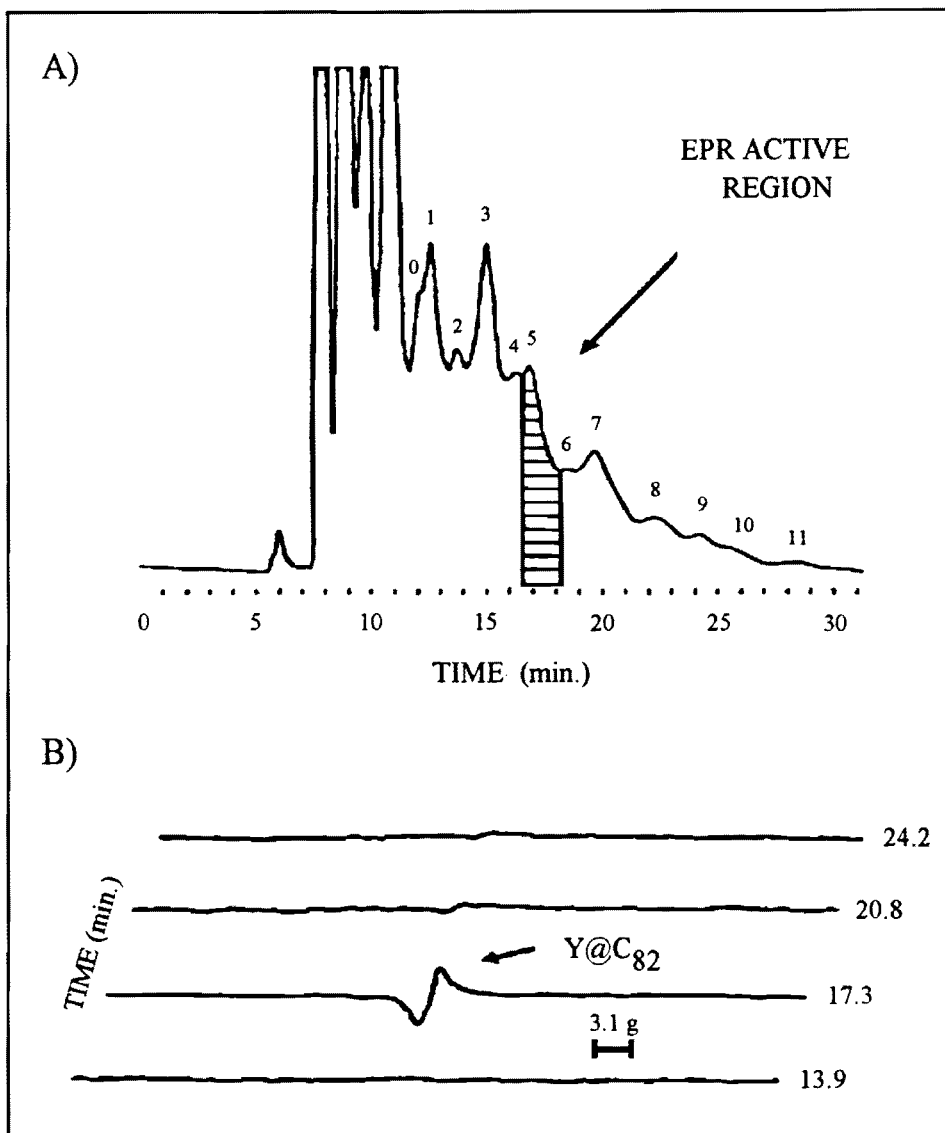


Figure 4.17 (a) HPLC-UV trace (340 nm), Buckyclutcher column, 2.0 mL/min of 80:20 toluene/decalin, and 250  $\mu$ L injection of the  $Y_m@C_{2n}$  EPR active fraction obtained from the final polystyrene pass. (b) on-line HPLC-EPR profile, 9.56 GHz, 3 scans/file, and 20 s/scan. Alternate files are not shown.



off-line fraction collection and characterization. The high selectivity of on-line EPR detection and its ability to chromatographically monitor labile species was demonstrated. Although a doublet with a small hyperfine coupling (0.48 G) has recently been reported for  $Y@C_{82}$  ( $I=1/2$ ) under high resolution, static conditions, the on-line EPR operating conditions (saturation, rapid sweeps, etc) were optimized for an improved signal-to-noise ratio. As a result, this small hyperfine coupling was not observed, and a broadened singlet was obtained. Nevertheless, an EPR active fraction (peak #5; 16.5 - 18.2 min.) was obtained. A recovery and re-injection of peak #5 for a second Buckyclutcher was performed. At this stage, a relatively symmetric UV trace was observed as indicated by Figure 4.18. However, the off-line negative-ion mass spectrum revealed that  $Y_2@C_{84}$  and  $Y_2@C_{90}$  co-eluted with  $Y@C_{82}$ . In addition, the higher mass  $C_{104}$  empty-cage fullerene was also present. At this point, further clean-up and isolation of the individual yttrium metallofullerenes was not attempted. Efforts shifted toward chromatographic separations involving other encapsulated metals (e.g. La, Er).

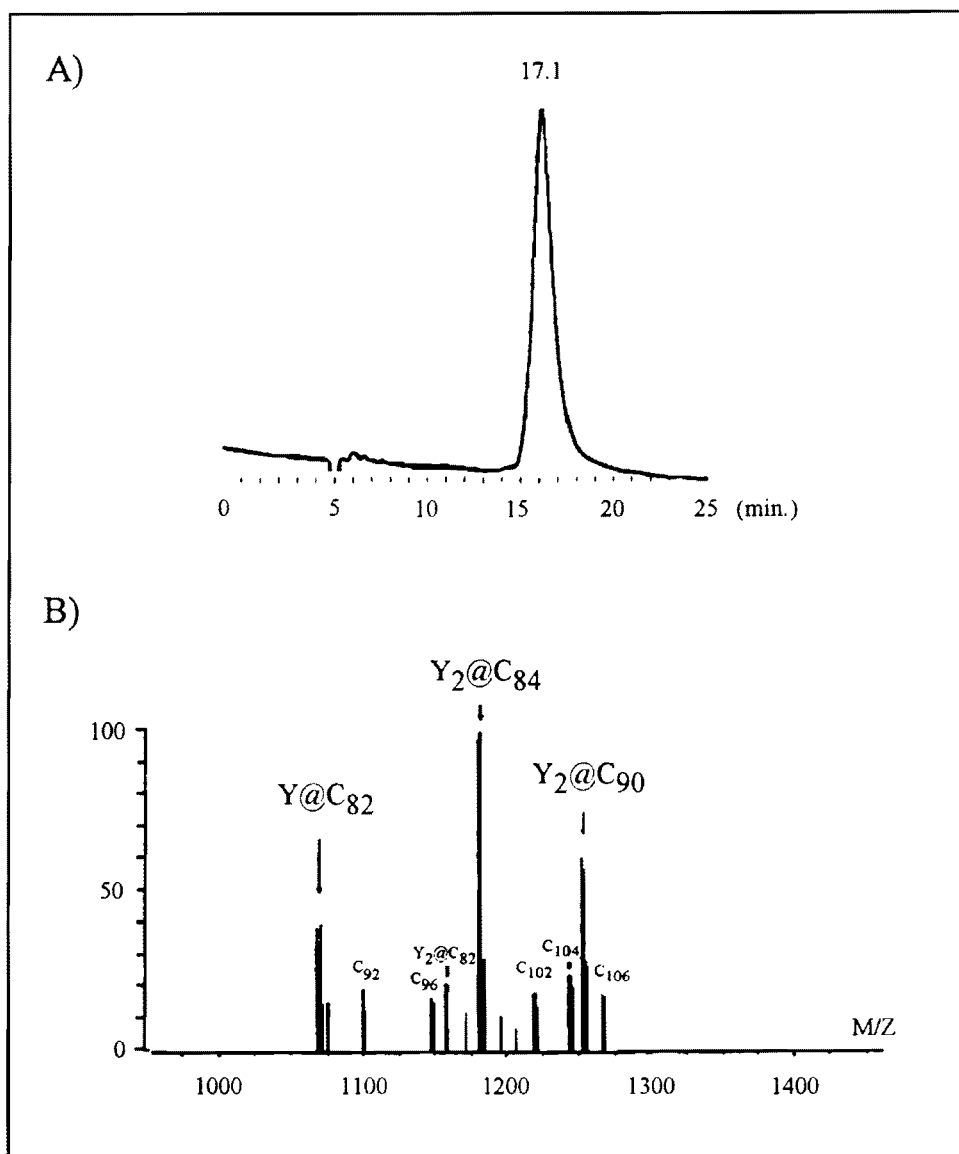


Figure 4.18 (a) Analytical HPLC-UV trace for isolated  $Y_m@C_{82}$  peak #5 (EPR active region), Buckyclutcher column, 2.0 mL/min, and 340 nm detection. (b) off-line negative ion mass spectrum of peak #5

### 4.13 $\text{La}_m@C_{2n}$

Depending on the production methodology, a lanthanum-containing raw extract can possess fewer metallofullerene species to separate. In a typical  $\text{La}_m@C_{2n}$  stock solution, the mono-metal  $\text{La}@C_{82}$  is often the most dominant metallofullerene with certain di-metal  $\text{La}_2@C_{2n}$  species also being abundant. For these reasons, it was initially believed that  $\text{La}@C_{82}$  could be readily isolated.

From ~50 mg of raw  $\text{La}_m@C_{2n}$  extract, a stock solution was made at 3 mg/mL. Since the  $\text{La}@C_{82}$  on-line detection limits were not established, a relatively large sample volume (5 mL) was injected. The resulting chromatogram (Figure 4.19a) once again suggests an overloaded column with poor resolution. Analogous to both the  $\text{Sc}_m@C_{2n}$  and  $\text{Y}_m@C_{2n}$  case, this  $\text{La}_m@C_{2n}$  chromatogram is similar in that the  $\text{La}@C_{82}$  EPR active region also occurs underneath the tailing region of the peak. Specifically, the EPR active region (Figure 4.19b) occurs between 28 and 35 minutes. Once again, the unshaded region consists of lower mass  $C_{60}$  -  $C_{84}$  empty-cage fullerenes. To effectively remove these empty-cage contaminants, five polystyrene passes were necessary. The 1<sup>st</sup>, 3<sup>rd</sup>, and 5<sup>th</sup> pass UV traces are summarized in Figure 4.20. The chromatogram and on-line HPLC-EPR spectra (Figure 4.21) for the 5<sup>th</sup> polystyrene pass clearly demonstrate that the EPR active region corresponds to the final peak on

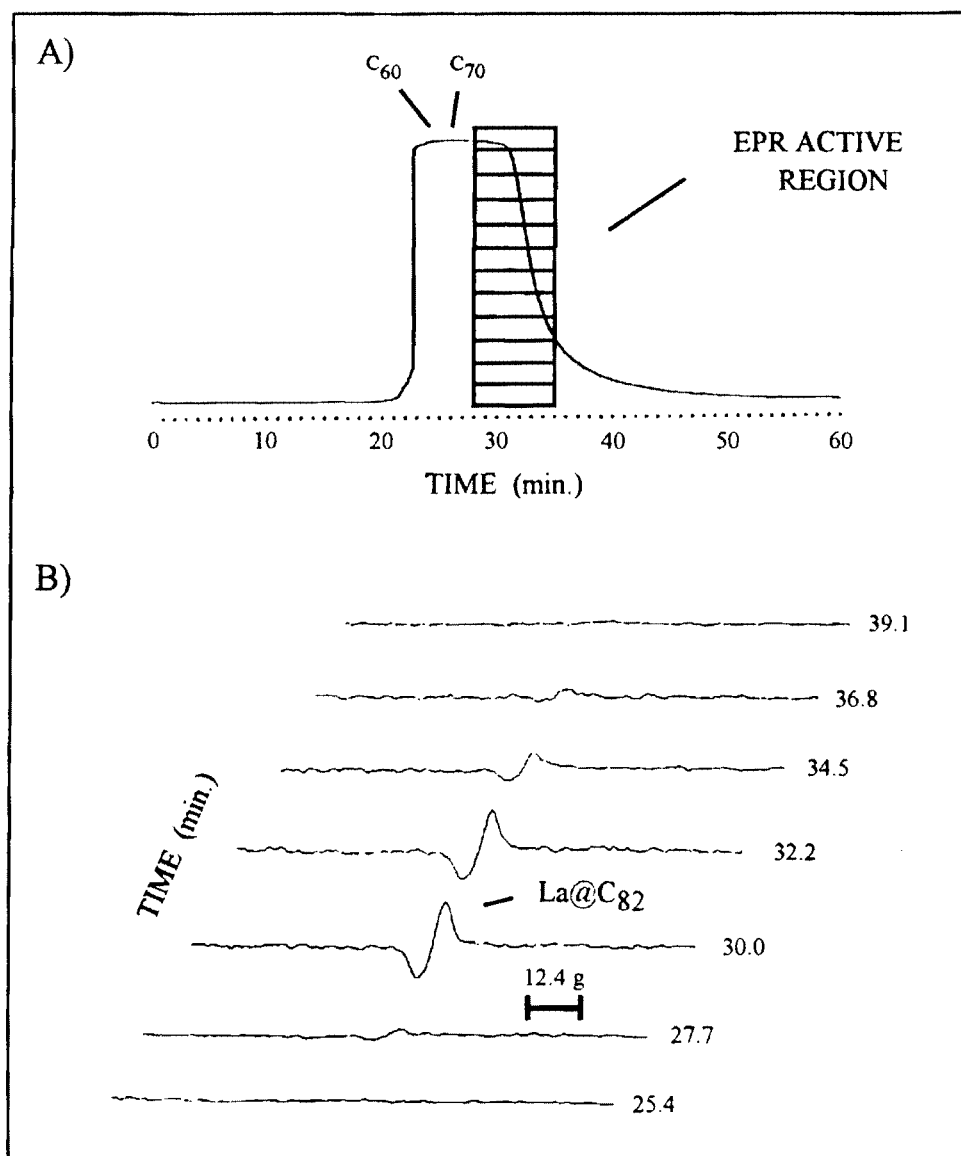


Figure 4.19 (a) HPLC-UV trace of 10 mg  $La_m@C_{2n}$  raw extract, first polystyrene pass, 1.0 mL/min, 80:20 toluene/decalin, and 340 nm detection. (b) on-line HPLC-EPR profile, 4 scans/file, 20 s/scan, sweep width 130 G, and 9.55 GHz.

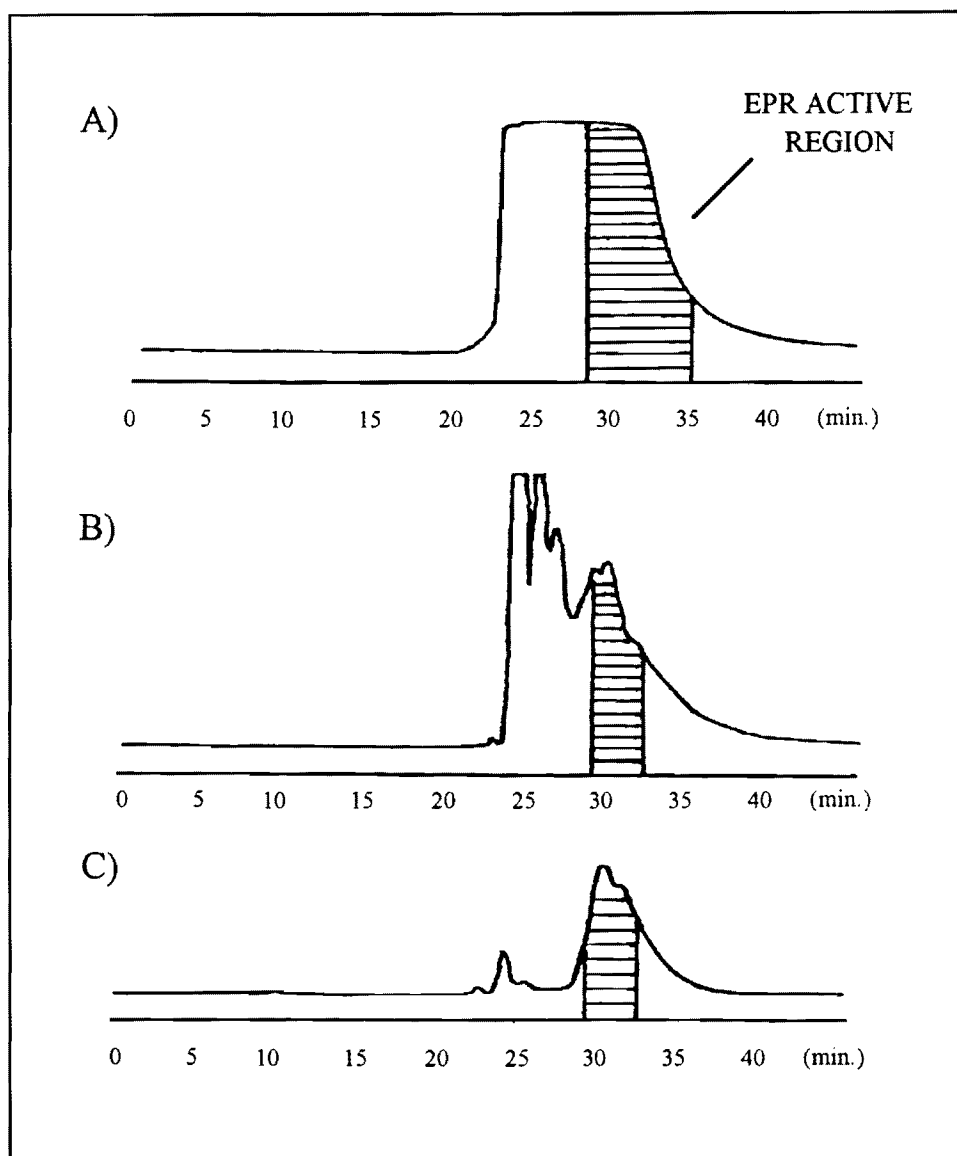


Figure 4.20 HPLC-UV trace representing the recovery and re-injection of the EPR active  $L_{a_m}@C_{2n}$  fraction: (a) first polystyrene pass, (b) third polystyrene pass, and (c) fifth polystyrene pass. Chromatographic conditions: 1.0 mL/min, 80:20 toluene/decalin, and 340 nm detection.

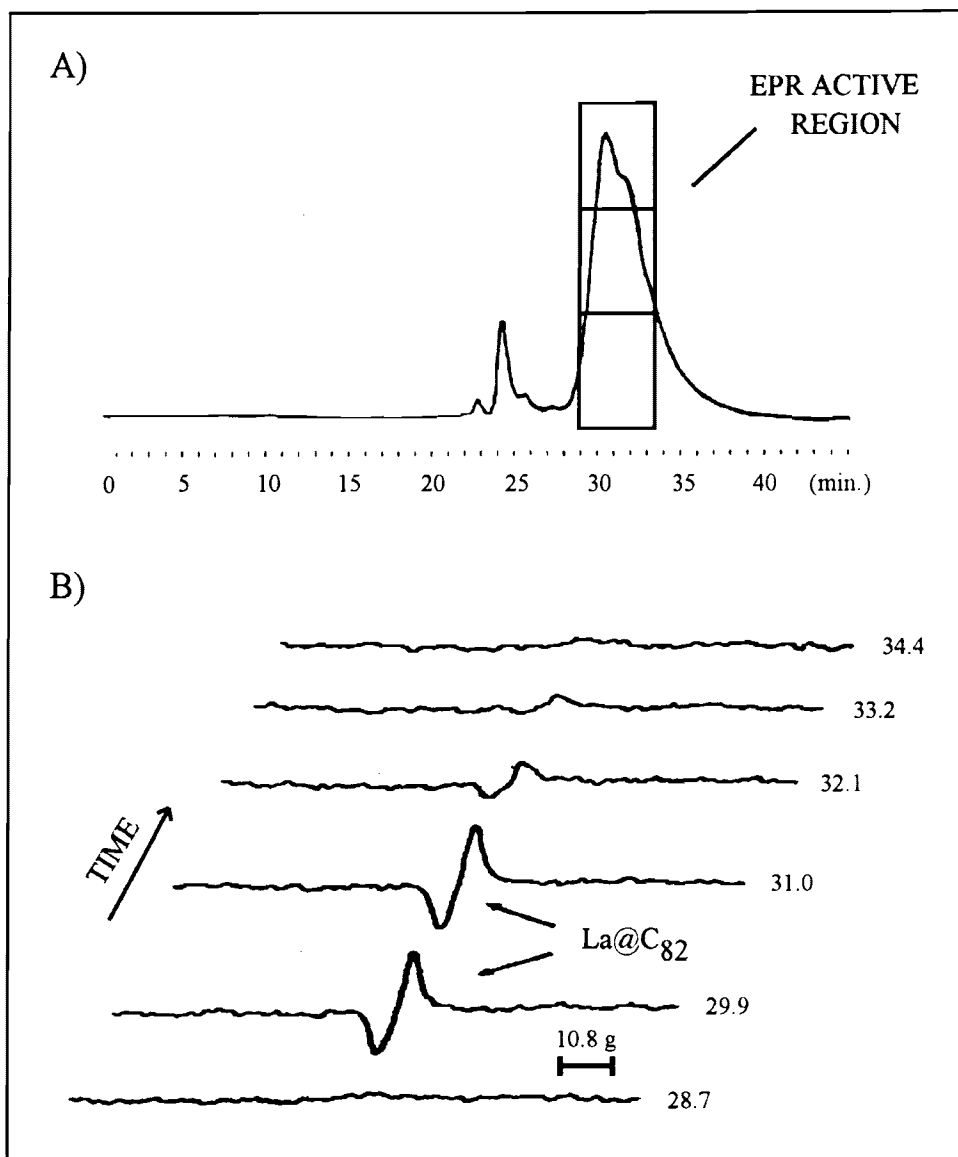


Figure 4.21 HPLC-UV trace of the fifth polystyrene pass, 1.0 mL/min, 80:20 toluene/decalin, 340 nm detection, and 200  $\mu$ L of  $\text{La}_m@C_{7n}$  sample. (b) on-line HPLC-EPR profile, 2 scans/file, 20 s/sweep, sweep width 130 g, and 9.55 GHz.

the chromatogram. Note that the expected octet for  $\text{La}@C_{82}$  ( $I = 7/2$ ) was observed as a broadened singlet. This feature is due, in part, to rapid scanning, oversaturation, and a small hyperfine coupling constant (1.2 g). An off-line negative-ion mass spectrum of this EPR active fraction revealed that  $\text{La}@C_{82}$  and  $\text{La}_2@C_{72}$  were the dominant peaks. However, low but significant levels of higher mass empty-cage  $C_{96}$  -  $C_{112}$  were also present.

Next, this metallofullerene sample was injected into the selective Buckyclutcher column to observe whether a series of resolvable peaks could be obtained. The chromatogram following a 110  $\mu\text{L}$  injection is presented in Figure 4.22. Note that the four dominant metallofullerene peaks are peaks #0, 3, 4, and 5. To determine which peak was the EPR active  $\text{La}@C_{82}$ , a subsequent injection was performed with the HPLC-EPR apparatus. According to the on-line EPR spectra, the EPR active region (17.0 to 19.5 min) corresponds to peaks 4 and 5. The composition of peak #0 was still unknown. Two Buckyclutcher passes permitted the isolation of samples corresponding to peaks 0, 4, and 5. Off-line mass spectral data indicated that peak #0 was purified  $\text{La}_2@C_{72}$  (> 98% purity, Figure 4.23) whereas peaks #4 and #5 consisted of  $\text{La}@C_{82}$  (~60% purity) co-eluting with several higher mass  $C_{102}$  to  $C_{106}$  empty-cage fullerenes.

Although < 1 mg of  $\text{La}_2@C_{72}$  sample was obtained, this compound could be very

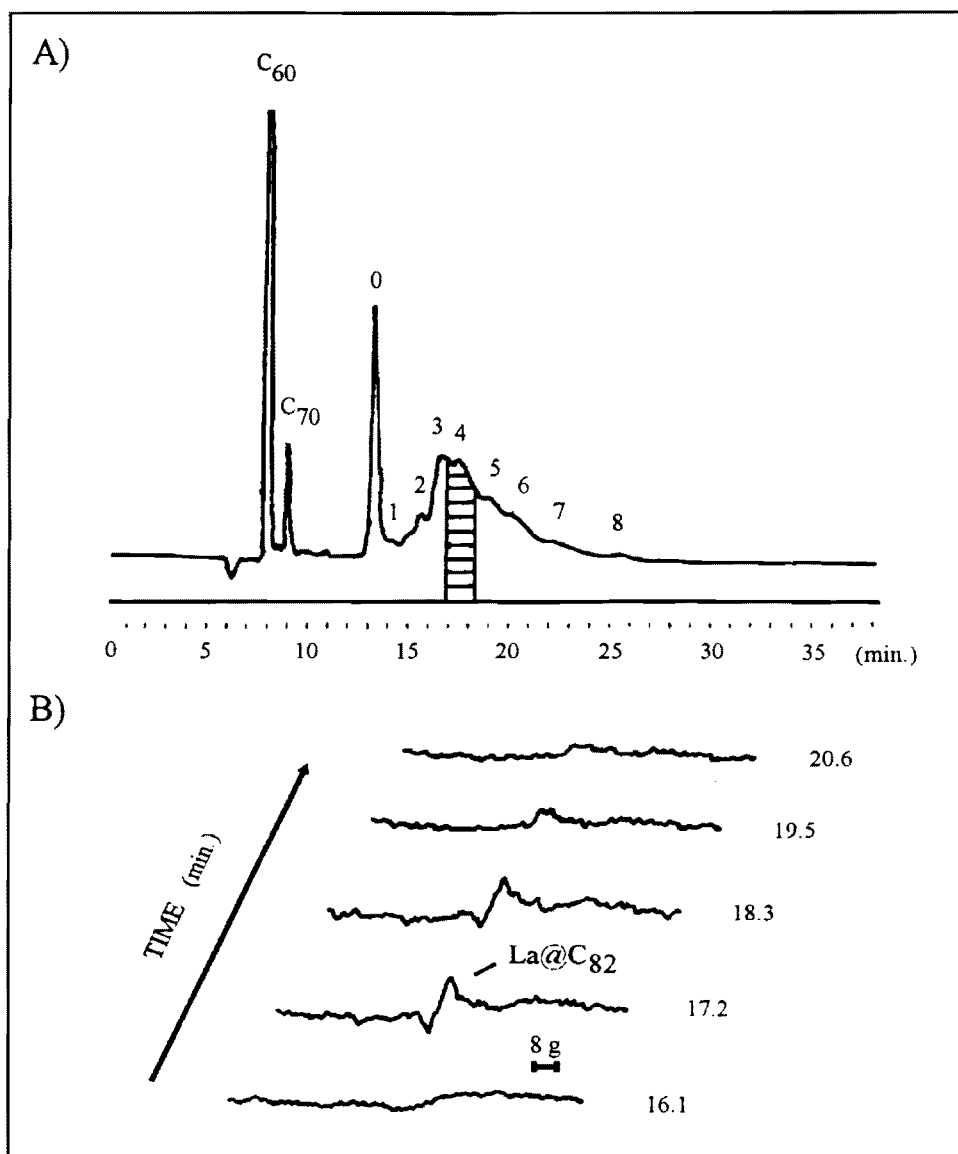


Figure 4.22 Fifth polystyrene pass,  $\text{La}_m@C_{2n}$  EPR active fraction on the Buckyclutcher column: (a) 110  $\mu\text{L}$  injection, 2.0 mL/min, 80:20 toluene/decalin, and 340 nm detection. (b) on-line HPLC-EPR profile, 2 scans/file, 20 s/sweep, sweep width 130 g, and 9.55 GHz.



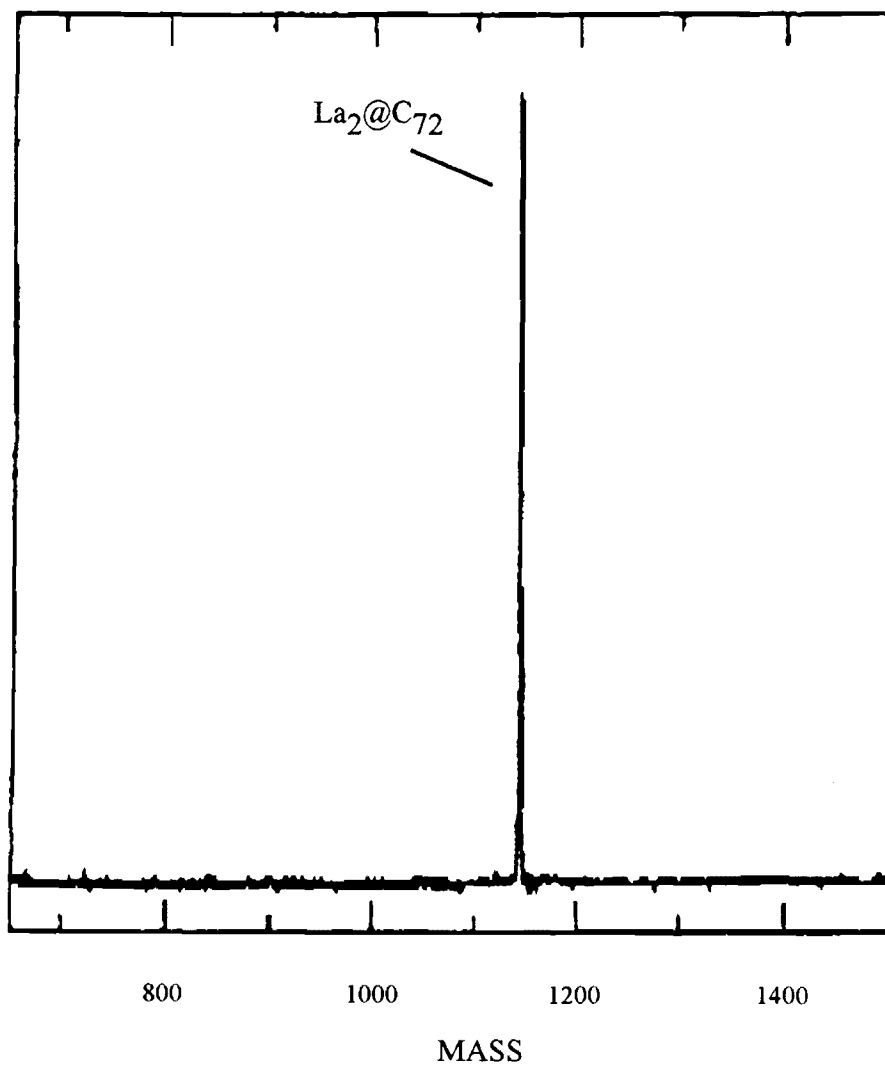


Figure 4.23 LD-TOF mass spectrum of isolated  $\text{La}_m@C_{2n}$  fraction #0. (mass spectrum courtesy of IBM, Almaden).

useful from  $^{13}\text{C}$  NMR viewpoint. Specifically, the highly symmetrical  $\text{C}_{72} (\text{D}_{6h})^{135}$  empty-cage could yield as few as four  $^{13}\text{C}$  NMR lines - depending on the position of the two lanthanum atoms inside the cage. At this writing, a definitive  $^{13}\text{C}$  NMR spectra elucidating the carbon cage structure of any endohedral metallofullerene has not been published.

#### 4.14 $\text{Er}_m@C_{2n}$

At this point, a shift toward chromatographic separations of erbium metallofullerenes was initiated for primarily two reasons. First, a preliminary mass spectrum (Figure 4.24) of the erbium raw extract indicated that  $\text{Er}@C_{82}$  and  $\text{Er}_2@C_{82}$  are the only significant metallofullerenes present in the initial stock. As noted in Figure 4.24, there is a paucity of di-metal erbium compounds - especially relative to the scandium and yttrium cases. The high abundance of  $\text{Er}_2@C_{82}$  and  $\text{Er}@C_{82}$  in the initial raw extract rendered  $\text{Er}@C_{82}$  quite amenable to chromatography and off-line sample handling. In addition, it was anticipated that  $\text{Er}@C_{82}$  would be sufficiently stable to oxygen. Note that with the previous mono-metal  $\text{Sc}@C_{82}$ ,  $\text{Y}@C_{82}$ , and  $\text{La}@C_{82}$  separations, the time-consuming safeguards and constant anxiety of their possible decomposition made these compounds difficult to handle. Finally, it was

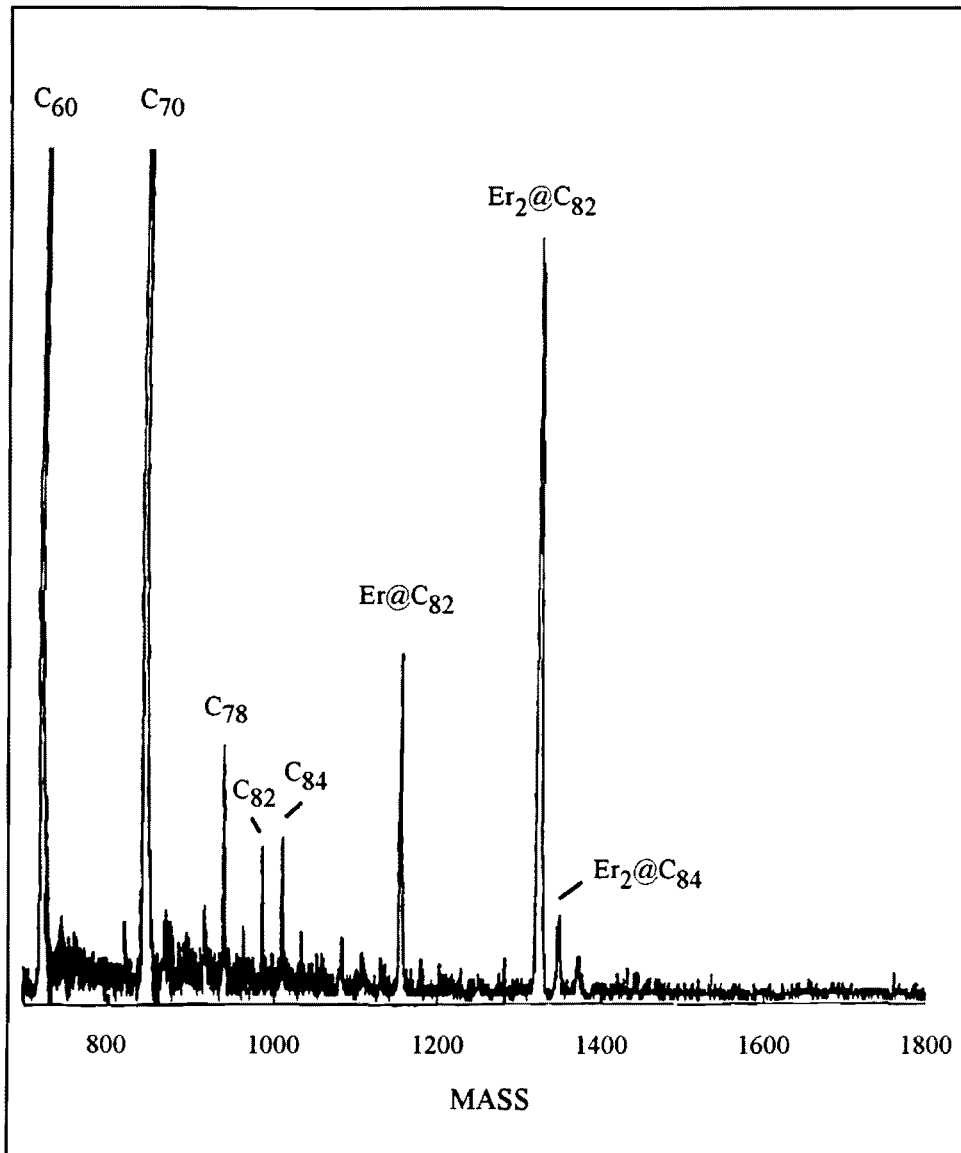


Figure 4.24 LD-TOF mass spectrum of  $Er_m@C_{2n}$  raw extract. (mass spectrum courtesy of IBM, Almaden).

predicted that  $\text{Er}_m@C_{2n}$  species could possess optical-limiting or non-linear optical properties.

Thus, a stock solution (3 mg/mL) of  $\text{Er}_m@C_{2n}$  was made and subsequently injected into two Buckyclutcher columns connected in series (Figure 4.25). Off-line mass spectra for these peaks were obtained. According to mass spectral data, three isomers (I,II, and III) of  $\text{Er}_2@C_{82}$  were observed in three distinct peaks. For this experiment, 400 - 500 mg of additional  $\text{Er}_m@C_{2n}$  extract was then separated and fraction collection focused on these three regions. After "recovery and re-injection" using a second Buckyclutcher pass, three samples containing I,II, and III of improved purity were obtained. Off-line mass spectra confirmed  $\text{Er}_2@C_{82}$  as a dominant peak for each fraction. A mixture of these three samples was made and subsequently injected into the Buckyclutcher column. The chromatogram (Figure 4.26) clearly indicates three well-resolved peaks corresponding to  $\text{Er}_2@C_{82}$  isomers I, II, and III.

However, these three samples were not yet pure. There were still low-lying levels of higher mass  $C_{100}$  -  $C_{106}$  empty-cage fullerenes present. To remove these contaminants, a tetraphenyl-porphyrin (TPP) column was utilized with  $\text{CS}_2$  as the mobile phase. The high solubility of the metallofullerenes in carbon disulfide permitted improved sample throughput. As an example, 500  $\mu\text{L}$  of the isomer III  $\text{Er}_2@C_{82}$  sample was injected into the TPP. The chromatogram (Figure 4.27) revealed

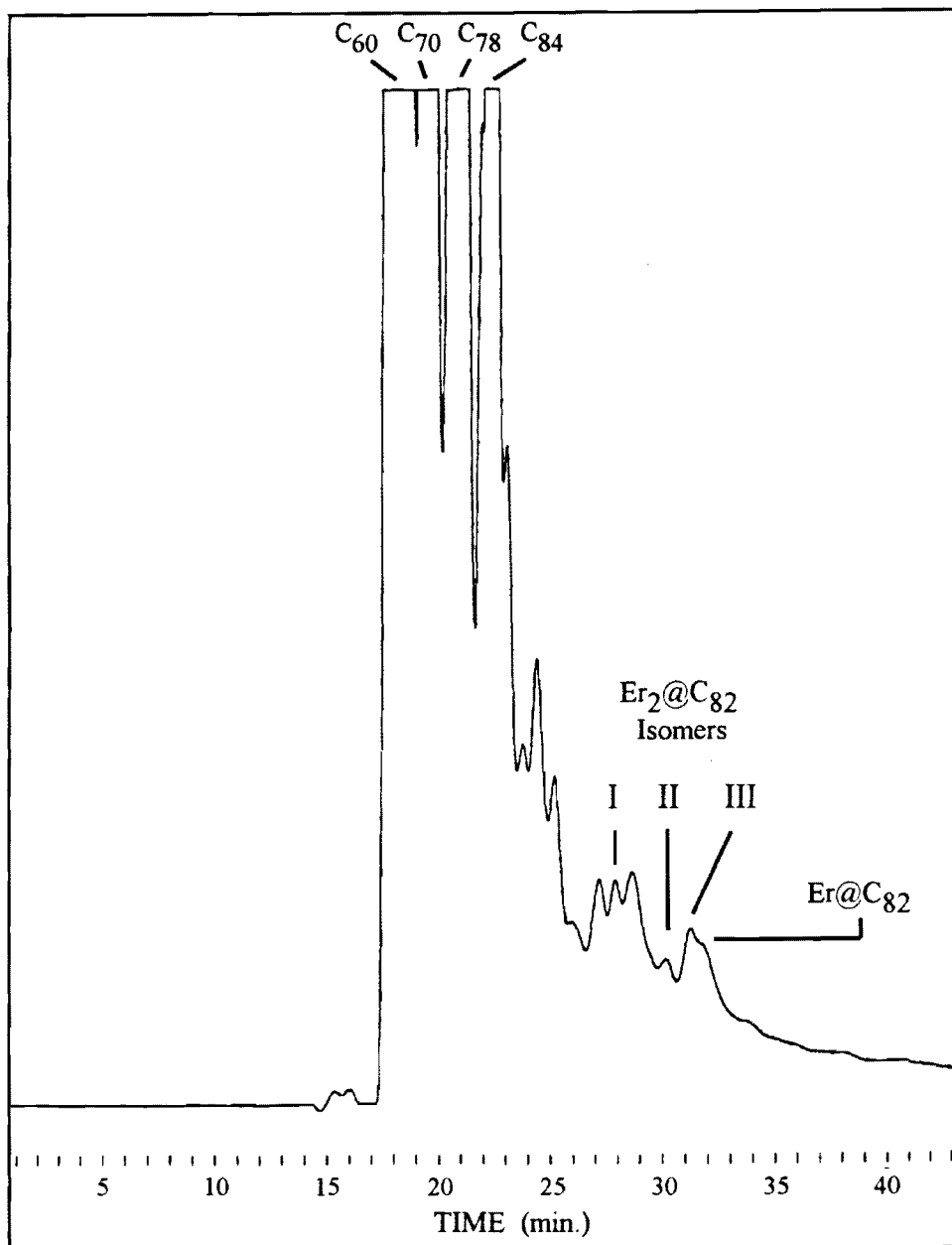


Figure 4.25 HPLC-UV trace of  $\text{Er}_m@C_{2n}$  raw extract, Buckyclutcher column, 200  $\mu\text{L}$  injection, 1.2 mL/min, 80:20 toluene/decalin, and 354 nm UV detection.

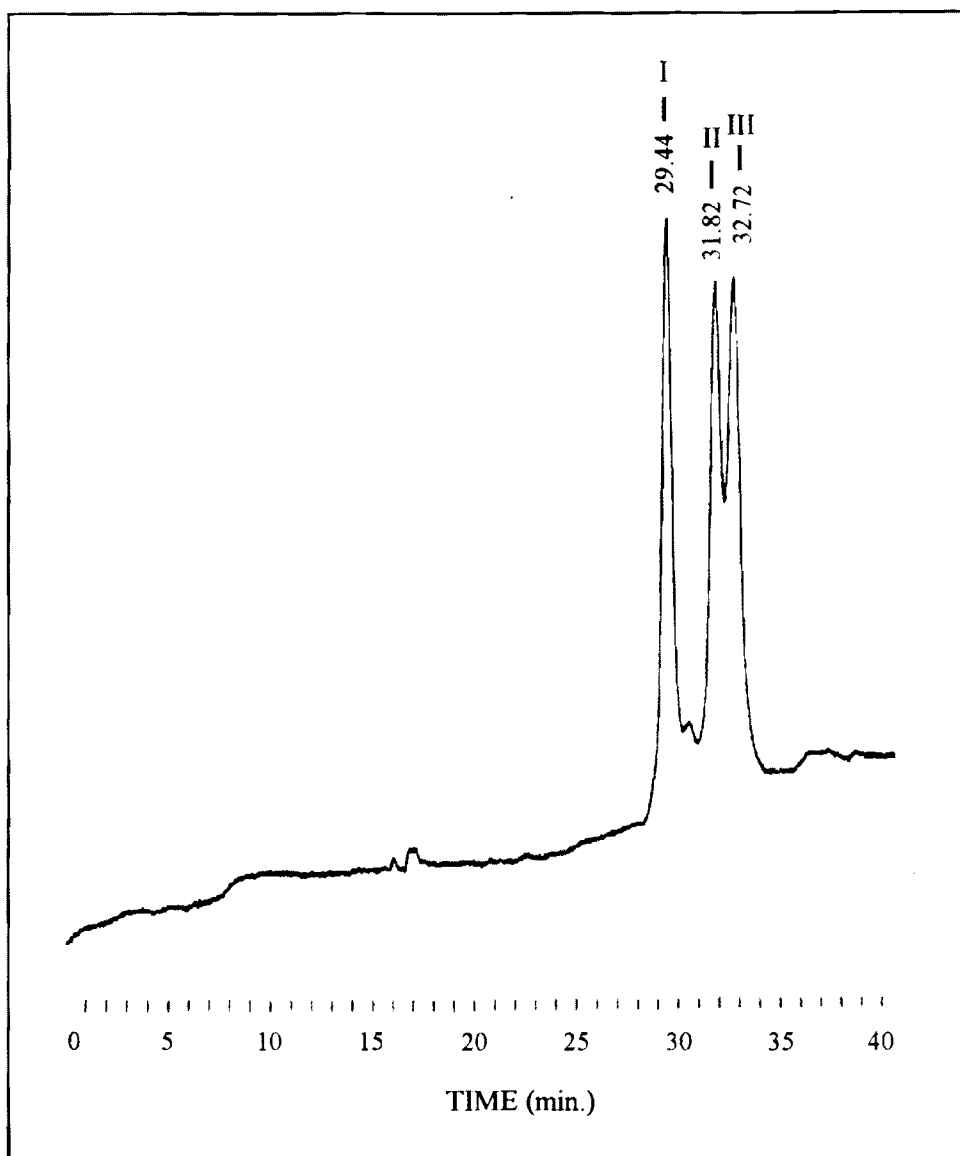


Figure 4.26 HPLC-UV trace of  $\text{Er}_2@C_{82}$  isomers I, II, and III. Chromatographic conditions: Two Buckyclutcher columns in series, 1.55 mL/min, 80:20 toluene/decalin, and 340 nm UV detection.

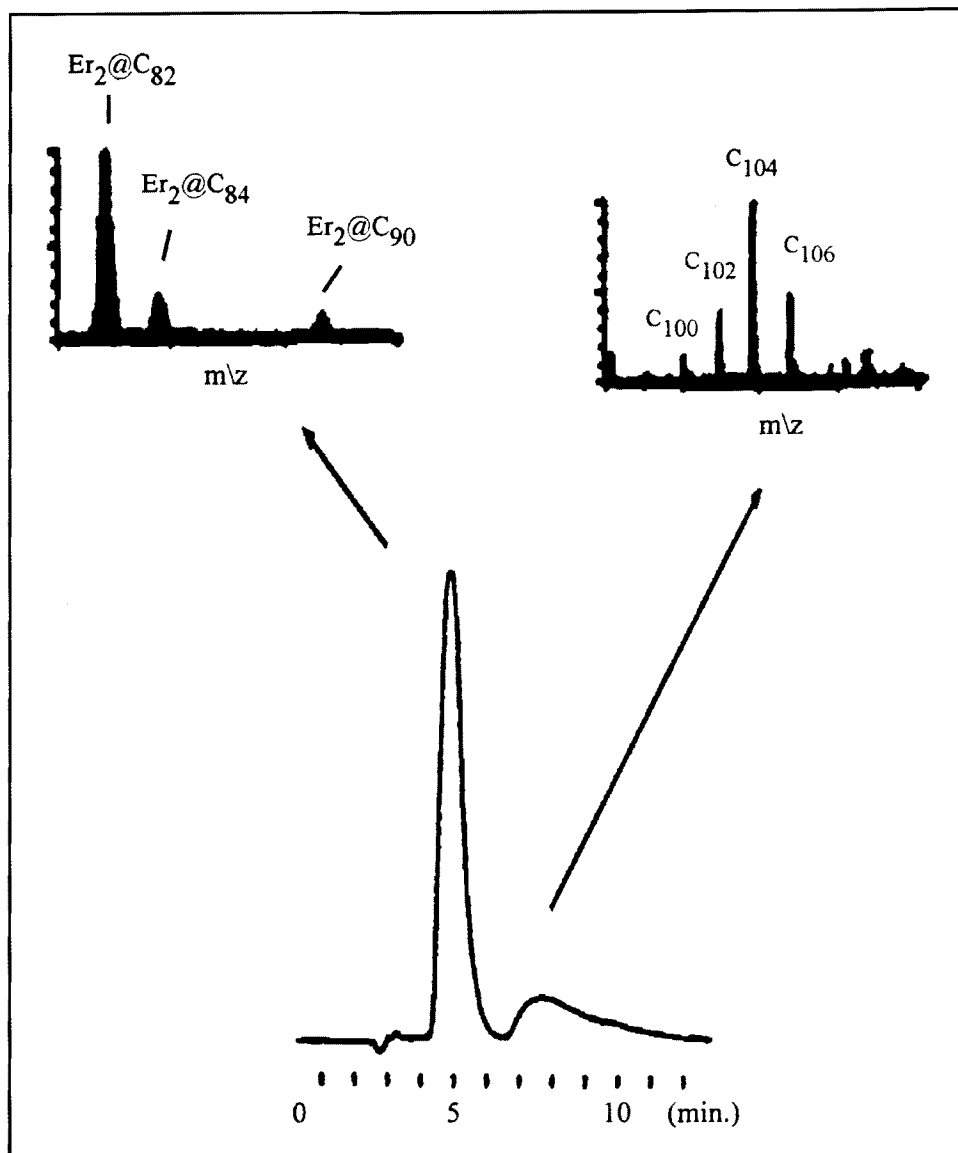


Figure 4.27 HPLC-UV chromatogram for an  $Er_2@C_{2n}$  (isomer III fraction), sample obtained from initial Buckyclutcher separations. Chromatographic conditions: TPP column, 1.0 mL/min  $CS_2$ , and 340 nm UV detection.

two peaks which were collected for mass spectral characterization. According to the data, the first peak corresponds to  $\text{Er}_2@C_{82}$  and small amounts of  $\text{Er}_2@C_{84}$  and  $\text{Er}_2@C_{90}$ . In contrast, the second peak contains only higher mass  $C_{100} - C_{106}$  fullerenes. Thus, a methodology to separate empty-cages from  $\text{Er}_m@C_{2n}$  species was developed with this Buckyclutcher/TPP "two-stage" procedure. In contrast to the Sc, Y and La case, it was no longer necessary to perform five polystyrene passes to remove the empty-cage fullerenes. In summary, sample loadability and decreased experimental time were the dominant features of this newly discovered Buckyclutcher/TPP "two-stage" methodology.

At this stage,  $\text{Er}_2@C_{82}$  had not yet been isolated in high purity. Following collection of the first peak ( $\text{Er}_2@C_{2n}$ ), it was soon realized that the TPP column did not adequately resolve the  $\text{Er}_2@C_{84}$  and  $\text{Er}_2@C_{90}$  contaminants. This sample (1st peak) was then injected into the Buckyclutcher column to obtain purified  $\text{Er}_2@C_{82}$  isomer III (> 98% purity). The analytical trace and mass spectrum for this highly purified sample are presented in Figure 4.28. The other samples (I and II) were also separated with the same methodology as just described for isomer III. Isomer I was a 50/50 mixture of  $\text{Er}_2@C_{82}$  and  $\text{Er}_2@C_{84}$ . In contrast, isomer II was pure  $\text{Er}_2@C_{82}$  (> 90% purity).

As previously discussed, one objective was to isolate the mono-metal  $\text{Er}@C_{82}$



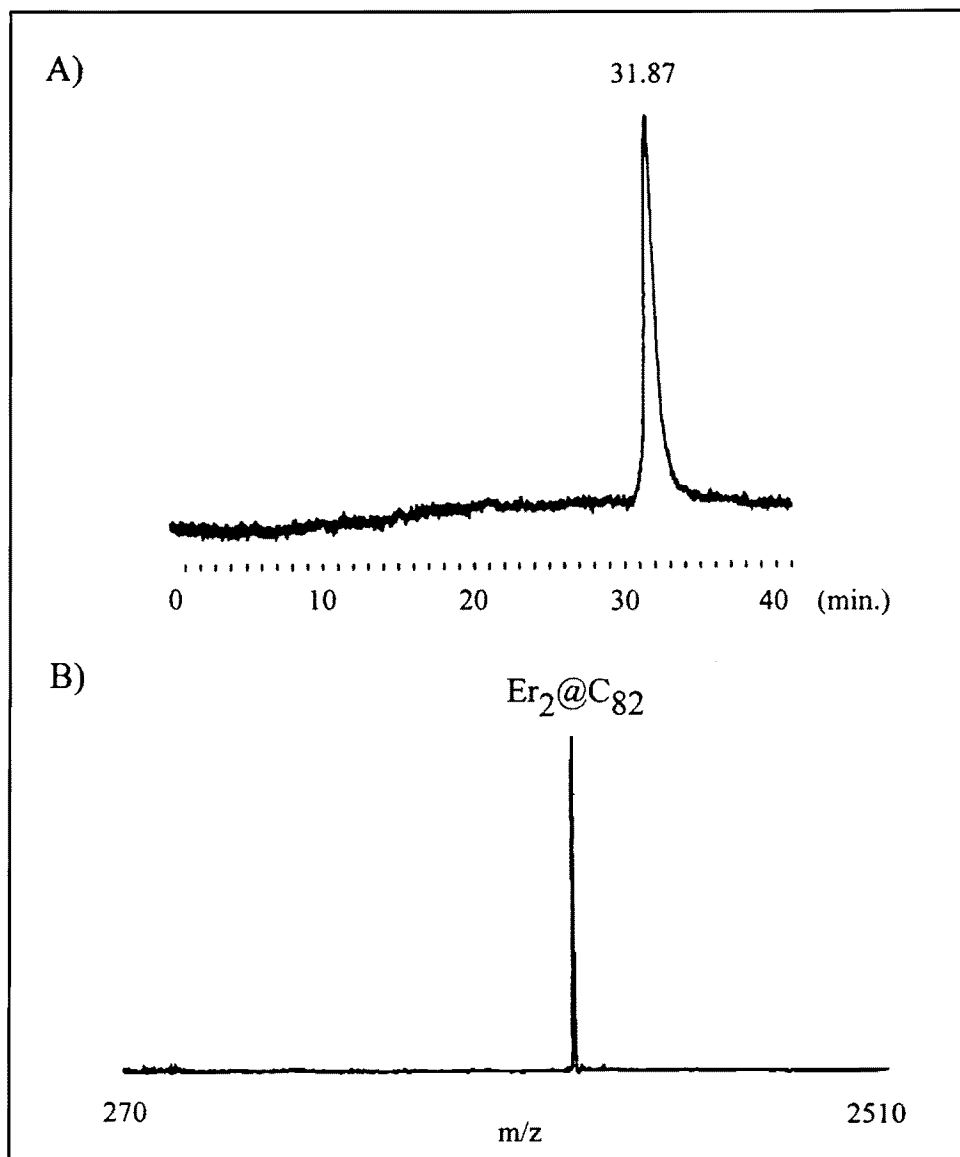


Figure 4.28 (a) HPLC-UV analytical trace for isolated Er<sub>2</sub>@C<sub>82</sub> (isomer III), Buckyclutcher columns, 1.0 mL/min, 80:20 toluene/decalin, and 340 nm detection. (b) LD-TOF mass spectrum of above (courtesy of IBM, Almaden).

species. Chromatographically,  $\text{Er@C}_{82}$  was located beyond  $\text{Er}_2\text{@C}_{82}$  (III) through off-line mass spectra of collected Buckyclutcher fractions. The fraction containing  $\text{Er@C}_{82}$  was then injected into the TPP column for further separation, and a new  $\text{Er@C}_{82}$  sample (~60 % purity, Figure 4.29) from the TPP was obtained.

Attempts were now made to isolate other erbium metallofullerenes (e.g.  $\text{Er}_2\text{@C}_{88}$ ,  $\text{Er}_2\text{@C}_{92}$ , etc) which were present as low abundant species in the initial raw extract. Chromatographically,  $\text{Er}_2\text{@C}_{92}$  was located beyond  $\text{Er@C}_{82}$  during the initial Buckyclutcher clean-up procedure. This  $\text{Er}_2\text{@C}_{92}$  fraction obtained from the Buckyclutcher was then injected into the TPP column for removal of other  $\text{Er}_2\text{@C}_{2n}$  and higher-mass empty-cage fullerenes. A re-injection into the Buckyclutcher column yielded an isolated  $\text{Er}_2\text{@C}_{92}$  sample (~80% purity). The analytical trace and mass spectrum are presented in Figure 4.30.

## 4.2 Improved Separation Methodology

### 4.21 PBB column

In August 1995, another chromatographic column became commercially available. This pentabromobenzyl-based stationary phase was originally obtained for its high

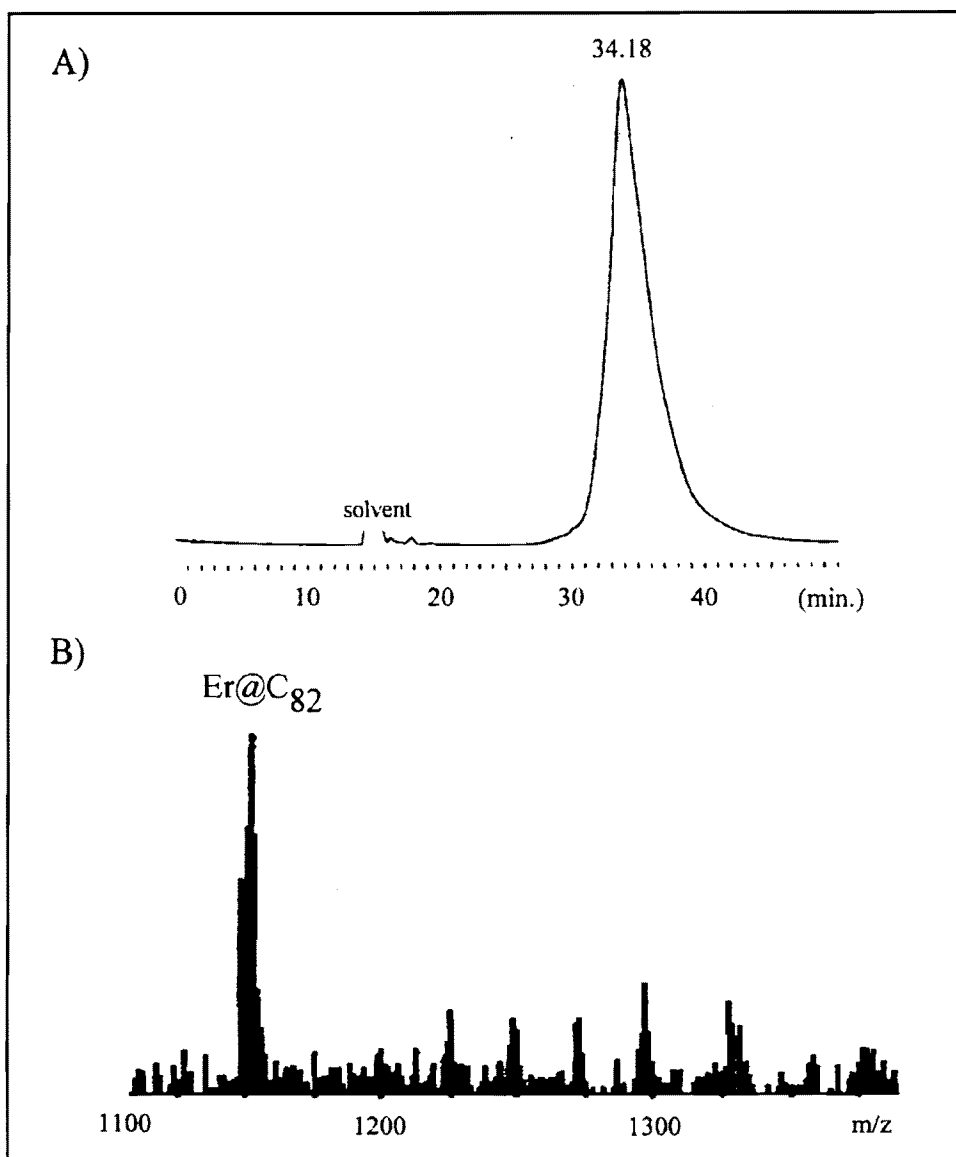


Figure 4.29 Isolated  $\text{Er}@C_{82}$  sample obtained after Buckyclutcher and TPP column separations. (a) HPLC-UV analytical trace, Buckyclutcher columns, 1.0 mL/min, 80:20 toluene/decalin, and 340 nm UV detection. (b) negative-ion chemical ionization mass spectrum of above using Ultramark 1621 as the calibration standard.

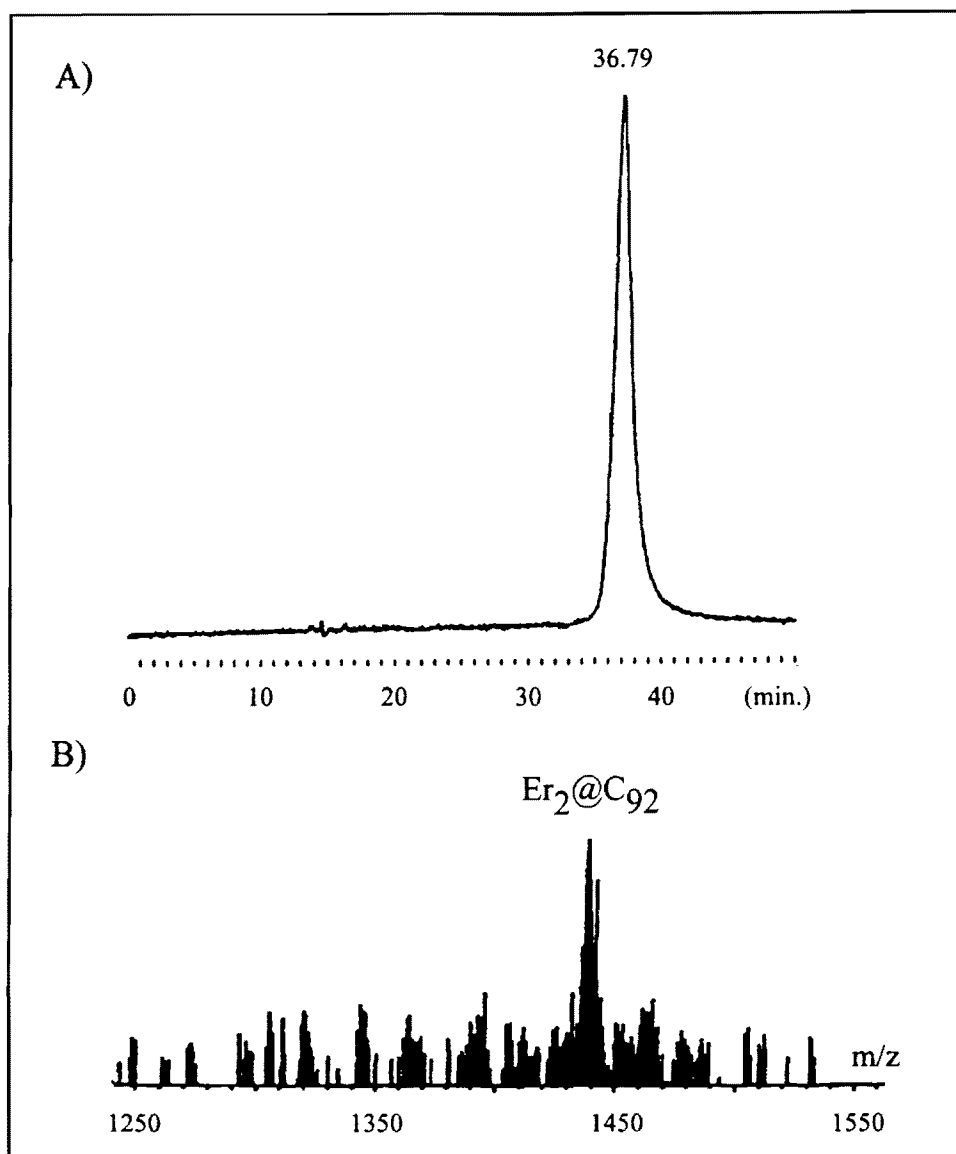


Figure 4.30 Isolated Er<sub>2</sub>@C<sub>92</sub> sample obtained after Buckyclutcher and TPP column separations. (a) HPLC-UV analytical trace, Buckyclutcher columns, 1.0 mL/min, 80:20 toluene/decalin, and 340 nm UV detection. (b) negative-ion chemical ionization mass spectrum of above using Ultramark 1621 as the calibration standard.

sample loadability. With carbon disulfide as a mobile phase, this column could handle ~50 mg of injected material. For these separations, 1000 mg of  $\text{Sc}_m@C_{2n}$  initial raw extract was prepared with an increased Sc loading (3-4 %) to produce a higher abundance of  $\text{Sc}_3@C_{82}/\text{Sc}@C_{82}$ . This initial raw extract was separated using the PBB column in conjunction with the automated system as described in Section 4.3. After the initial PBB automated separation, a metallofullerene fraction ( $\text{Sc}_m@C_{74}-\text{Sc}_m@C_{90}$ ) was collected. Note that this fraction overlapped chromatographically with the empty-cage region of  $C_{76} - C_{86}$ .

This metallofullerene-enriched fraction was further separated with the Buckyclutcher column using 80:20 toluene/decalin solvent system. The resulting chromatogram (similar to Figure 4.5) also revealed  $\text{Sc}_m@C_{2n}$  peaks #0 - 6. Each of these peaks was re-injected into the Buckyclutcher column until single peaks were obtained. Each of these seven peaks (#0-6) was then further separated with the PBB column for final purification. (Note that although single peaks were obtained with the Buckyclutcher column, the peak would typically further separate into 5 - 8 additional peaks with the PBB column.) From these separations, additional purified  $\text{Sc}_m@C_{2n}$  samples were obtained. A listing of these isolated metallofullerene samples are summarized in Table 4.2 - Table 4.5.

It should be noted that the mass spectrum for PBB  $\text{Sc}_m@C_{2n}$  fraction 4.B (Table

TABLE 4.2

Composition of Sc<sub>m</sub>@C<sub>2n</sub> fractions (#2 Buckyclutcher series)  
from PBB chromatographic column

PEAK NUMBER	COMPOSITION	RETENTION TIME (min.)
2.A	C82	10.80
2.B	(ScC@C82) ?	11.98
2.C	Sc2@C82	12.24
2.D	Sc2@C86	13.40

TABLE 4.3

Composition of PBB Sc<sub>m</sub>@C<sub>2n</sub> fractions (#3 Buckyclutcher series)  
from PBB chromatographic column

PEAK NUMBER	COMPOSITION	RETENTION TIME (min.)
3.A	Sc <sub>2</sub> @C78	11.40
3.B	(Sc <sub>2</sub> C)@C82 ?	11.77
3.C	Sc <sub>2</sub> @C82	12.31
3.D	Sc <sub>2</sub> @C84	12.62
3.E	Sc <sub>2</sub> @C86	13.00
3.F	Sc <sub>2</sub> @C88	13.60

TABLE 4.4

Composition of PBB Sc<sub>m</sub>@C<sub>2n</sub> fractions (#4 Buckyclutcher series)  
from PBB chromatographic column

SAMPLE NUMBER	COMPOSITION	RETENTION TIME (min.)
4.A	Sc2@C80	12.22
4.B	Sc4@C82	12.42
4.C	Sc2@C86	13.08
4.D	Sc4@C80	13.57
4.E	Sc2@C90	14.85



TABLE 4.5

Composition of PBB Sc<sub>m</sub>@C<sub>2n</sub> fractions (#5 Buckyclutcher series)  
from PBB chromatographic column

SAMPLE NUMBER	COMPOSITION	RETENTION TIME (min.)
5.A	Sc2@C76	11.47
5.B	Sc2@C80	12.28
5.C	Sc4@C82 / Sc2@C82	12.50
5.D	Sc3@C84	13.02
5.E	Sc2@C86	13.41
5.F	Sc2@C88	14.17
5.G	Sc2@C90	14.78

4.4) indicated the presence of  $\text{Sc}_4@C_{82}$ . This was exciting since there had been no precedence for encapsulating *four* metal atoms. Although  $\text{Sc}_4@C_{82}$  was the dominant species, this fraction was still contaminated with minor amounts of  $\text{Sc}_2@C_{80}$  -  $\text{Sc}_2@C_{84}$ . Since the PBB HPLC-UV trace (Figure 4.31a) revealed a symmetrical peak, further re-injection into this PBB column would not have effectively resulted in a purified  $\text{Sc}_4@C_{82}$  sample.

An injection into the Buckyclutcher column demonstrated that further separation was possible. Collection of the peak centered at 15.26 minutes (Figure 4.31b) resulted in a purified  $\text{Sc}_4@C_{82}$  sample with > 90% purity (Figure 4.31c). Although this mass spectrum was not obtained under satisfactory conditions for an accurate isotope distribution analysis, a mass spectrum (Figure 4.32) for a separate  $\text{Sc}_4@C_{82}$  sample was obtained under optimal conditions. A subsequent isotope distribution analysis suggests that the intensities for the experimental and theoretical M, M+1, M+2, M+3, and M+4 peaks are comparable. Note that the nearest empty-cage peak ( $C_{94}$ ) would possess a "M+1" peak of higher intensity than its "M" peak. Other possible  $\text{Sc}_m@C_{2n}$  species were inconsistent with this molecular weight.

In addition, a purified  $\text{Sc}_2@C_{74}$  sample was also obtained from injection of  $\text{Sc}_m@C_{2n}$  Buckyclutcher peak "0" (see Table 4.1 or Figure 4.5) into the PBB column. The HPLC-UV chromatogram for the final PBB injection is presented in Figure

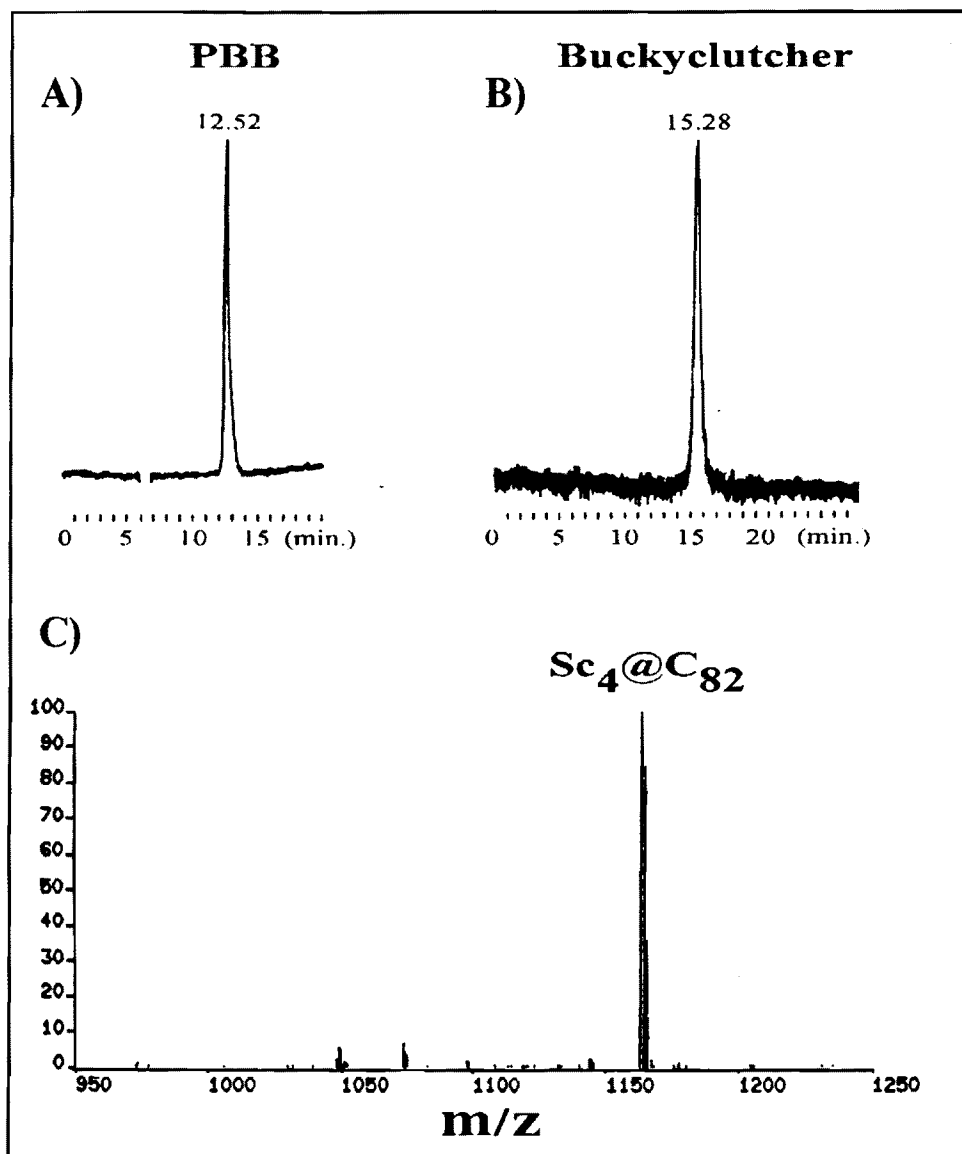


Figure 4.31 (a) HPLC-UV analytical trace of PBB fraction 4.B, CS<sub>2</sub> mobile phase, 380 nm UV detection, PBB column, and 2.0 mL/min. (b) HPLC-UV analytical trace of the final purified Sc<sub>4</sub>@C<sub>82</sub> sample, Buckyclutcher column, 2.0 mL/min, 380 nm UV detection, and 80:20 toluene/decalin mobile phase. (c) negative-ion chemical ionization mass spectrum of the above final purified Sc<sub>4</sub>@C<sub>82</sub> sample using Ultramark 1621 as the calibration standard.

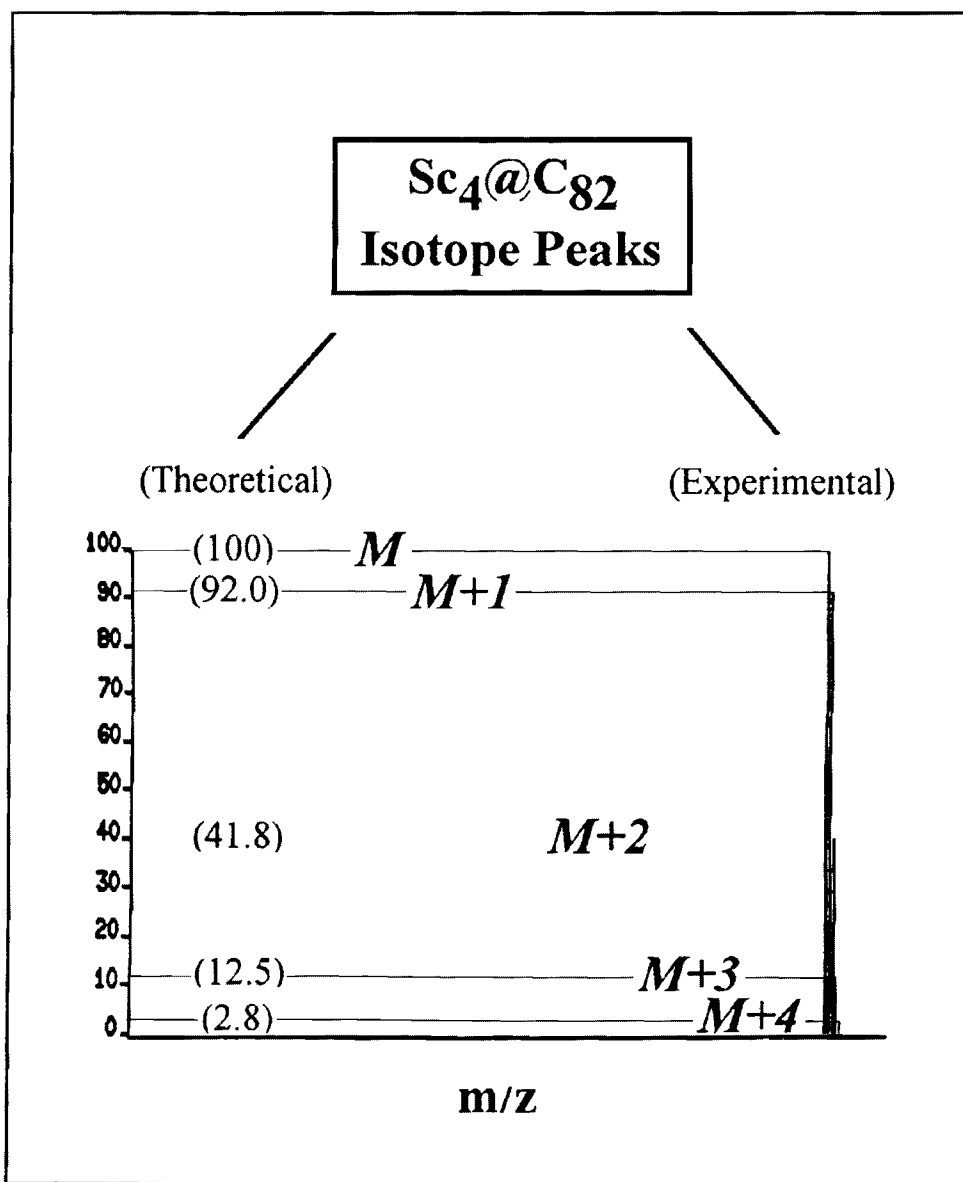


Figure 4.32 Negative-ion chemical ionization mass spectrum for the Sc<sub>4</sub>@C<sub>82</sub> sample using Ultramark 1621 as the calibration standard. Obtained under optimal high resolution mass spectral condition, this mass spectrum was used for analyzing predicted isotope distribution patterns for Sc<sub>4</sub>@C<sub>82</sub>.

4.33a. The purity of this  $\text{Sc}_2@C_{74}$  sample is estimated at  $> 95\%$ . A  $^{13}\text{C}$  NMR experiment for this metallofullerene was performed. Although several real  $^{13}\text{C}$  NMR peaks were suspected to be emerging above the noise, the results were nevertheless inconclusive.

Next, an attempt was made to obtain a  $^{45}\text{Sc}$  NMR spectrum for  $\text{Sc}_2@C_{74}$  to determine if the two Sc atoms were equivalent on the NMR time-scale. This experiment was successful, and the  $^{45}\text{Sc}$  NMR spectrum is presented in Figure 4.33b. Obtained under ambient conditions, this NMR spectrum suggests that the metal atoms are equivalent within the cage structure. Note that the  $^{45}\text{Sc}$  NMR signal is broadened due to quadrupolar interactions from the scandium nuclei.

### 4.3 Automated Metallofullerene Separations<sup>173</sup>

Because the amount of experimental time became a significant consideration, a quicker, if not better, methodology needed to be developed. Depending on the amount of initial raw extract, a typical series of five polystyrene passes required days to weeks. Once that metallofullerene-enriched fraction was obtained, another block of time was required. Based on the number of peaks to be collected and number of re-injections, one to three weeks was often necessary. In addition, off-line collection

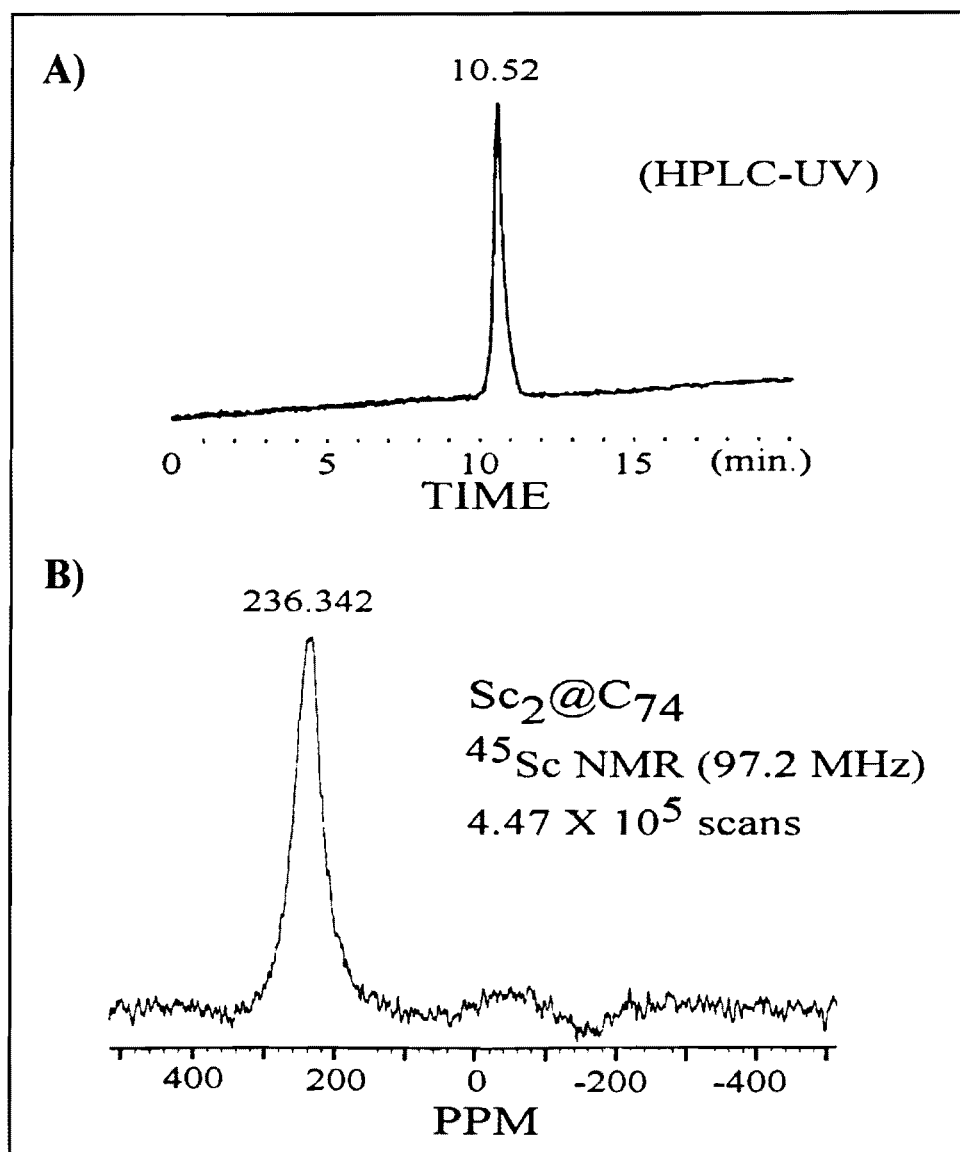


Figure 4.33 (a) HPLC-UV analytical trace for purified Sc<sub>2</sub>@C<sub>74</sub>, PBB column 2.0 mL/min, carbon disulfide mobile phase, and 380 nm UV detection. This sample was previously separated using the Buckyclutcher column and injected into the PBB column for final purification. (b)  $^{45}\text{Sc}$  NMR spectrum for the above purified Sc<sub>2</sub>@C<sub>74</sub> sample obtained under ambient conditions. Under these conditions, ScCl<sub>3</sub> would have a chemical shift of 114 ppm.

of eluents was often done manually. This increased the risk of sample contamination and required an inordinate amount of limited manpower. For these reasons, the following automated methodology was developed for unattended operation. It should be noted that Paul Burbank (see Acknowledgement Section) played the integral role in developing this automated system. Although details of this work have been recently published,<sup>173</sup> a diagram of this automated apparatus is presented in Figure 4.34.

#### 4.31 Er<sub>m</sub>@C<sub>2n</sub>

This automated approach can be effective for chromatographic separations of metallofullerenes. As an example, it will be demonstrated in this section that Er<sub>2</sub>@C<sub>82</sub> (isomer III) can be *isolated solely from the automated approach*.

From ~1000 mg of Er<sub>m</sub>@C<sub>2n</sub> extract, a stock solution (3 mg/mL) was prepared and separated using the Buckyclutcher columns as the separation columns. The automated system was initiated and the resulting chromatograms are presented in Figure 4.35a. Based on preliminary results (see Er<sub>m</sub>@C<sub>2n</sub> separations; Section 4.14), the Er<sub>2</sub>@C<sub>82</sub> (isomer III) species elutes at ~54 minutes in the automated experiments due to a lower flow rate in comparison with previous experiments. A narrow fraction centered at this region resulted in a sample containing Er<sub>2</sub>@C<sub>82</sub> and the empty-cages

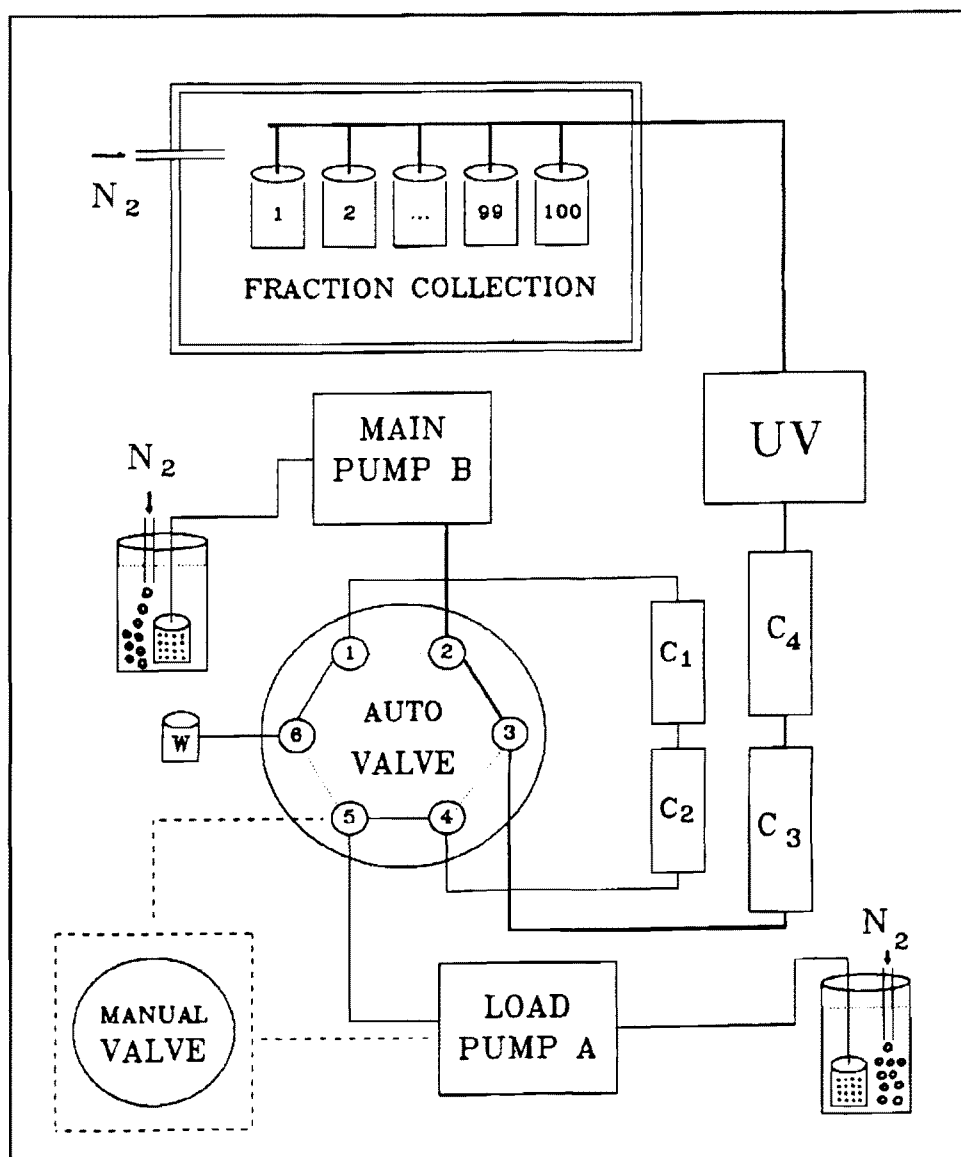


Figure 4.34 Automated HPLC apparatus: Load and separation columns are C1, C2 and C3, C4, respectively. The manual valve is an optional feature (details in ref. 173).



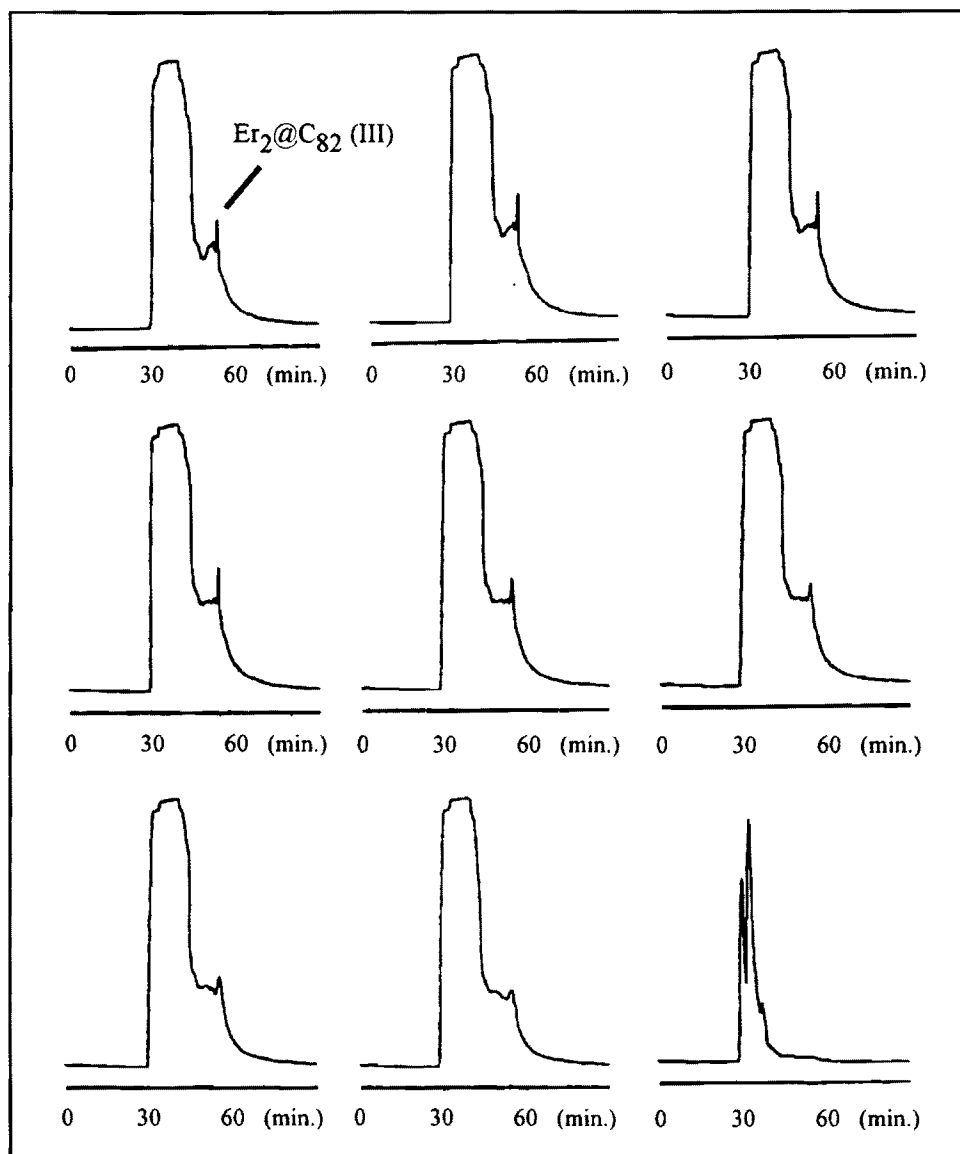


Figure 4.35 (a) Automated sequence of  $Er_m@C_{2n}$  injections. Chromatographic conditions: first Buckyclutcher pass, 1.0 mL/min, 80:20 toluene/decalin, and 340 nm detection.

$C_{100}$  -  $C_{106}$  fullerenes. In order to remove the  $C_{60}$  -  $C_{92}$  empty-cage fullerenes which had "tailed" into the metallofullerene fraction, the  $Er_2@C_{82}$  concentrated fraction (isomer III) was subsequently re-injected for a second Buckyclutcher automated sequence (Figure 4.35b).

To remove the higher-mass empty-cage contaminants, a series of automated-TPP injections were performed. The results are illustrated in Figure 4.36. A narrow fraction centered around the peak maxima (~5 min) resulted in a highly purified sample of  $Er_2@C_{82}$  (isomer III, > 90% purity). In summary, this automated approach went from an initial  $Er_m@C_{2n}$  extract to a final, isolated metallofullerene. This total-automated system represented a significant advancement in the savings of manpower and time.

#### 4.4 Empty-cage $C_{2n}$ Separations

In the course of the chromatography of metallofullerene samples, the empty-cage species were concomitantly separated for other characterization studies. For example, isolation of empty-cage species are important models to determine the cage symmetry based on  $^{13}C$  NMR data. In addition, empty-cage fullerenes serve as chromatographic "standards" for newly purchased columns and for characterization experiments of

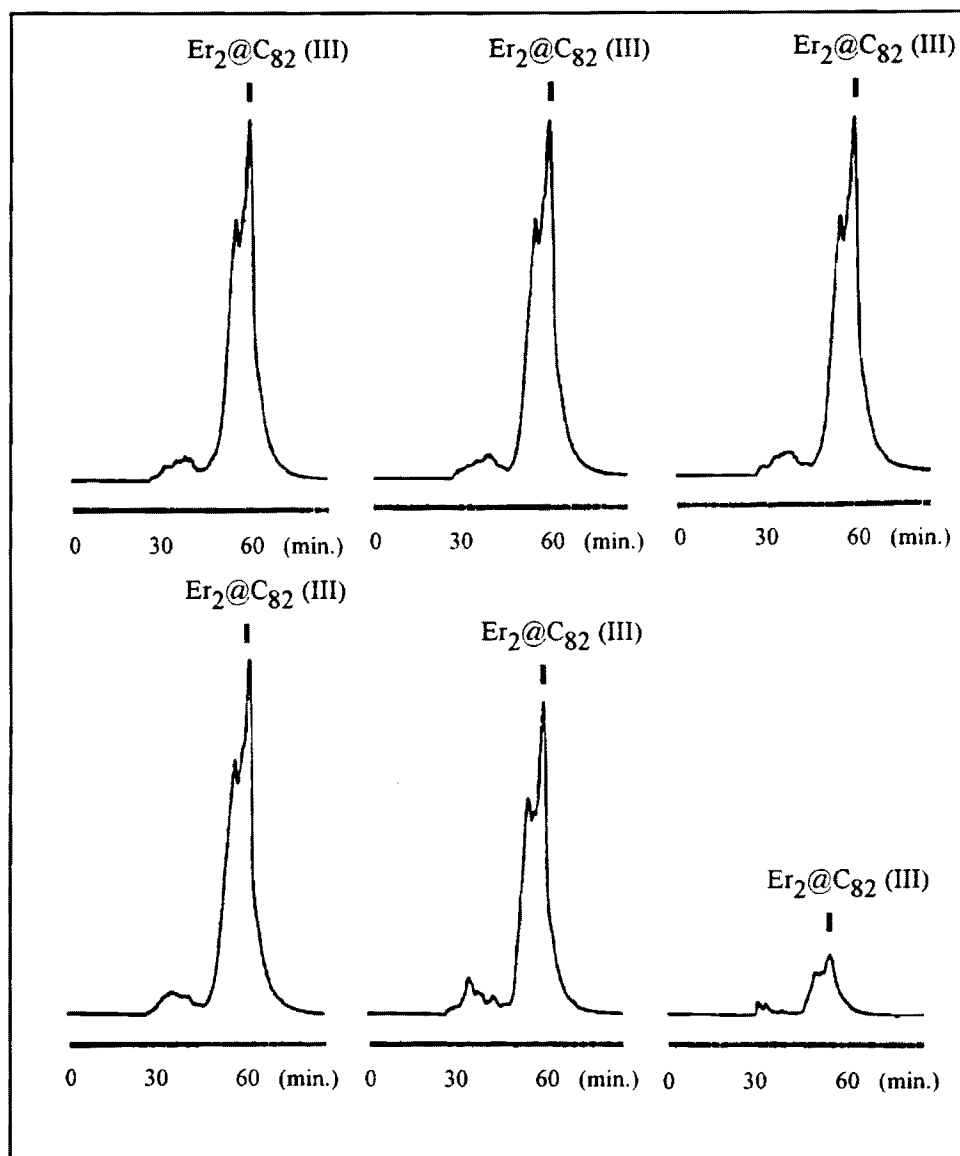


Figure 4.35 (b) Re-injection of the  $\text{Er}_2\text{@C}_{82}$  fraction into the automated apparatus. Chromatographic conditions: second Buckyclutcher pass, 1.0 mL/min, 80:20 toluene/decalin, and 340 UV nm detection. The dominant peak corresponds to  $\text{Er}_2\text{@C}_{82}$  (isomer III).

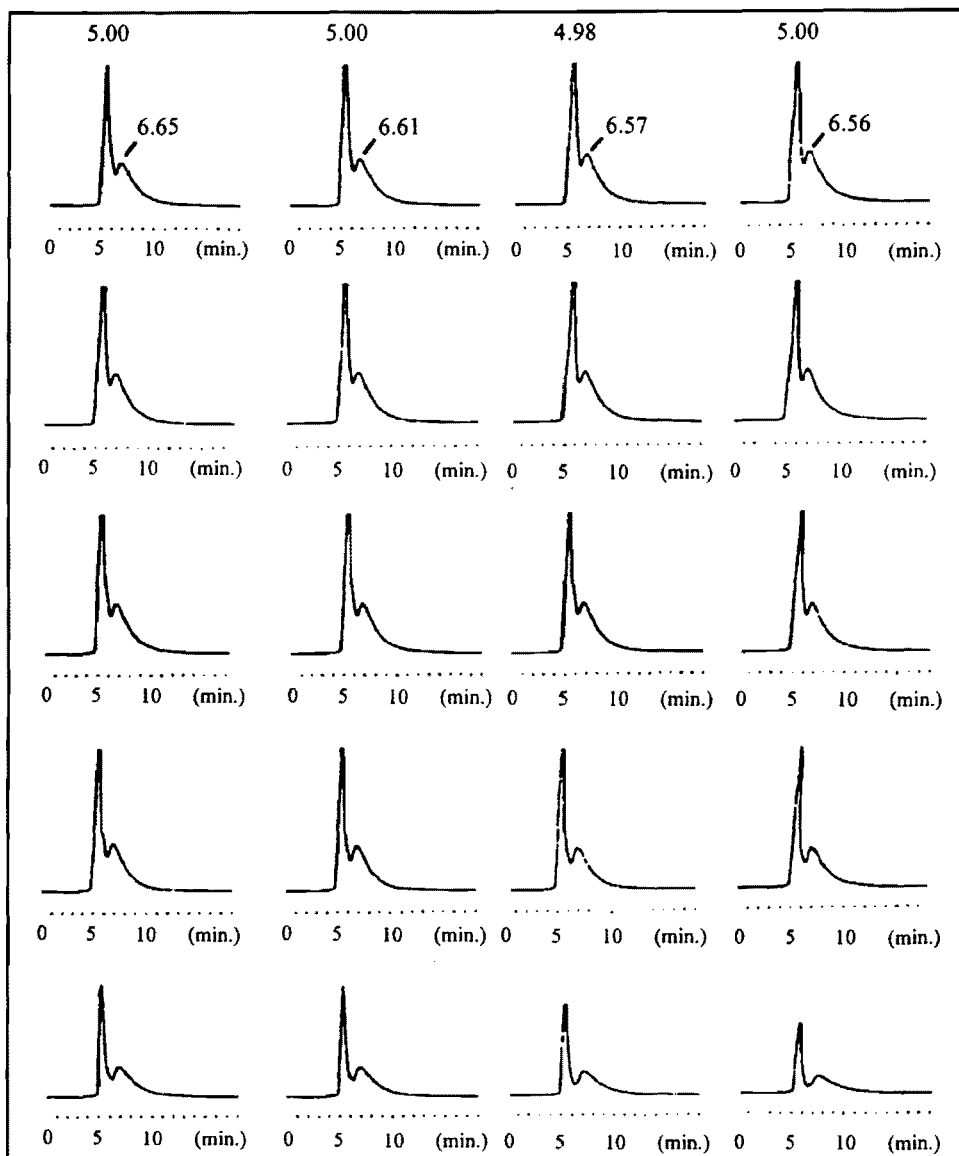


Figure 4.36 Automated sequence of the  $\text{Er}_2@C_{82}$  fraction (isomer III) obtained after two Buckyclutcher passes yielded a single, symmetric peak. Chromatographic conditions: TPP column, 1.0 mL/min, carbon disulfide, and 340 nm UV detection.

purified metallofullerenes. For example, the UV-Vis spectrum of  $\text{Sc}_3@C_{82}$  can be compared to the corresponding empty-cage  $C_{82}$  fullerene. Thus, subtle differences between a metallofullerene and its corresponding empty-cage can be compared to determine whether a given property arises from the empty-cage carbon network or as a result of metal encapsulation. In our laboratory, isolated empty-cage samples include  $C_{60}$  (> 98 % purity),  $C_{70}$  (> 98% purity),  $C_{78}$  (~80% purity),  $C_{82}$  (> 90% purity),  $C_{84}$  (> 90% purity),  $C_{86}$  (~85% purity),  $C_{88}$  (~70% purity),  $C_{90}$  (> 90% purity),  $C_{92}$  (~80% purity), and  $C_{96}$  (> 90% purity).

Although the polystyrene column lacked the desired selectivity for separating individual metallofullerenes, it was adequate resolution for isolation of  $C_{60}$ ,  $C_{70}$ , and  $C_{84}$  samples. As an example, Figure 4.37 illustrates a typical chromatogram following a polystyrene injection. Note that the column is not overloaded as was often the case in the initial polystyrene (1<sup>st</sup> pass) clean-up step previously used for obtaining the "EPR active" fraction (see section on metallofullerene separations).

However, the majority of purified empty-cage fullerenes were obtained with the more selective Buckyclutcher column. The analytical chromatograms and corresponding mass spectra for several isolated empty-cage fullerene fractions obtained from Buckyclutcher separations are presented in Figures 4.38a through 4.38f.

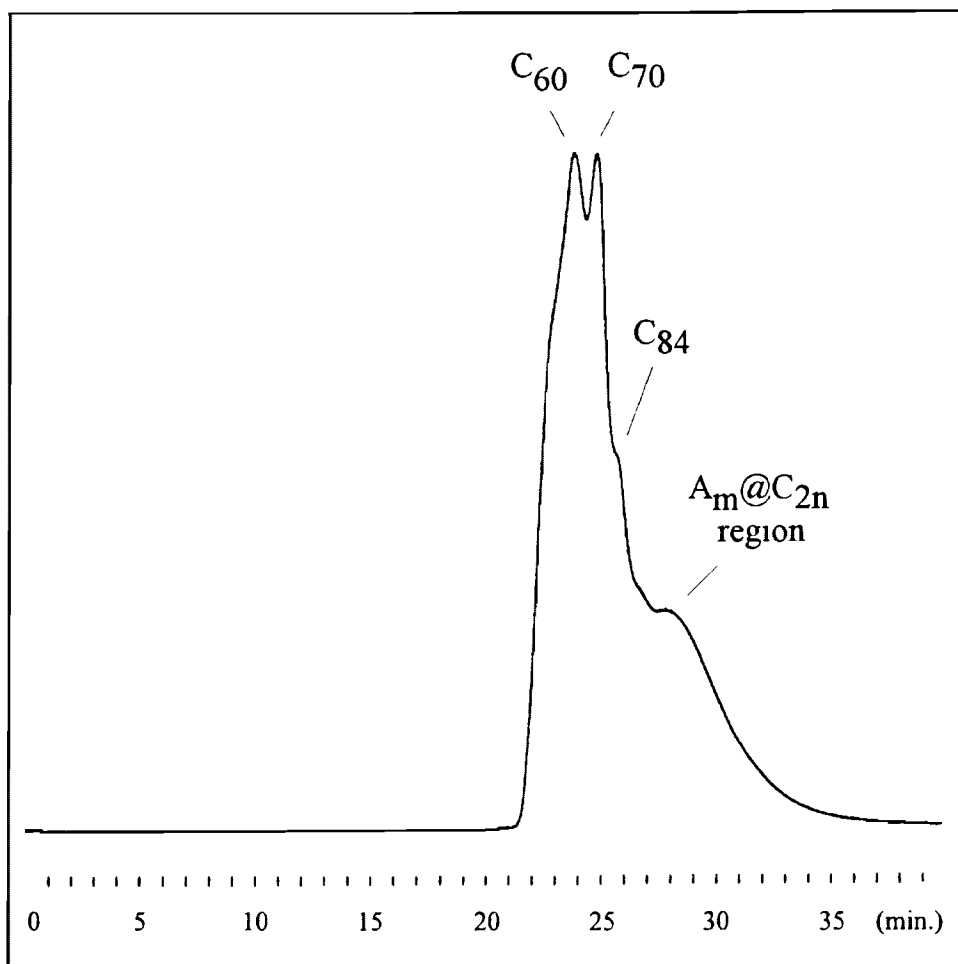


Figure 4.37 HPLC-UV chromatograms for a typical polystyrene separation. Chromatographic conditions: second polystyrene pass of the  $Y_m@C_{2n}$  fraction, 1.0 mL/min, 80:20 toluene/decalin, and 340 nm UV detection.

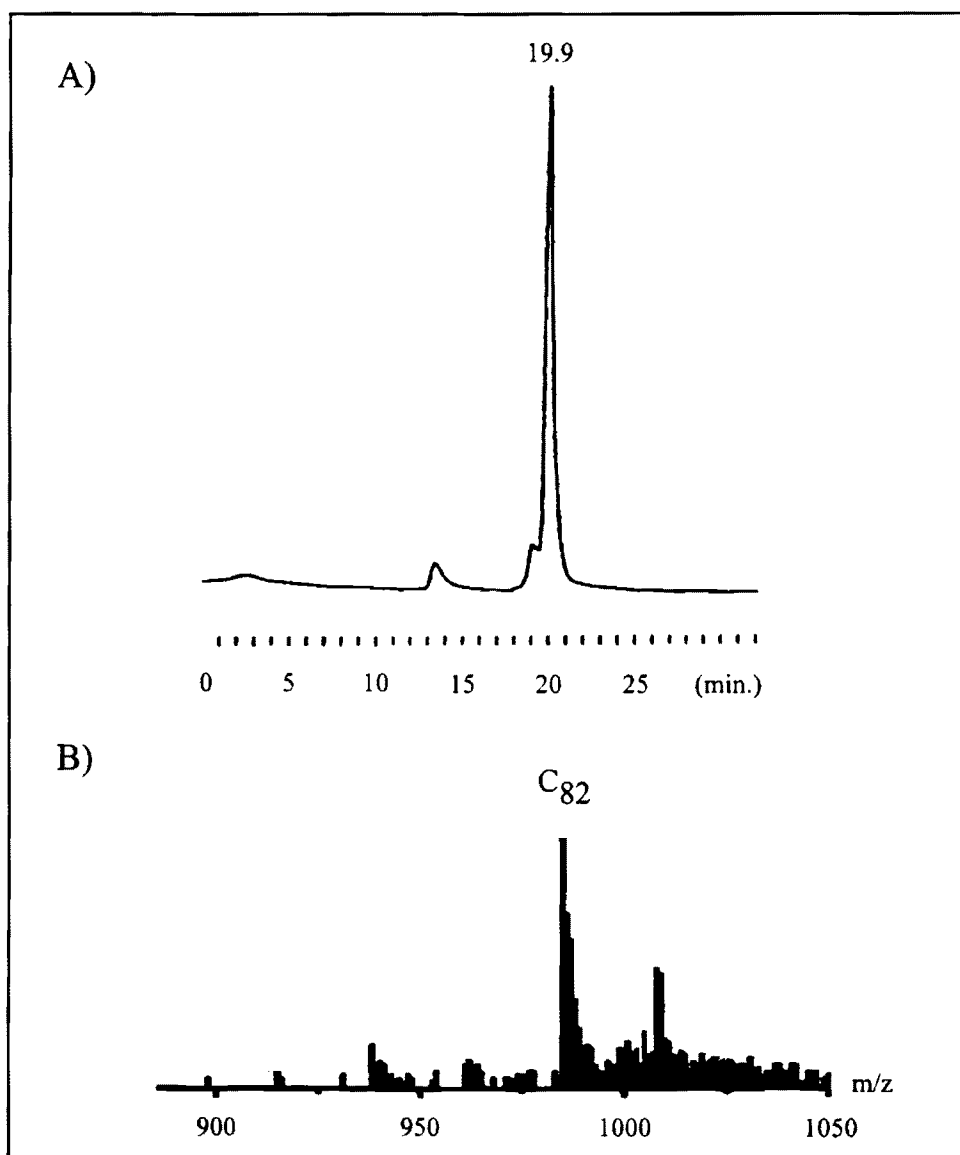


Figure 4.38a Analytical HPLC-UV trace of an isolated C<sub>82</sub> fraction, Buckyclutcher column, 1.0 mL/min, 80:20 toluene/decalin, and 340 nm UV detection.

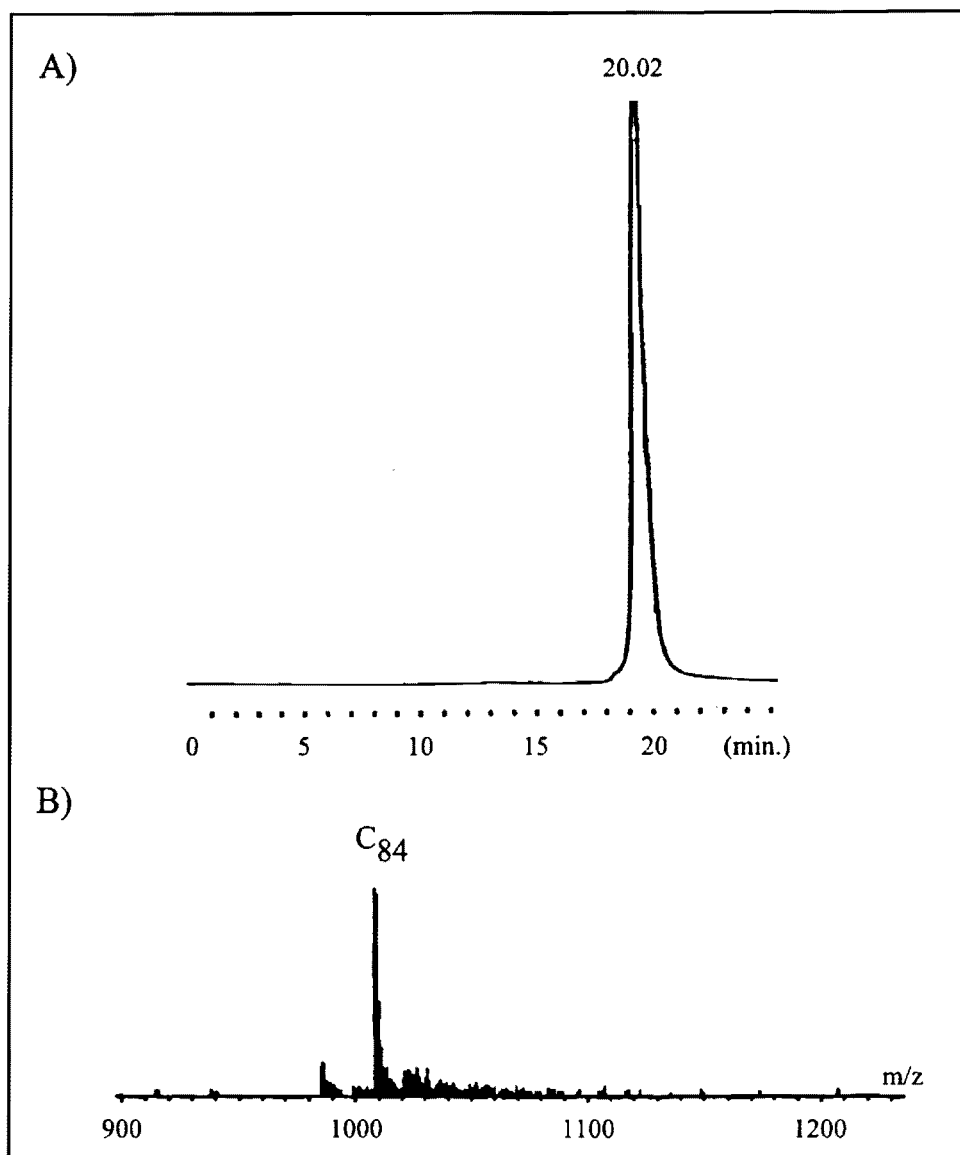


Figure 4.38b Analytical HPLC-UV trace of an isolated C<sub>84</sub> fraction, Buckyclutcher column, 1.0 mL/min, 80:20 toluene/decalin, and 340 nm UV detection.



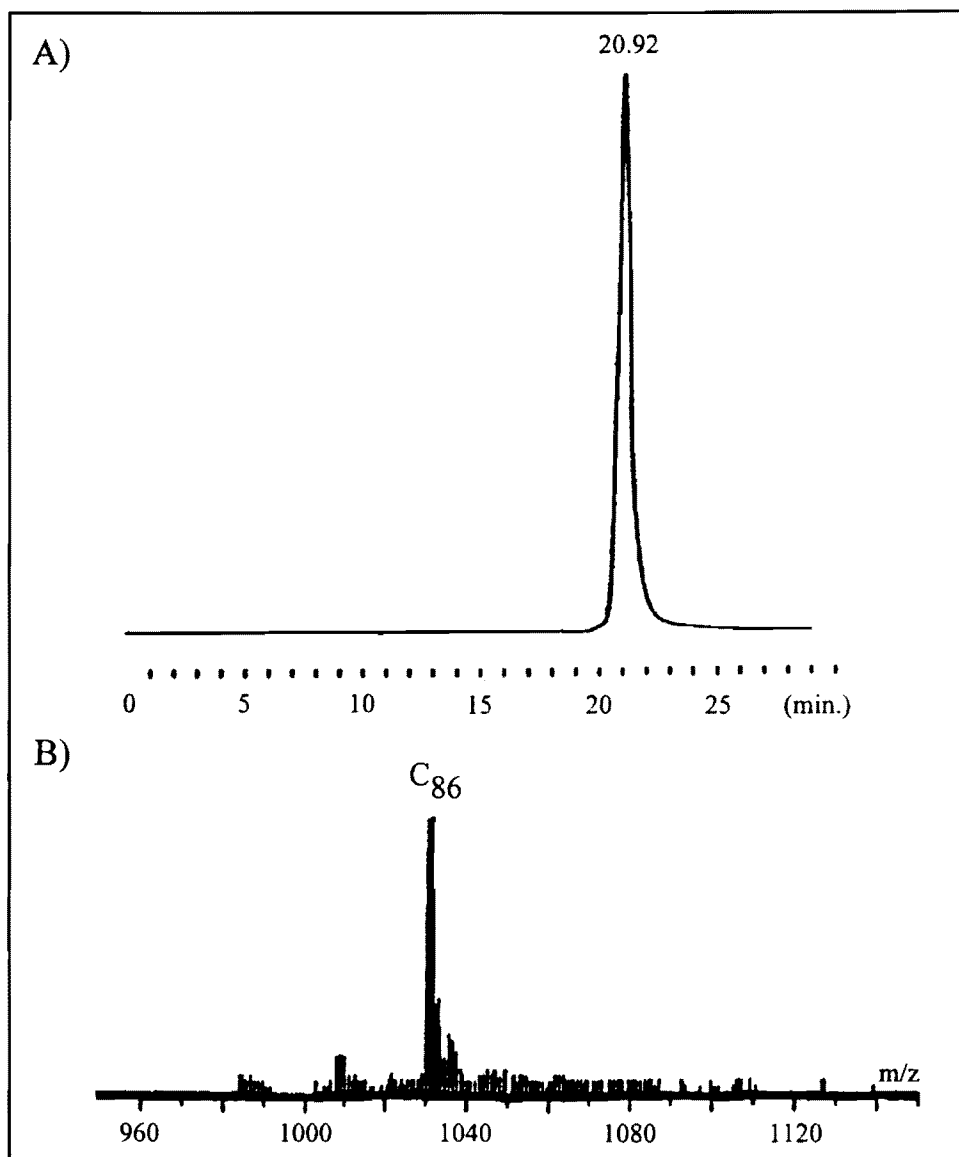


Figure 4.38c Analytical HPLC-UV trace of an isolated C<sub>86</sub> fraction, Buckyclutcher column, 1.0 mL/min, 80:20 toluene/decalin, and 340 nm UV detection.

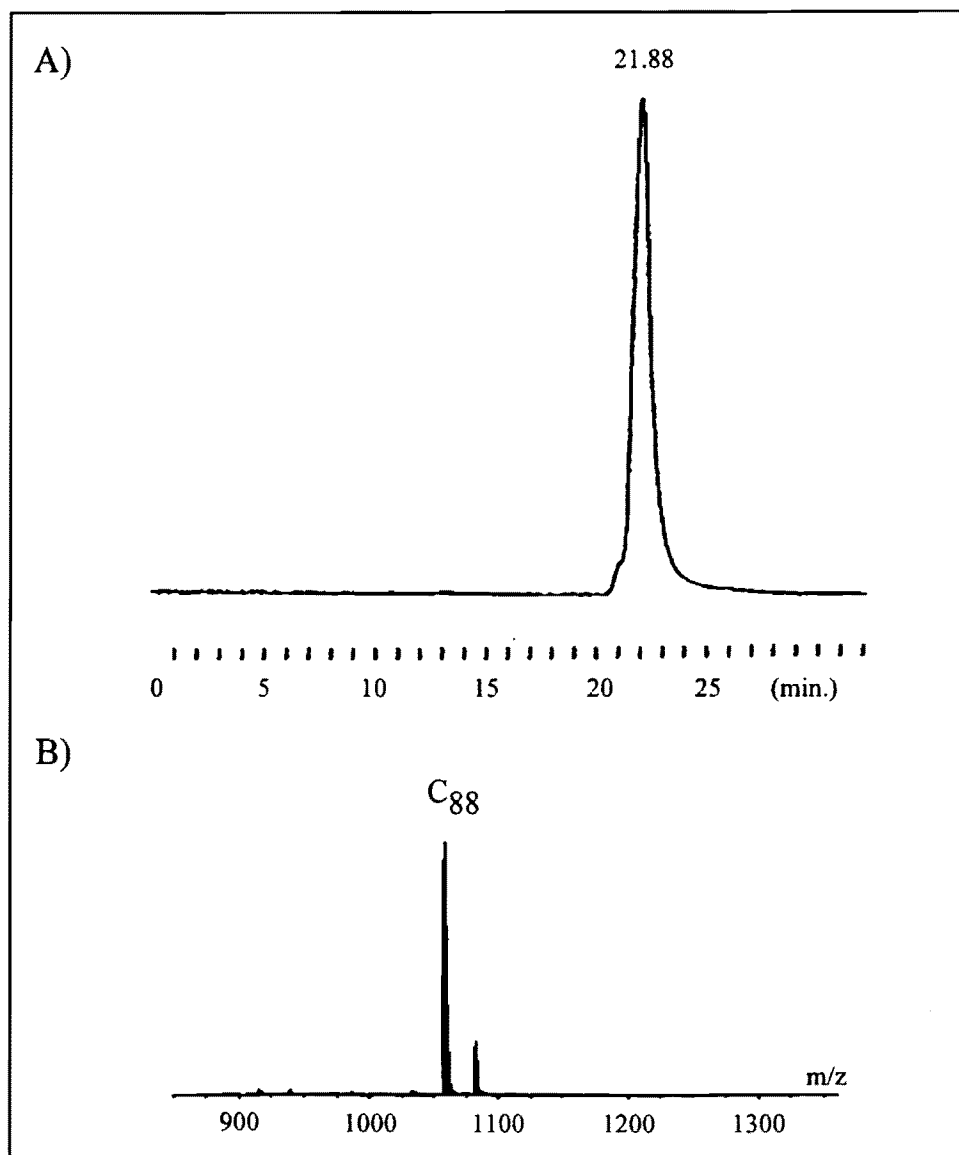


Figure 4.38d Analytical HPLC-UV trace of an isolated C<sub>88</sub> fraction, Buckyclutcher column, 1.0 mL/min, 80:20 toluene/decalin, and 340 nm UV detection.

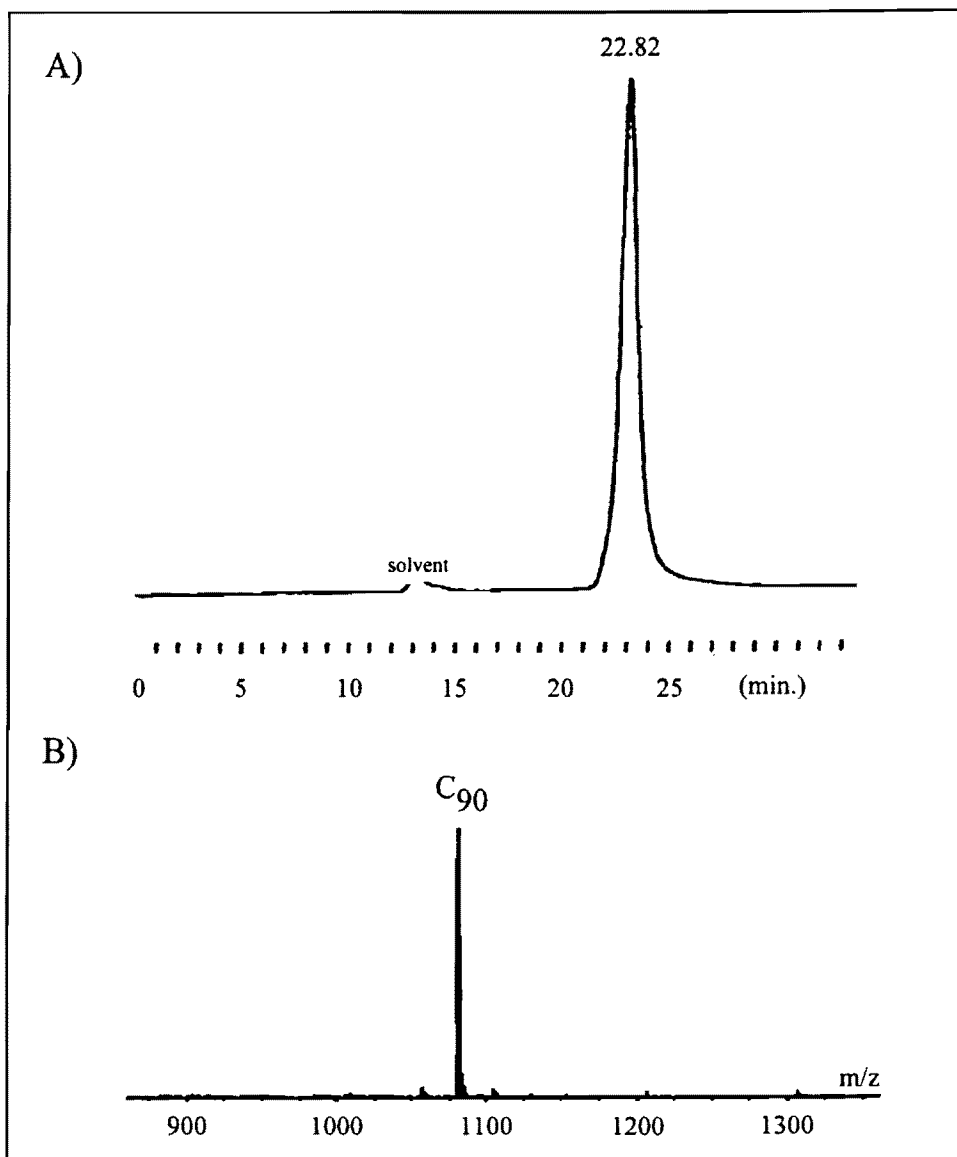


Figure 4.38e Analytical HPLC-UV trace of an isolated  $C_{90}$  fraction, Buckyclutcher column, 1.0 mL/min, 80:20 toluene/decalin, and 340 nm UV detection.

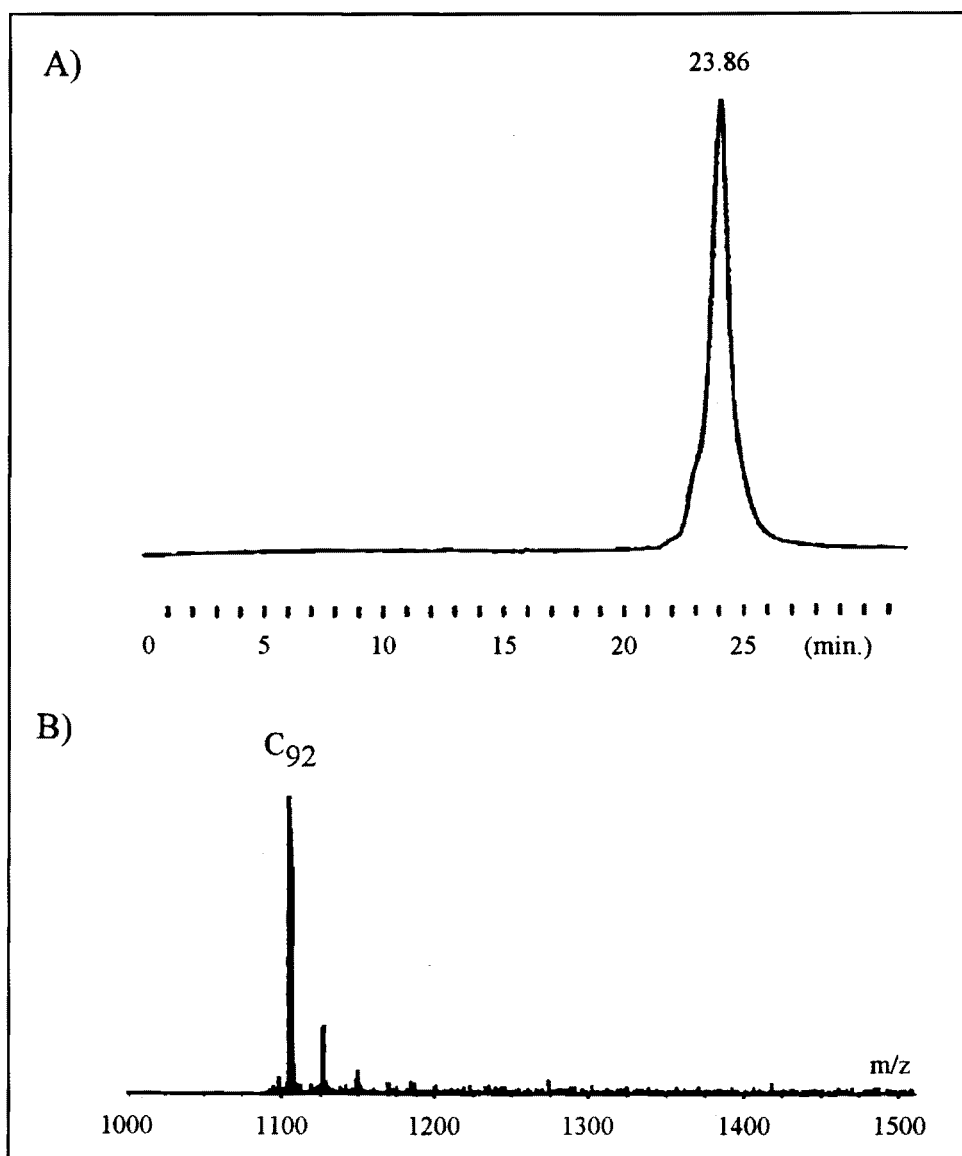


Figure 4.38f Analytical HPLC-UV trace of an isolated C<sub>92</sub> fraction, Buckyclutcher column, 1.0 mL/min, 80:20 toluene/decalin, and 340 nm UV detection.

#### 4.5 Trends in $A_m@C_{2n}$ Separations

In this research, the polystyrene, Buckyclutcher, TPP, and PBB columns have been the most useful for separation of endohedral metallofullerenes. Following years of metallofullerene separations on different types of chromatographic columns, valuable experimental data has been obtained. This data can provide a more fundamental understanding of separation processes of the endohedral metallofullerenes. Specifically, the chromatographic retention behavior [e.g. retention time ( $t_r$ ) and capacity factor ( $k'$ )] of empty-cage fullerenes ( $C_{60}$ - $C_{120}$ ) as well as endohedral metallofullerenes ( $Sc_m@C_{2n}$ ,  $Y_m@C_{2n}$ ,  $La_m@C_{2n}$ , and  $Er_m@C_{2n}$ ) has been characterized and evaluated for several columns. With the 80:20 toluene/decalin mobile phase, individual capacity factors were determined for each metallofullerene.

To unambiguously assign retention times for the paramagnetic metallofullerene species, HPLC-EPR detection was utilized as an on-line technique. In addition, off-line characterization methods included the following mass spectrometric techniques: time-of-flight (LD-TOF) and negative-ion desorption chemical ionization (NI-DCI). Off-line fractions were also characterized by EPR analysis of static samples. Chromatographic parameters of all metallofullerene separations have been obtained and are summarized in Figure 4.39 - a graphical representation of the log  $k'$  (capacity

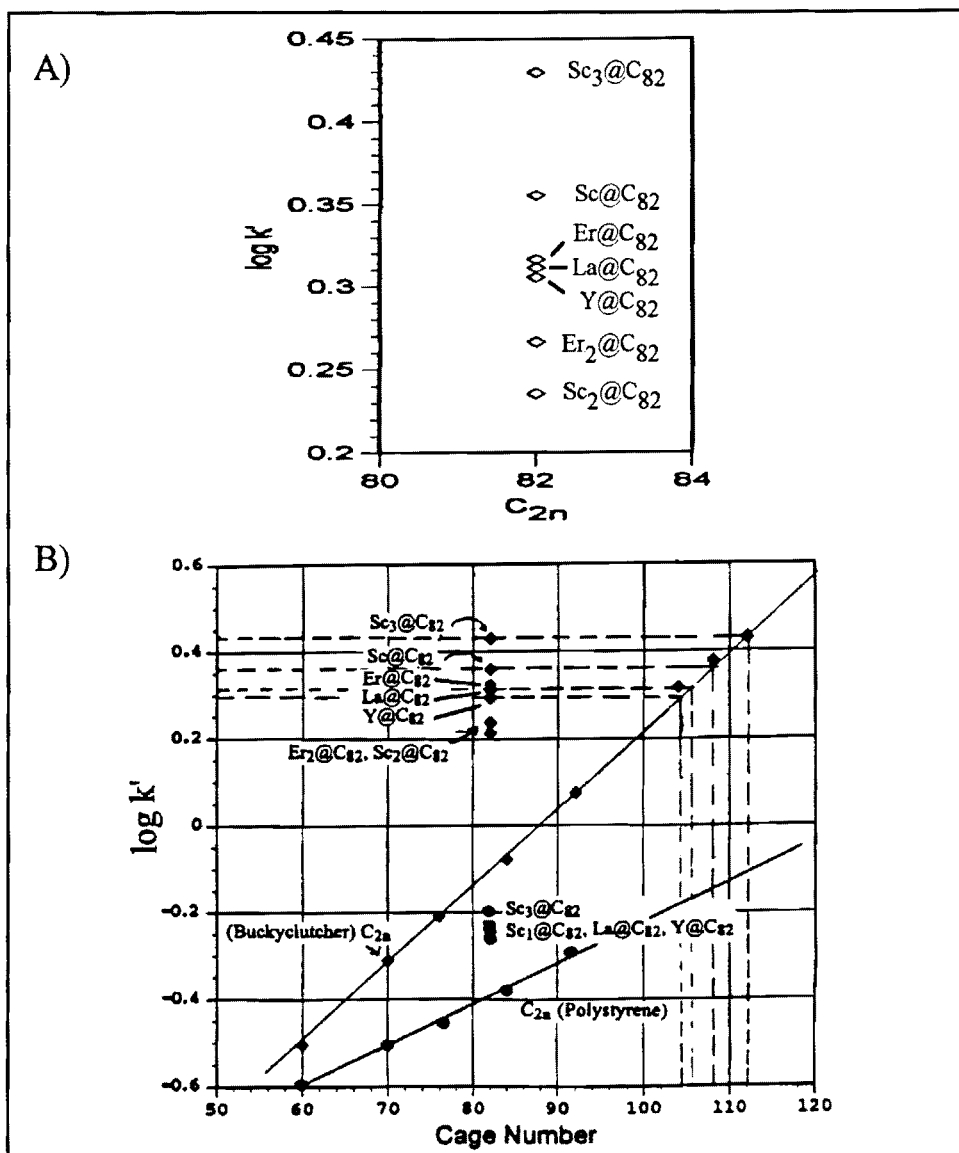


Figure 4.39 Plot of chromatographic capacity factor ( $\log k'$ ) versus cage size (number of carbon atoms), ● polystyrene column, ◆ Buckyclutcher column, and 80:20 toluene/decalin mobile phase. (a) is an expanded inset from (b).

factor) versus the number of carbon atoms in the outer fullerene cage network. Since plotting all metallofullerene data points would result in a cluttered graph, only metallofullerenes with a  $C_{82}$  outer-cage are presented. This graph addresses one of the primary concerns of metallofullerene separations. Namely, it provides information regarding where a particular metallofullerene would elute relative to the empty-cage fullerenes. Thus, a practical feature of Figure 4.39 is its ability to predict which empty-cage fullerene(s) will be the dominant contaminant for a specific metallofullerene. As an example, a  $Sc_3@C_{82}$  fraction obtained from a polystyrene column will possess  $C_{104}$  as the primary empty-cage contaminant. On the Buckyclutcher column, however, the identical  $Sc_3@C_{82}$  species would co-elute with the empty-cage  $C_{112}$  fullerene of slightly higher mass. In this regard, it would then be possible to isolate  $Sc_3@C_{82}$  using a combination of these two columns. Specifically, a  $Sc_3@C_{82}$  fraction from a polystyrene separation could be injected into the Buckyclutcher column to obtain a purified  $Sc_3@C_{82}$  sample. This "two-stage" system would be effective since the  $C_{104}$  and  $C_{112}$  species would be removed with a combination of these two different types of columns.

Figure 4.39 also reveals valuable information regarding metallofullerene separations. It should be noted that regardless of which type of column was used (polystyrene or Buckyclutcher), all of the empty-cage fullerenes were eluted as a

homologous series as indicated by the  $C_{2n}$  line connecting their data points. Based on this feature, a powerful statement is made regarding the chromatographic separations of metallofullerenes. Namely, there is an extremely high probability that any selected metallofullerene will co-elute with some empty-cage fullerene. For this reason, at least two different types of columns must often be utilized in the isolation of individual metallofullerenes. This explains why the "two-stage" systems (see Isolation; Section 2.29) have presently become the dominant methodology in metallofullerene isolation schemes. However, there is an exception. It is possible that, by chance, a metallofullerene could elute between two empty-cages in the  $C_{2n}$  homologous series (e.g.  $C_{86} < \text{La}@C_{82} < C_{38}$ ). This situation could occur for columns possessing adequate resolution of the *higher-mass* empty-cage  $C_{86}$ - $C_{112}$  species. Metallofullerenes often elute in this region regardless of which type of column is employed. However, it should be noted that these "one-step" purifications involving only one type of column have been rare.

In addition, the data in Figure 4.39 reveals other overall trends in metallofullerene separations. As an example,  $\text{Sc}_3@C_{82}$  possesses a large  $\log k'$  value and is a strongly retained metallofullerene. With slightly lower  $\log k'$  values, the mono-metal, endohedral metallofullerene series ( $\text{Y}@C_{82}$ ,  $\text{La}@C_{82}$ ,  $\text{Sc}@C_{82}$ , and  $\text{Er}@C_{82}$ ) are clustered together. These mono-metal species are less strongly retained than the tri-



metal  $\text{Sc}_3@C_{82}$  metallofullerene. Individually,  $\text{Y}@C_{82}$ ,  $\text{La}@C_{82}$ ,  $\text{Sc}@C_{82}$ , and  $\text{Er}@C_{82}$  possess minor differences in retention times. In contrast, the di-metal series ( $\text{Sc}_2@C_{82}$ ,  $\text{Y}_2@C_{82}$ ,  $\text{La}_2@C_{82}$ , and  $\text{Er}_2@C_{82}$ ) are noticeably the most weakly retained metallofullerenes. These di-metal species tend to elute in families or groups - possibly determined by which  $C_{82}$  empty-cage isomer is surrounding the metal atoms. Disregarding obvious differences in retention times of various individual isomers ( $\text{Er}_2@C_{82}$ , I, II, and III), it appears that the identity of the metal atoms (e.g.  $\text{Sc}_2$ ,  $\text{Y}_2$ , etc) does not significantly influence their retention times since these species are clustered so closely together.

In addition, the plot illustrates the poor selectivity of polystyrene separations as indicated by a  $C_{2n}$  slope of only 0.0088. This lack of significant resolution between individual metallofullerene compounds is due to a weaker  $\pi$ - $\pi$  complexing stationary phase (relative to the Buckyclutcher). This poor selectivity addresses why the paramagnetic species ( $\text{Sc}@C_{82}$ ,  $\text{Sc}_3@C_{82}$ ,  $\text{Y}@C_{82}$ , and  $\text{La}@C_{82}$ ) effectively served as ideal "markers" for the overall metallofullerene fraction as previously discussed. This feature also explains why five polystyrene "recovery and re-injection" steps were necessary to sufficiently distinguish and separate the overall metallofullerene EPR active fraction from the lower-mass empty-cage region (e.g.  $C_{60}$ - $C_{84}$ ).

At this stage, an attempt was made to correlate the paramagnetic metallofullerenes

(Sc@C<sub>82</sub>, Y@C<sub>82</sub>, La@C<sub>82</sub>, and Sc<sub>3</sub>@C<sub>82</sub>) with their chromatographic retention behaviour. We noted that the elution order was always Y@C<sub>82</sub>, La@C<sub>82</sub>, Sc@C<sub>82</sub>, and Sc<sub>3</sub>@C<sub>82</sub>. This has been consistent regardless of which type of column (polystyrene or Buckyclutcher) was utilized. Although this feature is not presently understood, a relationship between the log k' versus the hyperfine coupling constant (a) has been created as illustrated in Figure 4.40. From this plot, the trend is increased retention times for the metallofullerenes with larger hyperfine coupling constants. Specifically, Y@C<sub>82</sub> has the smallest hyperfine value and is the earliest to elute.

A possible explanation for this elution trend might be the amount of electron spin density that the metal atom(s) transfers to the surrounding carbon cage network. For example, the large hyperfine coupling constant of Sc<sub>3</sub>@C<sub>82</sub> suggests a significant amount of unpaired electron spin density remains on the Sc<sub>3</sub> trimer and less electron density transferred to the cage (relative to Y@C<sub>82</sub>). Thus, a separation based on the amount of "charge-transfer" could be a significant factor for these mono-metal species. Note that the hyperfine coupling constant for Sc<sub>3</sub>@C<sub>82</sub> (6.8 g) has a similar value (8.5 g) relative to a Sc<sub>3</sub> trimer trapped in an argon matrix (4 K).<sup>188b</sup> These similar hyperfine coupling constants suggest further evidence that most of the unpaired electron spin density of Sc<sub>3</sub>@C<sub>82</sub> remains on the Sc atoms.

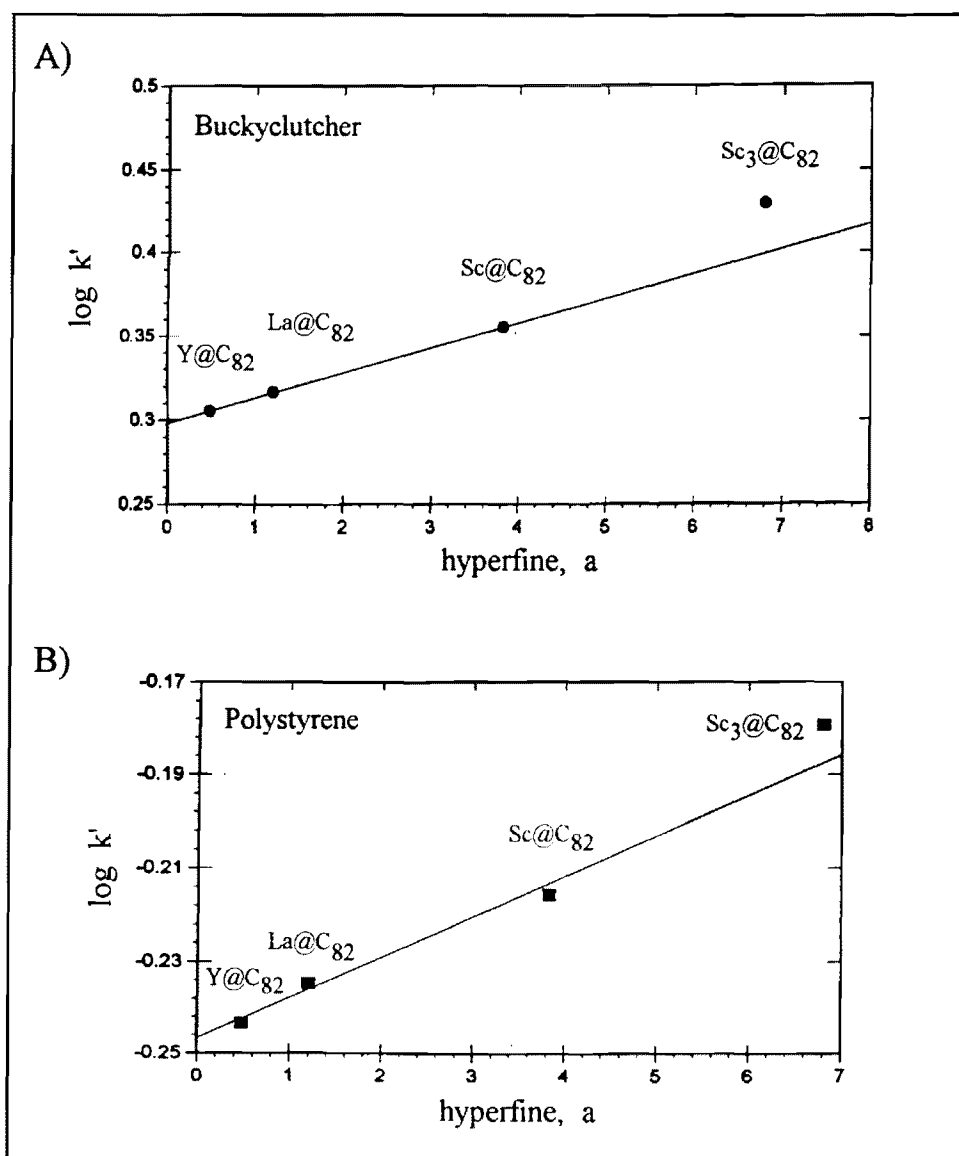


Figure 4.40 Plots of chromatographic capacity factor ( $\log k'$ ) versus the hyperfine coupling constant,  $a$ , for (a) Buckyclutcher and (b) polystyrene separations, respectively. The mobile phase is 80:20 toluene/decalin.

At first glance, this hyperfine data might appear to be inconsistent with the retention mechanism expected for the di-nitrophenyl stationary phase of the Buckyclutcher column. Namely, the nitrophenyl groups create a  $\pi$ -accepting stationary phase. However,  $\text{Sc}_3@C_{82}$  (less electron density transferred to the cage) would be then expected to interact to a lesser degree with this stationary phase and therefore elute earlier. Yet the elution trend for these mono-metal  $A_m@C_{2n}$  is reversed.

Another possible explanation for this elution trend might be the motional dynamics of the encapsulated metal atoms. Preliminary data<sup>296</sup> suggest that for the mono-metal endohedral species, the metal atom is off-center and bonded to the carbon cage atoms.<sup>296</sup> With the absence of other metal atoms to share the unpaired electron spin density, the charge and metal atom have no choice but to interact strongly with the carbon cage atoms. This would result in restricted motional dynamics for the metal atom. For the di-metal species, the electrons can now be shared between the two metal atoms. As a result, this metal dimer perhaps does not bond with the carbon cage and can then tumble freely within the cage. With the  $\text{Sc}_3$  trimer of  $\text{Sc}_3@C_{82}$ , any unpaired electrons could also be shared between the metal atoms instead of interacting strongly with the carbon cage atoms as discussed above. This  $\text{Sc}_3$  trimer is then free to move within the cage. This is consistent with our recent  $\text{Sc}_3@C_{82}$

motional dynamics study<sup>177</sup> indicating an energy rotational barrier of 28 meV and correlation time of  $5 \times 10^{-9}$  s. These features could relate to the elution trend in the following way. The rapidly moving Sc<sub>3</sub> trimer of Sc<sub>3</sub>@C<sub>82</sub> would strike the cage wall and briefly transfer a "bolus" of negative charge at a given instant. It could be this "concentration" of negative charge on the outer-cage wall that then interacts with the  $\pi$ -accepting dinitrophenyl ligands. This interaction could explain the longer retention of Sc<sub>3</sub>@C<sub>82</sub>.

It is possible that the nitro groups of the stationary influence the retention mechanism. As discussed previously for Sc<sub>3</sub>@C<sub>82</sub>, most of the charge remains on the metal with less charge transfer to the cage. Relative to the mono-metal A<sub>m</sub>@C<sub>2n</sub> species where there is the most charge-transfer to the cage, the outer-cage would therefore possess more negative charge to be repulsed by the negative charge on the NO<sub>2</sub> groups. Hence, these mono-metal species would be first to elute relative to Sc<sub>3</sub>@C<sub>82</sub>. The Sc<sub>3</sub>@C<sub>82</sub> with less charge-transfer to the cage would have a more positive charge on the cage and would therefore interact more strongly with the negative charge on the NO<sub>2</sub> group. Hence, the Sc<sub>3</sub>@C<sub>82</sub> would be last to elute.

It should be emphasized that the above discussion on retention mechanisms of the A<sub>m</sub>@C<sub>2n</sub> species with the various stationary phases are only presented as several possibilities. At present, a detailed study on the retention mechanisms for the

metallofullerenes on various stationary phases has not been published. Other possible retention mechanisms could involve the shape, size, and symmetry of the cage. In addition, recent electrochemical studies<sup>183,185</sup> have demonstrated that metallofullerenes can either accept or donate electrons to their cage structure. This feature could also contribute to the retention order of the metallofullerenes.

Despite the lack of fundamental understanding that these trends provide, other valuable and interesting information can be obtained. As a first example, an EPR spectrum of the paramagnetic  $\text{Er}@C_{82}$  species ( $I = 7/2$ ) would, in principle, yield an octet. Experimentally, however, a relatively sharp resonance signal<sup>189</sup> for  $\text{Er}@C_{82}$  with a g-factor (2.005) similar to  $\text{Sc}@C_{82}$ ,  $\text{Y}@C_{82}$ , and  $\text{La}@C_{82}$  is observed.<sup>189</sup> However, it is reported that the EPR signal for  $\text{Er}@C_{82}$  could not be resolved into the expected octet due to spin-spin interactions of the unpaired electron ( $S=1/2$ ) with the  $\text{Er}^{3+}$  4f-electrons ( $S=3/2$ ).<sup>189</sup> Thus it is difficult to assign an experimental hyperfine coupling value to  $\text{Er}@C_{82}$  for graphical purposes. However, the  $\text{Er}@C_{82}$  species can still be plotted in Figure 4.40 since the  $\log k'$  value has been obtained. After plotting, the striking feature is that, graphically speaking, the hyperfine coupling constant for  $\text{Er}@C_{82}$  coincidentally corresponds to  $\sim 0$  gauss. This feature may be related to the difficulty (spin-spin coupling) in observing hyperfine structure for the sharp absorption ( $g = 2.005$ ) as discussed above. It should also be noted that a second EPR

signal was located for  $\text{Er}@C_{82}$ .<sup>189</sup> Located at a g-factor of 8.6 g (80 GHz), this observed resonance is very *broad* and originates from transitions of  $\text{Er}^{3+}$  4f electrons ( $S=3/2$ ). Similar g-values are found for  $\text{Er}^{3+}$  ions in salt crystals.<sup>189</sup>

An additional application of Figure 4.40 can be made in the yttrium case. As mentioned previously, the  $\text{Sc}_3@C_{82}$  metallofullerene has been the only tri-atomic, metal-encapsulated fullerene. The issue of whether other tri-atomic metal atoms (e.g.  $\text{Y}_3$ ,  $\text{La}_3$ , etc.) exist has often been debated. In a fraction obtained from a Buckyclutcher separation of an yttrium extract, a weak mass spectral signal corresponding to  $\text{Y}_3@C_{82}$  was found (Figure 4.41a). The  $m/z$  value of 1253 from this spectrum corresponds to a calculated mass of  $\text{Y}_3@C_{82}$  (1253). Other species containing mass values in this region include  $C_{104}$  (1249),  $\text{Y}@C_{96}$  (1242), and  $\text{Y}_2@C_{90}$  (1259). Other species in this fraction included  $C_{110}$  and  $\text{Y}_2@C_{94}$ . Chromatographically, a  $\log k'$  value was determined and subsequently plotted as indicated by Figure 4.41b. Assuming  $\text{Y}_3@C_{82}$  was found and assuming this plot is accurate, a predicted hyperfine coupling constant of 5.03 - 6.18 g would be obtained.

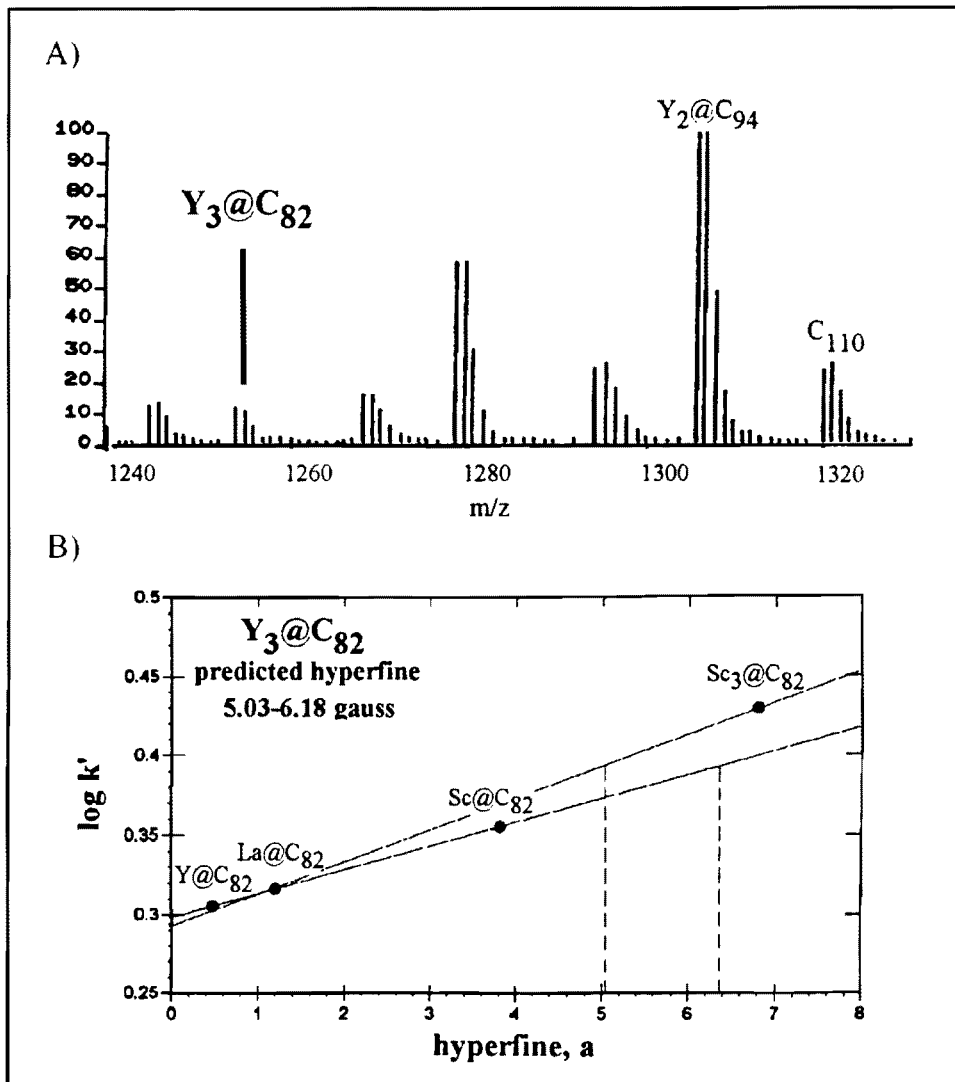


Figure 4.41 (a) mass spectrum of a  $Y_3@C_{82}$  - containing Buckyclutcher fraction. (b) Predicted hyperfine value for  $Y_3@C_{82}$  using a plot of  $\log k'$  versus hyperfine coupling constant.



## CHAPTER 5: FUTURE DEVELOPMENTS

### 5.1 Summary

At this writing, our laboratory has developed premier separation methodologies for the isolation of endohedral metallofullerenes. Purified metallofullerene samples have been obtained utilizing different types of columns. In summary, the polystyrene/Buckyclutcher two-stage system has resulted in purified  $\text{Sc}_2@C_{76}$ ,  $\text{Sc}_2@C_{84}$  (two isomers),  $\text{Sc}_3@C_{82}$ , and  $\text{La}_2@C_{72}$ . Meanwhile, the Buckyclutcher/TPP system has resulted in purified  $\text{Er}_2@C_{82}$  (two isomers) and  $\text{Er}@C_{82}$ . However, the optimal methodology involves a Buckyclutcher/PBB two-stage system. The high loadability of the Buckyclutcher column in conjunction with the high resolution of the PBB column has resulted in a valuable collection of purified metallofullerene samples. Specifically, isolated samples using this system include  $\text{Sc}_2@C_{74}$ ,  $\text{Sc}_2@C_{76}$ ,  $\text{Sc}_2@C_{78}$ ,  $\text{Sc}_2@C_{80}$ ,  $\text{Sc}_2@C_{82}$ ,  $\text{Sc}_2@C_{84}$  (two isomers),  $\text{Sc}_2@C_{86}$ ,  $\text{Sc}_2@C_{88}$ ,  $\text{Sc}_2@C_{90}$ ,  $\text{Sc}_3@C_{82}$ ,  $\text{Sc}_3@C_{84}$ , and  $\text{Sc}_4@C_{82}$ . These milligram quantities of purified samples can now be used in long-awaited characterization experiments (e.g.  $^{45}\text{Sc}$  NMR,  $^{13}\text{C}$  NMR, TEM, non-linear optical measurements, etc.).

The isolation of several unique metallofullerenes should be addressed. Namely,  $\text{Sc}_2@C_{74}$  and  $\text{La}_2@C_{72}$  possess only one possible cage structure in accordance with the isolated pentagon rule (Section 2.12). Holding the cage size constant, the influence of the encaged metal atoms can then be studied directly. These cage structures are also expected to be highly symmetrical. The  $C_{74}$  cage has  $D_{3h}$  symmetry, whereas the  $C_{72}$  cage structure has  $D_{6h}$  symmetry. From a NMR viewpoint, the  $\text{La}_2@C_{72}$  species would be an ideal sample and yield a  $^{13}\text{C}$  NMR spectrum of only four lines - assuming the La atoms do not lower the symmetry of the molecule.

At present, the  $\text{Sc}_2@C_{74}$  and  $\text{Sc}_2@C_{76}$  purified samples are currently being used in a  $^{45}\text{Sc}$  NMR study. Preliminary data has suggested that  $^{45}\text{Sc}$  NMR spectra are readily obtained only for those metallofullerenes with smaller  $C_{74}$ - $C_{76}$  cage sizes. In contrast,  $^{45}\text{Sc}$  NMR spectra for isolated metallofullerene samples with larger  $C_{82}$ - $C_{84}$  cage structures ( $\text{Sc}_2@C_{84}$ ,  $\text{Sc}_3@C_{82}$ ) were unsuccessful (room temperature) despite having a factor of 3-6 times more sample.

In addition, the discovery and isolation of purified  $\text{Sc}_4@C_{82}$  represented the first time a sample with four encaged metal atoms had been obtained. However, future characterization experiments will be limited since only  $\sim 100\ \mu\text{g}$  was isolated.

## 5.2 Concluding Remarks.

From 1990-1995, the field of metallofullerene science focused on developing a methodology to obtain purified samples. The recent advances in chromatographic separations have finally resulted in milligram quantities of isolated metallofullerenes. At present, columns are now commercially available and specifically designed for fullerene and metallofullerene separations. Although isolated samples are only present in milligram quantities, chemists can now finally probe into the unique characterization of metallofullerene species.

In recent years, there has been much discussion regarding the type of properties which metallofullerenes are believed to possess. Based on the novel arrangement of metal and carbon atoms, metallofullerenes are anticipated to have unique and exciting properties. Although purification methodologies have now been developed, more fundamental research into the *production* aspect needs to be performed. Despite having milligram-level samples, scientists are still often sample limited. Despite the fact that several research groups have now obtained purified metallofullerene species, the exact structure of any metallofullerene has yet to be elucidated. This is due, in part, to the difficulty of isolating macroscopic amounts of highly purified samples.

One could argue that the major problem area does not rest with the

chromatographic aspect but rather in the production step. Since the metallofullerene moiety typically represents only 1% of initial raw extract, more research should be performed in the production stage. For example, if a methodology could be developed to generate metallofullerenes in higher yield (20 - 70%), then separation scientists could likely obtain larger amounts of purified samples more efficiently. Unfortunately, until an improved production methodology is developed, the burden of obtaining purified metallofullerene samples will remain in the field of chromatographic science.

To date, scientists are on the edge of finally elucidating the exact structure for endohedral metallofullerene samples. NMR experiments have not provided conclusive information despite the fact that seemingly sufficient quantities (>10 mg) of purified endohedral samples have been obtained. This is likely due to any of the following: (1) presence of other co-eluting structural isomers (2) decreased symmetry of the carbon cage and/or (3) paramagnetism of the metal (e.g. Sc@C<sub>82</sub>).

Nevertheless, purified metallofullerene samples are now available, and a shift toward the "characterization aspect" should now be forthcoming. For example, Shinohara et al<sup>296</sup> have recently utilized scanning tunneling microscopy (STM) to observe an oriented "head-to-tail" cluster formation on a Cu(111) 1x1 surface for an isolated Y@C<sub>82</sub> sample. Their data indicates the presence of strong dipole-dipole and

charge-transfer interactions between the  $Y@C_{82}$  species. These  $Y@C_{82}$  molecules are similar to the "superatom" features that were theoretically proposed in a semiconductor heterostructure.<sup>296</sup> These  $Y@C_{82}$  metallofullerenes form quasi-molecules of the type ( $---Y@C_{82}---Y@C_{82}---Y@C_{82}---$ ).

In addition, this  $Y@C_{82}$  metallofullerene was subsequently characterized in a very recent X-ray diffraction study.<sup>297</sup> The analysis of  $Y@C_{82}$  microcrystals indicate that the molecules achieve a molecular alignment along the [001] direction in a "head-to-tail" manner. This orientation of  $Y@C_{82}$  molecules in a specific direction could lead to novel solid-state properties.<sup>297</sup>

### 5.3 Fullerene Related Materials.<sup>298-333</sup>

These initial emerging characterization experiments are encouraging for this endohedral type of fullerene compound. Nevertheless, it should be noted that the metallofullerenes represent only one member of the "fullerene family." Other intriguing species can also be created in arc-generated soot - depending on experimental considerations (e.g. choice of metal). For example, nanotubes<sup>298-328</sup> are cylindrical, tubular ( $\mu\text{m}$  length x nm diameter) shaped assemblies of carbon formed in arc-generated soot. These are formed when a metal such as cobalt<sup>299</sup> is introduced

to a cored graphite rod. Numerous predicted applications<sup>303,304,324,325</sup> include their use as composites,<sup>303</sup> catalysts,<sup>303</sup> and molecular wires.<sup>304</sup> Cylindrical layers of carbon nanotubes are predicted to be either metallic or semi-conducting.<sup>306,327,328</sup>

Shortly after the emergence of these hollow carbon nanotubes, scientists have successfully modified these nanotubes to encapsulate a metal (e.g. La, LaC, LaB<sub>6</sub>, YC, Pb, Mn, Gd, TiC, Nb, Fe<sub>3</sub>C, and Si).<sup>329-333</sup> Preliminary studies for several of these metallated nanoparticles do exhibit superconductivity and magnetism.<sup>329</sup>

For these reasons, there is a substantial interest in the endohedral metallofullerenes such as those purified in this research. With isolated metallofullerenes finally becoming available, scientists will soon be able to compare experimental data with their numerous, predicted properties. As previously discussed, anticipated applications have included the following: 1) tunable, non-linear-optical devices,<sup>175</sup> 2) biological studies<sup>2-4</sup> 3) superconductors,<sup>160</sup> and 4) novel catalytic materials.<sup>175</sup> With further research in the production, chromatography, and crystallization of metallofullerenes, one eagerly awaits characterization of their structural, electronic, and optical properties for this exciting new class of compounds.

## REFERENCES

1. Kroto H.W., Heath J.R., O'Brien S.C., Curl R.F., and Smalley R.E., Nature, **318**, 162-163, 1985.
2. Friedman S.H., Wudl F., Rubin Y., and Kenyon G.L., in Fullerenes: Recent Advances in the Chemistry and Physics of Fullerenes and Related Materials, (eds. Kadish K. and Ruoff R.), 662-669, (Electrochemical Society, 1994).
3. Scrivens W. A., Tour J.M., Creek K.E., and Pirisi L., in Fullerenes: Recent Advances in the Chemistry and Physics of Fullerenes and Related Materials, (eds. Kadish K. and Ruoff R.), 676-688, (Electrochemical Society, 1994).
4. Schinaza R.F., McMillan A., Juodawlkis A. S., Pharr J., Sijbsma R., Srdanov G., Hummelen J.C., Boudinot F.D., Hill C.L., and Wudl F., in Fullerenes: Recent Advances in the Chemistry and Physics of Fullerenes and Related Materials, (eds. Kadish K. and Ruoff R.), 689-696, (Electrochemical Society, 1994).
5. Welch C.J., and Pirkle W.H., J. Chromatogr., **609**, 89-101, 1992.
6. Krätschmer W., Lamb L.D., Fostiripoulos K., and Huffman D.R., Nature, **347**, 354-358, 1990.
7. Diederich F., Ettl R., Rubin Y., Whetten R.L, Beck R., Alvarez M., Anz S., Sensharma D., Wudl F., Khemani K.C., and Kuck A., Science, **252**, 548-551, 1991.
8. Diederich F., Whetten R.L., Thilgen C., Ettl R., Chao I., and Alvarez M., Science, **254**, 1768, 1991.
9. Parker D.H., Wurz P., Chatterjee K., Lykke K.R, Hunt J.E., Pellin M.J., Hemminger J.C., Gruen D.M., and Stock L.M., J.Amer.Chem. Soc., **113**, 7499-7503, 1991.
10. Kroto H.W., Angew Chem. Int. Ed. Engl., **31**, 111-129, 1992.

11. Kikuchi K., Nakahara N., Wakabayashi T., Honda M., Matsumiya H., Moriwaka T., Shiromaru H., Sato K., Yamauchi K., Ikemoto I., and Achiba Y., Chem. Phys. Lett., **188**, 177-180, 1992.
12. Kikuchi K., Nakahara N., Wakabayashi T., Suzuki S., Shiromaru H., Miyake Y., Saito K., Ikemoto I., Kainosho M., and Achiba Y., Nature, **357**, 142-145, 1992.
13. Diack M., Hettich R.L., Compton R.N., and Guichon G., Anal. Chem., **64**, 2143-2148, 1992.
14. Diederich F., and Whetten R.L., Acc. Chem. Res., **25**, 119-126, 1992.
15. Smalley R.E., Acc. Chem. Res., **25**, 98-105, 1992.
16. Manolopolous D.E., and Fowler P.W., J.Chem. Phys., **96**, 7603-7614, 1992.
17. Dhamodara R., Kaliappam I., Sivaraman N., Srinivasan T.G., Rao P.R.V., and Mathews C.K., Ind. J. Chem., **31A&B**, F32-F35, 1992.
18. Weaver J.H., Acc. Chem. Res., **25**, 143-149, 1992.
19. Parker D.H., Chatterjee K., Wurz P., Lykke K.R., Pellin M.J., Stock L.M., and Hemminger J.C, Carbon, **30**, 1167-1182, 1992.
20. Nondek L. and Kuzilek V., Chromatographia, **33**, 344-346, 1992.
21. Jinno K., Yamamoto K., Veda T., Nagashima H., Itoh K., Fetzer J.C., and Biggs W.R., J. Chromatogr., **594**, 105-109, 1992.
22. McElvaney S.W., Ross M.M., Callahan J.H., Acc. Chem. Res., **25**, 162-168, 1992.
23. Campbell E.E.B. and Hertel I.V., Carbon, **30**, 1157-1165, 1992.
24. Hare J.P. and Kroto H.W., Acc. Chem. Res., **25**, 106-112, 1992.



25. Smart C., Eldridge B., Reuter W., Zimmerman J.A., Creasy W.R., Rivera N., and Ruoff R.S., Chem. Phys. Lett., **188**, 171-176, 1992.
26. Chatterjee K., Parker D.H., Wurz P., Lykke K.R., Gruen D.M., and Stock L.M., J. Org. Chem., **57**, 3253-3254, 1992.
27. Klute R.C., Dorn H.C., and McNair H.M., J. Chromatogr. Sci., **30**, 438-442, 1992.
28. Fowler P.W. and Manolopolous D.E., Nature, **355**, 428-432, 1992.
29. Ruoff R.S., Tse D.S., Malhotra R., and Lorents D.C., J. Phys. Chem., **97**, 3379-3383, 1993.
30. Gügel A. and Müllen K., J. Chromatogr., **628**, 23-29, 1993.
31. Fowler P.W., Manolopolous D.E., Redmond D.B., and Ryan P.R., Chem. Phys. Lett., **202**, 371-378, 1993.
32. Selegue J.P., Show J.P., Guarr T.F., and Meier M.S., in Fullerenes: Recent Advances in the Chemistry and Physics of Fullerenes and Related Materials, (eds. Kadish K. and Ruoff R.), 1275-1291, (Electrochemical Society, 1994).
33. Taylor R., Hare J.P., Abdul-Sada A.K., and Kroto H.W., J. Chem. Soc. Chem. Commun., **20**, 1423-1425, 1990.
34. (a) Johnson R.D., Meijer B., and Bethune D.S., J. Amer. Chem. Soc., **112**, 8983-8984, 1990. (b) Ajie H., Alvarez M.M., anz S.J., Beck R.D, Diederich F., Fostiropoulos K., Huffman D.R., Kratschmer W., Rubin Y., Schriver K.E., Sensharma D., and Whetten R.L., J. Phys. Chem., **94**, 8630-8633, 1990.
35. Hawkins J.M., Lewis T.A., Loren S.D., Meyer A., Heath J.R., Shibato Y., and Saykally R.J., J. Org. Chem., **55**, 6250-6252, 1990.
36. Cox D.M., Behal S., Disko M., Gorun S.M., Greaney M., Hsu C.S., Kollin E.B., Millar J., Robbins J., Robbins W., Sherwood R.D., and Tindall P., J. Amer. Chem. Soc., **113**, 2940-1944, 1991.

37. Taylor R., Avent A., Birkett P.R., Dennis J.S., Hare J.P., Hitchcock P.B., Holloway J.H., Hope E.G., Kroto K.W., Langley G.J., Meidine M.F, Parsons J.P., and Walton D.R.M., Pure & Appl. Chem., **65**, 135-142, 1993.
38. Cox D.M., Reichmann K.C., and Kaldor A., J. Chem. Phys., **88**, 1588-1597, 1988.
39. Kroto H., Science, **242**, 1139-1145. 1988.
40. Curl R.F. and Smalley R.E., Science, **242**, 1017-1022, 1988.
41. Haufler R.E., Conceicao J., Chibante L.P.F., Chai Y., Byrne N.E., Flanagan S., Haley M.M., O'Brien S.C., Pan C., Xiao Z., Bilups W.E., Ciufolini M.A., Hage R.H., Margrave J.L., Wilson L.J., Curl R.F., and Smalley R.E., J. Phys. Chem., **94**, 8634-8636, 1990.
42. Bethune D.S., Meijer G., Tang W.C., and Rosen H.J., Chem. Phys. Lett., **174**, 219-222, 1990.
43. Krätschmer W., Fostiropoulos K., and Huffman D.R., Chem. Phys. Lett., **170**, 167-170, 1990.
44. Kikuchi K., Nakahara N., Honda M., Suzuki S., Saito K., Shiromaru H., Yamauchi K., Ikemoto I., Kuramochi T., Hino S., and Achiba Y., Chem. Lett., 1607-1610, 1991.
45. Huang Y., Gilson D.F..R., and Butler I.S., J. Phys. Chem., **95**, 5723-5725, 1991.
46. Zimmerman J.A., Eyler J.R., Bach S.B.H., and MElvany S.W., J. Chem. Phys., **94**, 3556-3562, 1991.
47. Beck R.D., St. Hohn P., Alvarez M.M., Diederich F., and Whetten R.L., J. Phys. Chem., **95**, 8402-8409, 1991.
48. Arbogast J.W., Darmanyan A.P., Foote C.S., Rubin Y., Diederich F.N., Alvarez M.M., Anz S.J., and Whetten R.L., J. Phys. Chem., **95**, 11-12, 1991.

49. Achiba Y., Nakagawa T., Matsui Y., Suzuki S., Shiromaru H., Yamauchi K., Nishiyama K., Kainosho M., Hoshi H., Maruyama Y., and Mitani T., Chem. Lett., 1233-1236, 1991.
50. Bakowies D. and Thiel, J. Amer. Chem. Soc., **113**, 3704-3714, 1991.
51. Shinohara H., Sato H., Saito Y., Tohji., Matsuoka I., Udagawa Y., Chem. Phys. Lett., **183**, 145-148, 1991.
52. Cox D.M., Behal S., Disko M., Gorun S.M., Greaney M., Hsu C.S., Kollin E.B., Millar J., Robbins J., Robbins W., Sherwood R.D., and Tindall P., J. Amer. Chem. Soc., **113**, 2940-2944, 1991.
53. Terminello L.J., Shuh D.K., Himpfel F.J., Lapiano-Smith D.A., Stohr J., Bethune D.S., and Meijer G., Chem. Phys. Lett., **182**, 491-496, 1991.
54. Raghavachari K. and Rohlffing C.M., J. Phys. Chem., **95**, 5768-5773, 1991.
55. Kato T., Kodama T., Shida T., Nakagawa T., Matsui Y., Suzuki S., Shiromaru H., Yamauchi K., and Achiba Y., Chem. Phys. Lett., **180**, 446-450, 1991.
56. Ben-Amotz D., Cooks R.G., Dejarne L., Gunderson J.C., Hoke S.H., Kahr B., Payne G.L., and Wood J.M., Chem. Phys. Lett., **183**, 149-152, 1991.
57. Guo Y., Karasawa N., and Goddard W.A., Nature, **351**, 465-467, 1991.
58. Hedberg K., Hedberg L., Bethune D.S., Brown C.A., Dorn H.C., Johnson R.D., de Vries M.S., Science, **254**, 410-412, 1991.
59. McElvany S.W. and Callahan J.K., J. Phys. Chem., **95**, 6186-6191, 1991.
60. Manolopoulos D.E., J. Chem. Soc. Faraday Trans., **87**, 2861-2862, 1991.
61. Wang Y. and Cheng L.T., J. Phys. Chem., **96**, 1430-1532, 1992.
62. Kurita N., Kobayashi K., Kumahora H., Tago K., and Ozawa K., Chem. Phys. Lett., **188**, 181-186, 1992.

63. Bakowies D., Kolb M., Thiel W., Richard S., Ahlrichs R., and Kappes M.M., Chem. Phys. Lett., **200**, 411-417, 1992.
64. Rao C.N.R., Pradeep T., Seshadri R., Nagarajan R., Murthy V.N., Subbanna G.N., D'Souza F., Krishnan V., Nagannagowda G.A., Suryaprakash N.R., Khetrupal C.L., and Bhat S.V., Indian J. Chem., **31 A&B**, F5-F16, 1992.
65. Oshiyama A., Saito S., Hamada N., and Miyamoto Y., J. Phys. Chem. Solids, **53**, 1457-1471, 1992.
66. Heiney P.A., J. Phys. Chem. Solids, **53**, 1333-1352, 1992.
67. Terrones H. and Mackay A.L., Carbon, **30**, 1251-1260, 1992.
68. Dunne L.J., and Clark A.D., Chaplin M.F., and Katbamna H., Carbon, **30**, 1227-1233, 1992.
69. Hwang K.C. and Mauzerall D., Nature, **361**, 138-140, 1993.
70. Grivei E., Nysten B., Cassart M., Demain A., and Issi J.P., Solid State Commun., **85**, 73-75, 1993.
71. Wakisaka A., Sato H., Gaumet J.J., Shimizu Y., Tamori Y., Tsuchiya M., and Tokumaru K., J. Chem Soc., Chem. Commun., 77-78, 1993.
72. Creasy W.R., Zimmerman J.A., and Ruoff R.S., J. Phys. Chem., **97**, 973-979, 1993.
73. Howard J. B., Lafleur A. L., Makarovskiy Y., Mitra S., Pope C.J., and Yadav T.K., Carbon, **30**, 1183-1201, 1992.
74. Prassides K., Kroto H.W., Taylor R., Walton D.R.M., David W.I.F., Tomkinson J., Haddon R.C., Rosseinsky M.J., and Murphy D.W., Carbon, **30**, 1277-1286, 1992.
75. Sibley S.P., Argentine S.M., and Francis A.H., Chem. Phys. Lett., **188**, 187-193, 1992.

76. Saito Y., Inagaki M., Shinohara H., Nagashima H., Ohkohchi M., and Ando Y., Chem. Phys. Lett., **200**, 643-648, 1992.
77. Sandler P., Lifshitz C., Klots C.E., Chem. Phys. Lett., **200**, 445-450, 1992.
78. Mathews C.K., Baba M.S., Narasimhan T.S.L., Balasubramanian R., Sivaraman N., Srinivasan T.G., and Rao P.R.V., J. Phys. Chem., **96**, 3566-3568, 1992.
79. Curl R.F., Carbon, **30**, 1149-1155, 1992.
80. Bohme D.K., Chem. Rev., **92**, 1487-1508, 1992.
81. Diederich F. and Rubin Y., Angew. Chem. Int. Ed. Engl., **31**, 1101-1123, 1992.
82. Heiney P.A., J. Phys. Chem. Solids, **53**, 1333-1352, 1992.
83. Copley J.R.D., Neumann D.A., Cappelletti R.L., and Kamitakahara W.A., J. Phys. Chem. Solids, **53**, 1353-1371, 1992.
84. Wang X.Q., Wang C.Z., ZZhang B.L. and Ho K.M., Chem. Phys. Lett., **200**, 35-38, 1992.
85. Fowler P.W., Manolopoulos D.E., and Ryan R.P., Carbon, **30**, 1235-1250, 1992.
86. Creasy W.R., Zimmerman J.A., and Ruoff R.S., J. Phys. Chem., **97**, 973-979, 1993.
87. Hamilton B., Rimmer J.S., Anderson M. and Leigh D., Adv. Mater., **5**, 583-585, 1993.
88. Wakabayashi T., Shiromaru H., Kikuchi K. and Achiba Y., Chem. Phys. Lett., **201**, 470-474, 1992.

89. Dunsch L., in Fullerenes: Recent Advances in the Chemistry and Physics of Fullerenes and Related Materials, (ed. Kadish K.M. and Ruoff R.S.), 1068-1076, (Electromechanical Society, 1994).
90. Bendale R.D. and Zerner M.C., J. Phys. Chem., **99**, 13830-13833, 1995.
91. Radi P.P., Hsu M.T., Rincon M.E., Kemper P.R., and Bowers M.T., Chem. Phys. Lett., **174**, 223-228, 1990.
92. Hawkins J.M., Meyer A., Lewis T.A., Loren S., Hollander F.J., Science, **252**, 312-313, 1991.
93. Ross M.M. and Callahan J.H., J. Phys. Chem., **95**, 5720-5723, 1991.
94. Huang Y. and Freiser B.S., J. Amer. Chem. Soc., **113**, 8187-8188, 1991.
95. Pradeep T., Vijayakrishnan V., Santra A.K. and Rao C.N.R., J. Phys. Chem., **95**, 10564-10565, 1991.
96. Xie Q., Perez-Cordero E. and Echegoyen L., J. Amer. Chem. Soc., **114**, 3978-3980, 1992.
97. Fagan P.J., Chase B., Calabrese C., Dixon D.A., Harlow R., Kursic P.J., Matsuzawa N., Tebbe F.N., Thorn D.L., and Wasserman E., Carbon, **30**, 1213-1226, 1992.
98. McEwen C.N., McKay R.G. and Larsen B.S., J. Amer. Chem. Soc., **114**, 4412-4414, 1992.
99. Fischer J.E., Heiney P.A. and Smith A.B., Acc. Chem. Res., **25**, 112-117, 1992.
100. Hawkins J.M., Acc. Chem. Res., **25**, 150-156, 1992.
101. Wudl F., Acc. Chem. Res., **25**, 157-161, 1992.

102. Cardini G., Procacci P., Salvi P.R. and Schettino V., Chem. Phys. Lett., **200**, 39-45, 1992.
103. Vasella A., Uhlmann P., Waldruff C.A.A., Diederich F. and Thilgen C., Angew. Chem. Int. Ed. Engl., **21**, 1388-1390, 1992.
104. Olah G.A., Bucsi I., Aniszföld R., and Prakash G.K.S., Carbon, **30**, 1203-1211, 1992.
105. Karfunkel H.R. and Hirsch A., Angew. Chem. Int. Ed. Engl., **31**, 1468-1471, 1992.
106. Prato M., Li Q.C., Wudl F. and Lucchini V., J. Amer. Chem. Soc., **115**, 1148-1150, 1993.
107. Belik P., Gugel A., Spickermann J. and Mullen K., Angew. Chem. Int. E. Engl., **32**, 78-80, 1993.
108. Prato M., Suzuki T., Foroudian H., Li Q., Khemani K., Wudl F., Leonetti J., Little R.D., White T., Rickborn B., Yamago S., and Nakamura E., J. Amer. Chem. Soc., **115**, 1594-1595, 1993.
109. Akasaka T., Ando W., Kobayashi K. and Nagase S., in Fullerenes: Recent Advances in the Chemistry and Physics of Fullerenes and Related Materials, (ed. Kadish K.M. and Ruoff R.S.), 723-733, (Electromechanical Society, 1994).
110. Callahan J.H., Ross M.M., Weiske T. and Schwarz H., J. Phys. Chem., **97**, 20-22, 1993.
111. Gakh A.A., Tuinman A.A., Adcock J.L., Sachleben R.A., and Compton R.N., J. Amer. Chem. Soc., **116**, 819-820, 1994.
112. Jimenez-Vazquez H.A., Cross R.J., Saunders M. and Poreda R.J., Chem. Phys. Lett., **229**, 111-114, 1994.
113. Greaney M.A. and Gorun S.M., J. Phys. Chem., **95**, 7142-7144, 1991.

114. Blinc R., Cevc P., Arcon D., Mihailovic D. and Venturini P., in Fullerenes: Recent Advances in the Chemistry and Physics of Fullerenes and Related Materials, (ed. Kadish K.M. and Ruoff R.S.), 568-571, (Electromechanical Society, 1994).
115. Kukolich S.G. and Huffman D.R., Chem. Phys. Lett., **182**, 263-265, 1991.
116. Kinoshita N. Tanaka Y., Tokumoto M. and Matsumiya S., J. Phys. Soc. Jap., **60**, 4032-4035, 1991.
117. Krusic P.J., Wasserman E., Keizer P.N., Morton J.R. and Preston K.F., Science, **254**, 1183-1185, 1991.
118. Allemand P.M., Srdanov G., Koch A., Khemani K. and Whetten R.L., J. Amer. Chem. Soc., **113**, 2780-2781, 1991.
119. Krusic P.J., Wasserman E., Parkinson B.A., Malone B., Holler E.R., Keizer P.N., Morton J.R., and Preston K.F., J. Amer. Chem. Soc., **113**, 6274-6275, 1991.
120. Bennati M., Grupp A., Mehring M., Dinse K.P., and Fink J., Chem. Phys. Lett., **200**, 440-444, 1992.
121. Morton J.R., Preston K.F., Krusic P.J., Hill S.A., and Wasserman E., J. Phys. Chem., **96**, 3576-3678, 1992.
122. Kawata S., Yamauchi K., Suzuki S., Kikuchi K., Shiromaru H., Katada M., Saito K., Ikemoto I., and Achiba Y., Chem. Lett., 1659-1662, 1992.
123. Morton J.R., Preston K.F., Krusic P.J., Hill S.A., and Wasserman E., J. Amer. Chem. Soc., **114**, 5454-5455, 1992.
124. Morton J.R., Preston K.F., Krusic P.J., and Wasserman E., J. Chem. Soc. Perkin Trans., **2**, 1425-1429, 1992.
125. Pace M.D., Christidis T.C., Yin J.J., and Milliken J., J. Phys. Chem., **96**, 6855-6858, 1992.



126. Krusic P.J., Roe D.C., Johnston E., Morton J.R., and Preston K.F., J. Phys. Chem., **97**, 1736-1738, 1993.
127. Lezius M. Scheier P., and Mark T.D., Chem. Phys. Lett., **203**, 232-236, 1993.
128. Dimitrijevic N.M., Kamat P.V., and Fessenden R.W., J. Phys. Chem., **97**, 615-618, 1993.
129. Subramanian R., Boulas P., Vijayashree M.N., D'Souza F., Jones M.T., and Kadish K.M., in Fullerenes: Recent Advances in the Chemistry and Physics of Fullerenes and Related Materials, (ed. Kadish K.M. and Ruoff R.S.), 779-788, (Electromechanical Society, 1994).
130. Johnson R.D., Meijer G., Salem J.R., and Bethune D.S., J. Amer. Chem. Soc., **113**, 3619-3621, 1991.
131. Yannoni C.S., Johnson R.D., Meijer G., Bethune D.S., and Salem J.R., J. Phys. Chem., **95**, 9-10, 1991.
132. Walton J.H., Kamasa-Quashie A.K., Joers J.M., and Gullion T., Chem. Phys. Lett., **203**, 237-242, 1993.
133. Canet D., Robert J.B., and Tekely P., Chem. Phys. Lett., **212**, 483-486, 1993.
134. Chai Y., Guo T., Jin C., Haufler R.E., Chibante L.P.F., Fure J., Wang L., Alford J.M., and Smalley R.E., J. Phys. Chem., **95**, 7564, 1991.
135. Manolopoulos D.E. and Fowler P.W., Chem. Phys. Lett., **187**, 1-7, 1991.
136. Alvarez M.M., Gillan E.G., Holczer K., Kaner R.B., Min K.S., and Whetten R.L., J. Phys. Chem., **95**, 10561-10563, 1991.
137. Bandow S., Kitagawa H., Mitani T., Inokuchi H., Saito Y., Yamaguchi H., Hayashi N., Sato H., and Shinohara H., J. Phys. Chem., **96**, 9609-9612, 1992.
138. Soderholm L., Wurz P., Lykke K.R., Parker D.H., and Lytle F.W., J. Phys. Chem., **96**, 7153-7156, 1992.

139. Ross M.M., Nelson H.H., Callahan J.H., and McElvany S.W., Mat. Res. Soc. Symp. Proc., **270**, 269-274, 1992.
140. Johnson R.D., Yannoni C.S., deVries M.S., Dorn H.C., Salem J.R., and Bethune D.S., Nanotechnology, **3**, 164-166, 1992.
141. Laasonen K., Andreoni W., and Parrinello M., Science, **258**, 1916-1918, 1992.
142. Suzuki S., Kawata S., Shiromaru H., Yamauchi K., Kikuchi K., Kato T., and Achiba Y., J. Phys. Chem., **96**, 7159-7161, 1992.
143. Shinohara H., Sato H., Ohkohchi M., Ando Y., Kodama T., Shida T., Kato T., and Saito Y., Nature, **357**, 52-54, 1992.
144. Gillan E.G., Yeretzian C., Min K.S., Alvarez M.M., Whetten R.L., and Kaner R.B., J. Phys. Chem., **96**, 6869-6871, 1992.
145. Shinohara H., Sato H., Saito Y., Ohkohchi M., and Ando Y., J. Phys. Chem., **96**, 3571-3573, 1992.
146. Hoinkis M., Yannoni C.S., Bethune D.S., Salem J.R., Johnson R.D., Crowder M.S., and deVries M.S., Chem. Phys. Lett., **198**, 461-465, 1992.
147. Yannoni C.S., Hoinkis M., deVries M.S., Bethune D.S., Salem J.R., Crowder M.S., and Johnson R.D., Science, **256**, 1191-1193, 1992.
148. Manolopolous D.E., Fowler P.W., and Ryan R.P., J. Chem. Soc. Faraday Trans., **88**, 1225-1226, 1992.
149. Saito S. and Sawada S., Chem. Phys. Lett., **198**, 466-471, 1992.
150. Weaver J.H., Chai Y., Kroll G.H., Jin C., Oho T.R., Haufler R.E., Guo T., Alford J.M., Conceicao J., Chibante L.P.F., Jain A., Palmer G., and Smalley R.E., Chem. Phys. Lett., **190**, 460-465, 1992.
151. Johnson R.D., deVries M.S., Salem J.R., Bethune D.S., and Yannoni C.S., Nature, **355**, 239-240, 1992.

152. Johnson R.D., Yannoni C.S., Hoinkis M., deVries M.S., Salem J.R., Crowder M.S., and Bethune D.S., Mat. Res. Soc. Symp. Proc., **270**, 261-267, 1992.
153. McElvaney S.W., J. Phys. Chem., **96**, 4935-4937, 1992.
154. Yeretizian C., Hausen K., Alvares M.M., Min K.S., Gillan E.G., Holczer K., Kaner T.B., and Whetten R.L., Chem. Phys. Lett., **196**, 337-342, 1992.
155. Ross M.M., Nelson H.H., Callahan J.H., and McElvaney S.W., J. Phys. Chem., **96**, 5231-5234, 1992.
156. Yannoni C.S., Wendt H.R., deVries M.S., Siemens R.L., Salem J.R., Lyerla J., Johnson R.D., Hoinkis M., Crowder M.S., Brown C.A., and Bethune D.S., Synthetic Metals, **59**, 279-285, 1993.
157. Wang Y., Tomanek D., and Ruoff R.S., Chem Phys. Lett., **208**, 79-85, 1993.
158. Kato T., Suzuki S., Kikuchi K., and Achiba Y., J. Phys. Chem., **97**, 13425-13428, 1993.
159. Ungerer J.R. and Hughbanks T., J. Amer. Chem. Soc., **115**, 2054-2055, 1993.
160. Bethune D.S., Johnson R.D., Salem J.R., deVries M.S., and Yannoni C.S., Nature, **366**, 123-128, 1993.
161. Wan X.D., Hashizume T., Xue Q., Shinohara H., Saito Y., Nishina Y., and Sakurai T., Chem. Phys. Lett., **216**, 409-412, 1993.
162. Moro L., Ruoff R.S., Becker C.H., Lorents D.C., and Malhotra R., J. Phys. Chem., **97**, 6801-6805, 1993.
163. Yeretizian C., Wiley J.B., Holczer K., Su T., Nguyen S., Kaner R.B., and Whetten R.L., J. Phys. Chem., **97**, 10097-10101, 1993.
164. Nagase S., Kobayashi K., Kato T., and Achiba Y., Chem Phys. Lett., **201**, 475-480, 1993.

165. Ugarte D., Chem. Phys. Lett., **209**, 99-103, 1993.
166. Bandow S., Shinohara H., Saito Y., Ohkohchi M., and Ando Y., J. Phys. Chem., **97**, 6101-6103, 1993.
167. Nagase S. and Kobayashi K., Chem. Phys. Lett., **214**, 57-63, 1993.
168. Shinohara H., Yamaguchi H., Hayashi N., Sato H., Ohkohchi M., Ando Y., and Saito Y., J. Phys. Chem., **97**, 4259-4261, 1993.
169. Kikuchi K., Suzuki S., Nakao Y., Nakahara N., Wakabayashi T., Shiromaru H., Saito K., Ikemoto I., and Achiba Y., Chem. Phys. Lett., **216**, 67-71, 1993.
170. Suzuki T., Maruyama Y., Kato T., Kikuchi K., and Achiba Y., J. Amer. Chem. Soc., **115**, 11006-11007, 1993.
171. Hino S., Takahashi H., Iwasaki K., Matsumoto K., Miyazaki T., Hasegawa S., Kikuchi K., and Achiba Y., Phys. Rev. Lett., **71**, 4261-4263, 1993.
172. Dorn H.C., Stevenson S., Burbank P., Sun Z., Glass T., Harich K., van Loosdrecht P.H.M., Johnson R.D., Beyers R., Salem J.R., deVries M.S., Yannoni C.S., Bethune D.S., and Kiang C.H., Mat. Res. Soc. Symp. Proc., **359**, 123-135, 1995.
173. Stevenson S., Dorn H.S., Burbank P., Harich K., Haynes J., Kiang C.H., Salem J.R., deVries M.S., van Loosdrecht P.H.M., Johnson R.D., Yannoni C.S., and Bethune D.S., Anal. Chem., **66**, 2675, 2679, 1994.
174. Stevenson S., Dorn H.C., Burbank P., Harich K., Sun Z., Kiang C.H., Salem J.R., deVries M.S., van Loosdrecht P.H.M., Johnson R.D., Yannoni C.S., and Bethune D.S., Anal. Chem., **66**, 2680-2685, 1994.
175. Beyers R., Kiang C.H., Johnson R.D., Salem J.R., deVries M.S., Yannoni C.S., Bethune D.S., Dorn H.C., Burbank P., Harich K., and Stevenson S., Nature, **370**, 196-199, 1994.

176. van Loosdrecht P.H.M., Johnson R.D., Beyers R., Salem J.R., deVries M.S., Bethune D.S., Burbank P., Haynes J., Glass T., Stevenson S., Dorn H.C., Boonman M., van Bentum P.J.M., and Meijer G., in Fullerenes: Recent Advances in the Chemistry and Physics of Fullerenes and Related Materials, (ed. Kadish K.M. and Ruoff R.S.), 1320-1330, (Electromechanical Society, 1994).
177. van Loosdrecht P.H.M., Johnson R.D., deVries M.S., Kiang C.H., Bethune D.S., Dorn H.C., Burbank P., and Stevenson S., Phys. Rev. Lett., **73**, 3415-3418, 1994.
178. Bethune D.S., Kiang C.H., Beyers R., van Loosdrecht P.H.M., deVries M.S., Salem J.R., Yannoni C.S., Johnson R.D., Burbank P., Haynes J., Glass T., Stevenson S., and Dorn H.C., Proc. IWEPM 94, Kirchberg/Tirol, Austria, 5-12, March 1994.
179. Bartl A., Dunsch L., Frohner J., and Kirbach U., Chem. Phys. Lett., **229**, 115-121, 1994.
180. Capp C., Wood T.D., Marshall A.G, and Coe J.V., J. Amer. Chem. Soc., **116**, 4987-4988, 1994.
181. Suzuki S., Kojima Y., Nakao Y., Wakayabashi T., Kawata S., Kikuchi K., Achiba Y., and Kato T., Chem. Phys. Lett., **229**, 512-516, 1994.
182. Shinohara H., Inakuma M., Hayashi N., Sato H., Saito Y., Kato T., and Bandow S., J. Phys. Chem., **98**, 8597-8599, 1994.
183. Kikuchi K., Nakao Y., Achiba Y., and Nomura M., in Fullerenes: Recent Advances in the Chemistry and Physics of Fullerenes and Related Materials, (ed. Kadish K.M. and Ruoff R.S.), 1300-1308, (Electromechanical Society, 1994).
184. Savina M.R., Martin G., Xiao J., Milanovich N., Meyerhoff M.E., and Francis A.H., in Fullerenes: Recent Advances in the Chemistry and Physics of Fullerenes and Related Materials, (ed. Kadish K.M. and Ruoff R.S.), 1309-1319, (Electromechanical Society, 1994).

185. Suzuki T., Maruyama Y., Kato T., Kikuchi K., Achiba Y., Yamamoto K., Funasaka H., and Takahashi T., in Fullerenes: Recent Advances in the Chemistry and Physics of Fullerenes and Related Materials, (ed. Kadish K.M. and Ruoff R.S.), 1077-1086, (Electromechanical Society, 1994).
186. (a) Kato T., Bandow S., Inakuma M., Shinohara H., Hayashi N., and Saito Y., in Fullerenes: Recent Advances in the Chemistry and Physics of Fullerenes and Related Materials, (ed. Kadish K.M. and Ruoff R.S.), 1331-1339, (Electromechanical Society, 1994). (b) Kato T., Bandow S., Inakuma M., and Shinohara H., J. Phys. Chem., **99**, 856-858, 1995.
187. Shinohara H., Kishida M., Nakane T., Kato T., Bandow S., Saito Y., Wang X.D., Hashizume T., and Sakurai T., in Fullerenes: Recent Advances in the Chemistry and Physics of Fullerenes and Related Materials, (ed. Kadish K.M. and Ruoff R.S.), 1361-1381, (Electromechanical Society, 1994).
188. (a) Yamamoto K., Funasaka H., Takahashi T., and Akasaka T., J. Phys. Chem., **98**, 2008-2011, 1994. (b) Knight L.B., Woodward R.W., Van Zee R.J., and Weltner W., J. Chem. Phys., **79**, 5820-5827, 1983.
189. Boonman M.E.J., van Loosdrecht P.H.M., Bethune D.S., Holleman I., Meijer G.J.M., and van Bentum P.J.M., to be published, 1995.
190. Funasaka H., Sugiyama K., Yamamoto K., and Takahashi T., J. Phys. Chem., **99**, 1826-1830, 1995.
191. Funasaka H., Sakurai K., Oda Y., Yamamoto K., and Takahashi T., Chem. Phys. Lett., **232**, 273-277, 1995.
192. Cox D.M., Trevor D.J., Reichmann K.C., and Kaldor A., J. Am. Chem. Soc., **108**, 2457-2458, 1986.
193. Rosen A. and Wastberg B., J. Amer. Chem. Soc., **110**, 8701, 8703, 1988.
194. (a) Weiss F.D., Elkind J.L., O'Brien S.C., Curl R.f., and Smalley R.E., J. Amer. Chem. Soc., **110**, 4464-4465, 1988. (b) Rosen A. and Wastberg B., Z. Phys. D - Atoms, Molecules and Clusters, **12**, 387-390, 1989.

195. Wilson L.J., Flanagan S., Khabashesku V., Alford M., Chibante F., Diener M., Fargason C., and Roche E., Appl. Superconductivity, **1**, 913-923, 1993.
196. Chang. A.H.H., Ermler W.C., and Pitser R.M., J. Chem. Phys., **94**, 5004-5010, 1991.
197. Schmidt P.P., Dunlap B.I., and White C.T., J. Phys. Chem., **95**, 10537-10541, 1991.
198. Caldwell K.A., Giblin D.E., Hsu C.S., Cox D., and Gross M.L., J. Amer. Chem. Soc., **113**, 8519-8521, 1991.
199. Mowrey R.C., Ross M.M., and Callahan J.H., J. Phys. Chem., **96**, 4755-4761, 1992.
200. Cioslowski J. and Nanayakkara A., J. Phys. Chem., **96**, 8354-8362, 1992.
201. van Cleef G.W., Renkes G.D., and Coe J.V., J. Chem. Phys., **98**, 860-864, 1993.
202. Bethune D.S., Yannoni C.S., Hoinkis M., de Vries M.S., Salem J.R., Crowder M.S., and Johnson R.D., Z. Phys. D. - Atoms, Molecules, and Clusters, **26**, 153-158, 1993.
203. Ying Z.C., Jin C., Hettich R.L., Poretzky A.A., Haufler R.E., and Compton R.N., in Fullerenes: Recent Advances in the Chemistry and Physics of Fullerenes and Related Materials, (ed. Kadish K.M. and Ruoff R.S.), 1402-1412, (Electromechanical Society, 1994).
204. Capp C., Wood T.D., Marshall A.G., and Coe J.V., in Fullerenes: Recent Advances in the Chemistry and Physics of Fullerenes and Related Materials, (ed. Kadish K.M. and Ruoff R.S.), 1340-1350, (Electromechanical Society, 1994).
205. Scuseria G.E., in Fullerenes: Recent Advances in the Chemistry and Physics of Fullerenes and Related Materials, (ed. Kadish K.M. and Ruoff R.S.), 1294-1298, (Electromechanical Society, 1994).

206. Poirier D.M., Knupfer M., Weaver J.H., Andreoni W., Laasonen K., Parrinello M., Bethune D.S., Kikuchi K., and Achiba Y., Phys. Rev. B, submitted Feb. 1994.
207. Bartl A., Dunsch L., Frohner J., and Kirbach U., Chem. Phys. Lett., **229**, 115-121, 1994.
208. Okabe N., Ohba Y., Suzuki S., Kawata S., Kikuchi K., Achiba Y., and Iwaizumi M., Chem. Phys. Lett., **235**, 564-569, 1995.
209. Lorents D.C., Yu D.H., Brink C., Jensen N., Gvelplund P., Chem. Phys. Lett., **236**, 141-149, 1995.
210. Rubsam M., Pluschau M., Schweitzer P., Kinse K.P., Fuchs D., Rietschel H., Michel R.H., Benz M., and Kappes M.M., Chem. Phys. Lett., **240**, 615-621, 1995.
211. Laskin J., Jimenez-vazquez H.A., Shimshi R., Saunders M., deVries M.S., and Lifshitz C., Chem. Phys. Lett., **242**, 249-252, 1995.
212. Kroto H.W., Nature, **329**, 529-531, 1987.
213. Schmalz T.G., Seitz W.A., Hein D.J., and Hite G.E., J. Amer. Chem. Soc., **110**, 1113-1127, 1988.
214. Manolopolous D.E., J. Chem. Soc. Faraday Trans., **87**, 2861, 1991.
215. Heath J.R. et al., J. Amer. Chem. Soc., **107**, 7779-7780, 1985.
216. Chai et al., J. Phys. Chem., **95**, 7504-7568, 1991.
217. Chen C.T., Tjeng L.H., Rudolf P., Meigs G., Rowe J.E., Chen J., McCauler J.P., Smith A.B., McGhie A.R., Romanow W.J., and Plummer E.W., Nature, **352**, 603-607, 1991.
218. Zhou O., Fischer J.E., Coustel N., Kycia S., Zhu Q., McGhie A.R., Romanow W.J., McCauler J.P., Smith A.B., and Cox D.E., Nature, **351**, 462-464, 1991.



219. Fleming R.M., Rosseinsky M.J., Ramirez A.P., Murphy D.W., Tully J.C., Haddon R.C., Siegrist T., Tycko R., Glarum S.H., Marsh P., Dabbagh G., Zahurak S.M., Makhija A.V., and Hampton C., Nature, **352**, 701-703, 1991.
220. Zhou O. and Cox D.E., J. Phys. Chem. Solids, **53**, 1373-1390, 1992.
221. Haddon R.C., Kochanski G.P., Hebard A.F., Fiory A.T., and Morris R.C., Science, **258**, 1636-1643, 1992.
222. Eklund P.C., Zhou P., Wang K.A., Dresselhaus G., and Dresselhaus M.S., J. Phys. Chem. Solids, **53**, 1391-1413, 1992.
223. Haddon R.C., Acc. Chem. Res., **25**, 127-133, 1992.
224. Xiang X.D., Hou J.G., Crespi H., Zettl A., and Cohen M.L., Nature, **361**, 54-56, 1993.
225. Ostling D. and Rosen A., Chem. Phys. Lett., **202**, 389-393, 1993.
226. Messaoudi A., Conard J., Setton R., and Beguin F., Chem. Phys. Lett., **202**, 506-508, 1993.
227. Haddon R.C., Kochanski G.P., Hebard A.F., Fiory A.T., Morris R.C., and Perel A.S., Chem. Phys. Lett., **203**, 433-437, 1993.
228. Ruoff R.S., Wang Y., and Tomanek D., Chem. Phys. Lett., **203**, 438-443, 1993.
229. Kosaka M., Tanigaki K., Hirose I., Shimakawa Y., Kuroshima S., Ebbesen T.W., Mizuki J., and Kubo Y., Chem. Phys. Lett., **203**, 429-432, 1993.
230. Murphy D.W., Rosseinsky M.J., Fleming R.M., Tycko R., Ramirez A.P., Haddon R.C., Siegrist T., Dabbagh G., Tully J.C., and Walstedt R.E., J. Phys. Chem. Solids, **53**, 1321-1332, 1992.
231. Hebard A.F., Rosseinsky M.J., Haddon R.C., Murphy D.W., Glarum S.H., Palstra T.T.M., Ramirez A.P., and Kortan A.R., Nature, **350**, 600-601, 1991.

232. Haddon R.C., Hebard A.F., Rosseinsky M.J., Murphy D.W., Duclos S.J., Lyons K.B., Miller B., Rosamilia J.M., Fleming M., Kortan A.R., Glarum S.H., Makhija A.V., Muller A.J., Eick R.H., Zahurak S.M., Tycko R., Dabbagh G., and Thiel F.A., Nature, **350**, 320-322, 1991.
233. Rosseinsky M.J., Ramirez A.P., Glarum S.H., Murphy D.W., Haddon R.C., Hebard A.F., Palstra T.T., Kortan A.R., Zahurak S.M., and Makhija A.V., Phys. Rev. Lett., **66**, 2830-2832, 1991.
234. Holczer K., Klein O., Huang S.M., Kaner R.B., Fu K.J., Whetten R.L., and Diederich F., Science, **252**, 1154-1157, 1991.
235. Tanigaki K., Ebbesen t.W., Saito S., Mizuki J., Tsai J.S., Kubo Y., and Kuroshima S., Nature, **352**, 222-223, 1991.
236. Chen C.C., Kelty S.P., and Lieber C.M., Science, **253**, 886, 1991.
237. Stephens P.W., Mihaly L., Lee P.L., Whetten R.L., Huang S.M., Kaner R.D., Diederich F., and Holczer K., Nature, **351**, 632-634, 1991.
238. Fleming R.M., Ramirez A.P., Rosseinsky M.J., Murphy D.W., Haddon R.C., Zahurak S.M., and Makhija A.V., Nature, **352**, 787-788, 1991.
239. Holczer K. and Whetten R.L., Carbon, **30**, 1261-1276, 1992.
240. Chen C.C. and Lieber C.M., Science, **259**, 655-658, 1993.
241. Tanigaki K., Hirosawa I., Ebbesen T.W., Mizuki J., and Kuroshima S., Chem. Phys. Lett., **203**, 33-36, 1993.
242. Kortan A.R., Kopylou N., Glarum S., Gyorgy E.M., Ramirez A.P., Fleming R.M., Zhou O., Thiel F.A., Trevor P.L., and Haddon R.C., Nature, **360**, 566-571, 1992.
243. Pirkle W.H. and Welch C.J., J. Org. Chem., **56**, 6973-6974, 1991.

244. Cui Y., Lee S.T., Olesik S.V., Flory W., and Mearini M., J. Chromatogr., **625**, 131-140, 1992.
245. Jinno K., Uemura T., Nagashimo H., and Itoh K., J. High Resol. Chromatogr., **15**, 627-628, 1992.
246. Meier M.S., Guarr T.F., Selegue J.P., and Vance V.K., J. Chem. Soc., Chem. Commun., 63-65, 1993.
247. Kimata K., Hosoya K., Araki T., and Tanaka N., J. Org. Chem., **58**, 282-283, 1993.
248. Kibbey C.E., Savina M.R., Parseghian B.K., Francis A.H., and Meyerhoff M.E., Anal. Chem., **65**, 3717-3719, 1993.
249. Jinno K., Uemura T., Ohta H., Nagashima H., and Itoh K., Anal. Chem., **65**, 2650-2654, 1993.
250. Tse D.S., Ruoff R.S., Lorents D.C., and Malhotra R., in Fullerenes: Recent Advances in the Chemistry and Physics of Fullerenes and Related Materials, (ed. Kadish K.M. and Ruoff R.S.), 191-199, (Electromechanical Society, 1994).
251. Martin G.G., Xiao J., Savina M.R., Wilks M., Francis A.H., and Meyerhoff M.E., in Fullerenes: Recent Advances in the Chemistry and Physics of Fullerenes and Related Materials, (ed. Kadish K.M. and Ruoff R.S.), 178-190, (Electromechanical Society, 1994).
252. Kibbey C.E. and Meyerhoff M.E., J. Chromatogr., **641**, 49-55, 1993.
253. Kibbey C.E. and Meyerhoff M.E., Anal. Chem., **65**, 2189-2196, 1993.
254. Tanaka N., Tokuda Y., Iwaguchi K., and Araki M., J. Chromatogr., **239**, 761-772, 1982.
255. Kimata K., Hosoya K., Tanaka N., Araki T., and Patterson D.G., J. Chromatogr., **595**, 77-88, 1992.

256. Rokushika S., Taniguchi H., and Hatano H., Anal. Lett., **8**, 205-213, 1975.
257. Creber K.A.M. and Wan J.K.S., J. Amer. Chem. Soc., **103**, 2101-2102, 1981.
258. Ho T.I., Creber K.A.M., and Wan J.K.S., J. Amer. Chem. Soc., **103**, 6524-6526, 1981.
259. Evans J.C., Jackson A.H., Rao K.R.N., and Rowlands C.C., J. High Resolut. Chromat., Chromat. Commun., **8**, 269-270, 1985.
260. Zolotov Y.A., Petruhkin O.M., Timerbaev A.R., Eustiferov M.U., Salov V.V., and Vanifatora N.G., Analyst, **114**, 1337-1339, 1989.
261. Taniguchi H. and Aoshima H., Chem. Lett., (#11), 1599-1602, 1981.
262. Iwahashi H., Parker C.E., Mason R.P., and Tomer K.B., Biochem. J., **276**, 447-453, 1991.
263. Reich T., Chen K.S., and Wan J.K.S., J. Chromatogr., **206**, 139-142, 1981.
264. Makino K., Moriya F., and Hatano H., J. Chromatogr., **332**, 71-106, 1985.
265. Sugata R., Iwahashi H., Ishii T., and Kido R., J. Chromatogr., **487**, 9-16, 1989.
266. Iwahashi H., Parker C.E., Mason R.P., and Tomer K.B., Anal. Chem., **64**, 2244-2252, 1992.
267. Kominani S., Rokushika S., and Hatano h., Int. J. Radiat. Biol., **30**, 525-534, 1976.
268. Makino K., Suzuki N., Moriya F., Rokushika S., and Hatano H., Chem. Lett. 675-678, 1979.
269. Iwahashi H., Ikeda A., Negoro Y., and Kido R., Biochem. J., **236**, 509-514, 1986.

270. Iwahashi H., Negoro Y., Ikeda A., and Kido R., J. Chromatogr., **391**, 199-205, 1987.
271. Iwahashi H., Parker C.E., Mason R.P., and Tomer K.B., Anal. Chem., **64**, 2244-2252, 1992.
272. Suzuki N., Makino K., Moriya F., Rokushika S., and Hatano H., J. Phys. Chem., **85**, 263-268, 1981.
273. Makino K., J. Phys. Chem., **83**, 2520-2523, 1979.
274. Kominani S., Rokushika S., and Hatano H., Radiation Research, **72**, 89-99, 1977.
275. Makino K., J. Phys. Chem., **84**, 1012-1015, 1980.
276. Makino K., J. Phys. Chem., **84**, 1016-1019, 1980.
277. Makino K., J. Phys. Chem., **84**, 1968-1974, 1980.
278. Moriya F., Makino K., Suzuki N., Rokushika S., and Hatano H., J. Phys. Chem., **84**, 3085-3090, 1980.
279. Moriya F., Makino K., Suzuki N., Rokushika S., and Hatano H., J. Phys. Chem., **84**, 3614-3619, 1980.
280. Moriya F., Makino K., Suzuki N., Rokushika S., and Hatano H., J. Amer. Chem. Soc., **104**, 830-836, 1982.
281. Makino K. and Riesz P., Can. J. Chem., **60**, 1480-1485, 1982.
282. Makino K., Mossoba M.M., and Riesz P., J. Phys. Chem., **87**, 1074-1080, 1983.
283. Makino K., Moriya F., and Hatano H., Radiat. Phys. Chem., **23**, 217-228, 1984.

284. Moriya F., Makino K., Iguchi N., Suzuki N., Rokushika S., and Hatano H., J. Phys. Chem., **88**, 2373-2377, 1984.
285. Iguchi N., Moriya F., Makino K., Rokushika S., and Hatano H., Can. J. Chem., **62**, 1722-1730, 1984.
286. Moriya F., Iguchi N., Makino K., Rokushika S., and Hatano H., Can. J. Chem., **62**, 2206-2216, 1984.
287. Evans J.C., Rao K.R.N., Jackson S.K., Rowlands C.C., and Barratt M.D., J. High Resol. Chromat., Chromat. Commun., **8**, 829-830, 1985.
288. Makino K., J. Phys. Chem., **83**, 2520-2523, 1979.
289. Suzuki N., Makino K., Moriya F., Rokushika S., and Hatano H., J. Phys. Chem., **85**, 263-268, 1981.
290. Agnel J.P., Thiery C., Battesti C., Vincent P., and Raffi J., Anal. Lett., **18**, 1013-1025, 1985.
291. Raffi J.J., Vincent P.B., Agnel J.P.L., Battesti C.M., and Thiery C.L., J. Chem. Soc., Faraday Trans. 1, **83**, 225-230, 1987.
292. Sugata R., Iwahashi H., Ishii T., and Kido R., J. Chromatogr., **487**, 9-16, 1989.
293. Makino K., Suzuki N., Moriya F., Rokushika S., and Hatano H., Anal. Lett., **13**, 301-309, 1980.
294. Makino K. and Hatano H., Chem. Lett., 119-122, 1979.
295. Makino K., Moriyama F., and Hatano H., J. Chromatogr., **332**, 71-106, 1985.
296. Shinohara H., Inakuma M., Kishida M., Yamazaki S., Hashizume T., and Sakurai T., J. Phys. Chem., **99**, 13769-13771, 1995.
297. Takata M., Umeda B., Nishibori E., Sakata M., Saito Y., Ohno M., and Shinohara H., Nature, **377**, 46-49, 1995.

298. Dresselhaus M.S., Dresselhaus G., and Saito R., Solid State Communications, **84**, 201-205, 1992.
299. Bethune D.S., Kiang C.H., deVries M.S., Gorman G., Savoy R., Vazquez J., and Beyers R., Nature, **363**, 605-607, 1993.
300. Iijima S. and Ichihashi T., Nature, **363**, 603-605, 1993.
301. Hiura H., Ebbesen T.W., Tanigaki K., and Takahashi H., Chem. Phys. Lett., **202**, 509-512, 1993.
302. Ajayan P.M., Ichihashi T., and Iijima S., Chem. Phys. Lett., **202**, 384-388, 1993.
303. Brabec C.J., Maiti A., Roland C., and Bernholc J., Chem. Phys. Lett., **236**, 150-155, 1995.
304. Weldon D.N., Blau W.J., and Zandbergen H.W., Chem. Phys. Lett., **241**, 365-372, 1995.
305. Setton R., Carbon, **33**, 135-140, 1995.
306. de Heer W.A., Bacsá W.S., Chatelain A., Gerfin T., Humphrey-Baker R., Forro L., Ugarte D., Science, **268**, 845-847, 1995.
307. Saito Y., Okuda M., Tomita M., and Hayashi T., Chem. Phys. Lett., **236**, 419-426, 1995.
308. Zhou D. and Seraphin S., Chem. Phys. Lett., **238**, 286-289, 1995.
309. Guo T., Nikolaev P., Thess A., Colbert D.T., and Smalley R.E., Chem. Phys. Lett., **243**, 49-54, 1995.
310. Rinzler A.G., Hafner J.H., Nikolaev P., Lou L., Kim S.G., Tomanek D., Nordlander P., Colbert D.T., and Smalley R.E., Science, **269**, 1550-1553, 1995.

311. Chopra N.G., Benedict L.X., Crespi V.H., Cohen M.L., Louie S.G., and Zeltl A., Nature, **377**, 135-138, 1995.
312. Endo M., Takeuchi K., Kobori K., Takahashi K., Kroto H.W., and Sarkar A., Carbon, **33**, 873-882, 1995.
313. Dresselhaus M.S., Dresselhaus G., and Saito R., Carbon, **33**, 883-892, 1995.
314. Mintmire J.W. and White C.T., Carbon, **33**, 893-902, 1995.
315. Kiang C.H., Goddard W.A., Beyers R., and Bethune D.S., Carbon, **33**, 903-914, 1995.
316. Sattler K., Carbon, **33**, 915-920, 1995.
317. Colbert D.T. and Smalley R.E., Carbon, **33**, 921-924, 1995.
318. Ruoff R.S. and Lorents D.C., Carbon, **33**, 925-930, 1995.
319. Issi J.P., Langer L., Heremans J., and Olk C.H., Carbon, **33**, 941-948, 1995.
320. Wang X.K., Lin X.W., Song S.N., Dravid V.P., Ketterson J.B., and Chang R.P.H., Carbon, **33**, 949-958, 1995.
321. Eklund P.C., Holden J.M., and Jishi R.A., Carbon, **33**, 959-972, 1995.
322. Ebbesen T.W. and Takada T., Carbon, **33**, 973-978, 1995.
323. Saito Y., Carbon, **33**, 979-988, 1995.
324. Calvert P., Nature, **357**, 365, 1992.
325. Broughton J. and Pederson M., Phys. Rev. Lett., **69**, 2689-2692, 1992.
326. Mintmire J.W., Dunlap B.I., and White T., Phys. Rev. Lett., **68**, 631-634, 1992.



327. Hamada N., Sawada S., and Oshiyama S., Phys. Rev. Lett., **68**, 1579-1581, 1992.
328. Dresselhaus M.S., Nature, **358**, 195, 1992.
329. Dai H., Wong E.W., Lu Y.Z., Fan S., and Lieber C.M., Nature, **375**, 769-772, 1995.
330. Liu M. and Cowley J.M., Carbon, **33**, 749-756, 1995.
331. Funasaka H., Sugiyama K., Yamamoto K., and Takahashi T., Chem. Phys. Lett., **236**, 277-284, 1995.
332. Ajayan P.M., Stephan O., Redlich P., and Colliex C., Nature, **375**, 564-567, 1995.
333. Ajayan P.M. and Iijima S., Nature, **361**, 333-334, 1993.

APPENDIX I: EMPTY-CAGE, C<sub>2n</sub>  
 MASS SPECTROMETRY TABLE

C60	720.7	C88	1057.0	C116	1393.3
C62	744.7	C90	1081.0	C118	1417.3
C64	768.7	C92	1105.0	C120	1441.3
C66	792.7	C94	1129.0	C122	1465.3
C68	816.7	C96	1153.1	C124	1489.4
C70	840.8	C98	1177.1	C126	1513.4
C72	864.8	C100	1201.1	C128	1537.4
C74	888.8	C102	1225.1	C130	1561.4
C76	912.8	C104	1249.1	C132	1585.4
C78	936.9	C106	1273.2	C134	1601.4
C80	960.9	C108	1297.2	C136	1633.5
C82	984.9	C110	1321.2	C138	1657.5
C84	1008.9	C112	1345.2	C140	1681.5
C86	1032.9	C114	1369.2	C142	1705.5

APPENDIX II:  $Sc_m@C_{2n}$   
 MASS SPECTROMETRY TABLE

Sc@C60	765.6	Sc2@C60	810.6	Sc3@C60	855.5	Sc4@C60	900.7
Sc@C62	789.6	Sc2@C62	834.6	Sc3@C62	879.5	Sc4@C62	924.7
Sc@C64	813.7	Sc2@C64	858.6	Sc3@C64	903.6	Sc4@C64	948.7
Sc@C66	837.7	Sc2@C66	882.6	Sc3@C66	927.6	Sc4@C66	972.7
Sc@C68	861.7	Sc2@C68	906.7	Sc3@C68	951.6	Sc4@C68	996.7
Sc@C70	885.7	Sc2@C70	930.7	Sc3@C70	975.6	Sc4@C70	1020.8
Sc@C72	909.7	Sc2@C72	954.7	Sc3@C72	999.6	Sc4@C72	1044.8
Sc@C74	933.8	Sc2@C74	978.7	Sc3@C74	1023.7	Sc4@C74	1068.8
Sc@C76	957.8	Sc2@C76	1002.7	Sc3@C76	1047.7	Sc4@C76	1092.8
Sc@C78	981.8	Sc2@C78	1026.8	Sc3@C78	1071.7	Sc4@C78	1116.9
Sc@C80	1005.8	Sc2@C80	1050.8	Sc3@C80	1095.7	Sc4@C80	1140.9
Sc@C82	1029.9	Sc2@C82	1074.8	Sc3@C82	1119.8	Sc4@C82	1164.9
Sc@C84	1053.9	Sc2@C84	1098.8	Sc3@C84	1143.8	Sc4@C84	1188.9
Sc@C86	1077.9	Sc2@C86	1122.9	Sc3@C86	1167.8	Sc4@C86	1212.9
Sc@C88	1101.9	Sc2@C88	1146.9	Sc3@C88	1191.8	Sc4@C88	1237.0
Sc@C90	1125.9	Sc2@C90	1170.9	Sc3@C90	1215.9	Sc4@C90	1261.0
Sc@C92	1150.0	Sc2@C92	1194.9	Sc3@C92	1239.9	Sc4@C92	1285.0
Sc@C94	1174.0	Sc2@C94	1218.9	Sc3@C94	1263.9	Sc4@C94	1309.0
Sc@C96	1198.0	Sc2@C96	1243.0	Sc3@C96	1287.9	Sc4@C96	1331.1
Sc@C98	1222.0	Sc2@C98	1267.0	Sc3@C98	1311.9	Sc4@C98	1357.1
Sc@C100	1246.1	Sc2@C100	1291.0	Sc3@C100	1336.0	Sc4@C100	1381.1

APPENDIX III:  $Y_m@C_{2n}$   
 MASS SPECTROMETRY TABLE

Y@C60	810	Y2@C60	899	Y3@C60	988	Y4@C60	1077
Y@C62	834	Y2@C62	923	Y3@C62	1012	Y4@C62	1101
Y@C64	858	Y2@C64	947	Y3@C64	1036	Y4@C64	1125
Y@C66	882	Y2@C66	971	Y3@C66	1060	Y4@C66	1149
Y@C68	906	Y2@C68	995	Y3@C68	1084	Y4@C68	1173
Y@C70	930	Y2@C70	1019	Y3@C70	1108	Y4@C70	1197
Y@C72	954	Y2@C72	1043	Y3@C72	1132	Y4@C72	1221
Y@C74	978	Y2@C74	1067	Y3@C74	1156	Y4@C74	1245
Y@C76	1002	Y2@C76	1091	Y3@C76	1180	Y4@C76	1269
Y@C78	1026	Y2@C78	1115	Y3@C78	1204	Y4@C78	1293
Y@C80	1050	Y2@C80	1139	Y3@C80	1228	Y4@C80	1317
Y@C82	1074	Y2@C82	1163	Y3@C82	1252	Y4@C82	1341
Y@C84	1098	Y2@C84	1187	Y3@C84	1276	Y4@C84	1365
Y@C86	1122	Y2@C86	1211	Y3@C86	1300	Y4@C86	1389
Y@C88	1146	Y2@C88	1235	Y3@C88	1324	Y4@C88	1413
Y@C90	1170	Y2@C90	1259	Y3@C90	1348	Y4@C90	1437
Y@C92	1194	Y2@C92	1283	Y3@C92	1372	Y4@C92	1461
Y@C94	1218	Y2@C94	1307	Y3@C94	1396	Y4@C94	1485
Y@C96	1242	Y2@C96	1331	Y3@C96	1420	Y4@C96	1509
Y@C98	1266	Y2@C98	1355	Y3@C98	1444	Y4@C98	1533
Y@C100	1290	Y2@C100	1379	Y3@C100	1468	Y4@C100	1557

APPENDIX IV:  $\text{La}_m@C_{2n}$   
 MASS SPECTROMETRY TABLE

La@C60	859.6	La2@C60	998.5	La3@C60	1137.4	La4@C60	1276.3
La@C62	883.6	La2@C62	1022.5	La3@C62	1161.4	La4@C62	1300.3
La@C64	907.6	La2@C64	1046.5	La3@C64	1185.4	La4@C64	1324.3
La@C66	931.6	La2@C66	1070.5	La3@C66	1209.4	La4@C66	1348.3
La@C68	955.6	La2@C68	1094.5	La3@C68	1233.4	La4@C68	1372.3
La@C70	979.7	La2@C70	1118.6	La3@C70	1257.5	La4@C70	1396.4
La@C72	1003.7	La2@C72	1142.6	La3@C72	1281.5	La4@C72	1420.4
La@C74	1027.7	La2@C74	1166.6	La3@C74	1305.5	La4@C74	1444.4
La@C76	1051.7	La2@C76	1190.6	La3@C76	1329.5	La4@C76	1468.4
La@C78	1075.8	La2@C78	1214.7	La3@C78	1353.6	La4@C78	1492.5
La@C80	1099.8	La2@C80	1238.7	La3@C80	1377.6	La4@C80	1516.5
La@C82	1123.8	La2@C82	1262.7	La3@C82	1401.6	La4@C82	1540.5
La@C84	1147.8	La2@C84	1286.7	La3@C84	1425.6	La4@C84	1564.5
La@C86	1171.8	La2@C86	1310.7	La3@C86	1449.6	La4@C86	1588.5
La@C88	1195.9	La2@C88	1334.8	La3@C88	1473.7	La4@C88	1612.6
La@C90	1219.4	La2@C90	1358.8	La3@C90	1497.7	La4@C90	1636.6
La@C92	1243.9	La2@C92	1382.8	La3@C92	1521.7	La4@C92	1660.6
La@C94	1267.9	La2@C94	1406.8	La3@C94	1545.7	La4@C94	1684.6
La@C96	1292.0	La2@C96	1430.4	La3@C96	1569.8	La4@C96	1708.7
La@C98	1316.0	La2@C98	1454.9	La3@C98	1593.8	La4@C98	1732.7
La@C100	1340.0	La2@C100	1478.9	La3@C100	1617.8	La4@C100	1756.7

APPENDIX V:  $Er_m@C_{2n}$   
 MASS SPECTROMETRY TABLE

Er@C60	888	Er2@C60	1055	Er3@C60	1222
Er@C62	912	Er2@C62	1079	Er3@C62	1246
Er@C64	936	Er2@C64	1103	Er3@C64	1270
Er@C66	960	Er2@C66	1127	Er3@C66	1294
Er@C68	984	Er2@C68	1151	Er3@C68	1318
Er@C70	1008	Er2@C70	1175	Er3@C70	1342
Er@C72	1032	Er2@C72	1199	Er3@C72	1366
Er@C74	1056	Er2@C74	1223	Er3@C74	1390
Er@C76	1080	Er2@C76	1247	Er3@C76	1414
Er@C78	1104	Er2@C78	1271	Er3@C78	1438
Er@C80	1128	Er2@C80	1295	Er3@C80	1462
Er@C82	1152	Er2@C82	1319	Er3@C82	1486
Er@C84	1176	Er2@C84	1343	Er3@C84	1510
Er@C86	1200	Er2@C86	1367	Er3@C86	1534
Er@C88	1224	Er2@C88	1391	Er3@C88	1558
Er@C90	1248	Er2@C90	1415	Er3@C90	1582
Er@C92	1272	Er2@C92	1439	Er3@C92	1606
Er@C94	1296	Er2@C94	1463	Er3@C94	1630
Er@C96	1320	Er2@C96	1487	Er3@C96	1654
Er@C98	1344	Er2@C98	1511	Er3@C98	1678
Er@C100	1368	Er2@C100	1535	Er3@C100	1702

## VITA

Born in Clearlake Highlands, California , I was raised in a family of nine people. My father is a dedicated teacher whose career has been enlightening students at the grade school, high school, and university level. My mother is a dedicated housewife who raised five boys and two girls. Academically, my education has consisted of the following: Sharyland High School (Mission, TX, 1982-1986), Angelo State University (San Angelo, TX, 1986-1990, B.S. Chemistry, Magna Cumme Laude Honors), Virginia Polytechnic Institute & State University (Blacksburg, VA, 1990-1992, M.S. Chemistry), and Virginia Polytechnic Institute & State University (Blacksburg, VA, 1993-1995, Ph.D. Chemistry). On a personal level, I have two beautiful children, Jordan (5 years old) and 'Cole (3 years old).



---

Steven Stevenson